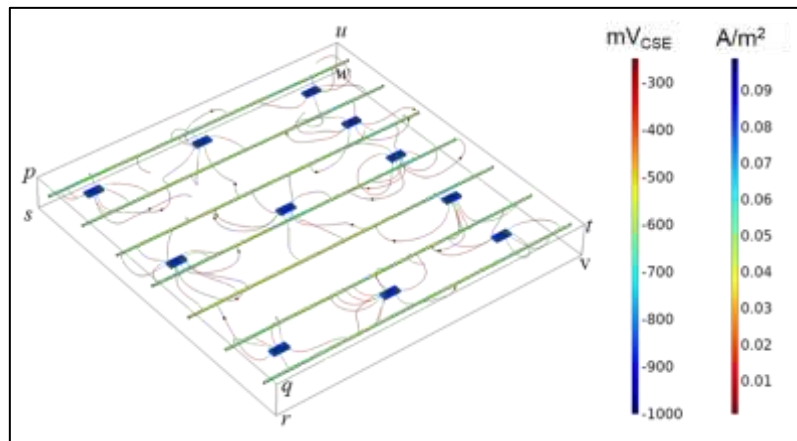DEPARTMENT OF CIVIL ENGINEERING

INDIAN INSTITUTE OF TECHNOLOGY MADRAS

CHENNAI – 600 036

FIELD PERFORMANCE ASSESSMENT AND

AN ATTEMPT FOR ELECTROCHEMICAL MODELLING OF

CATHODIC PROTECTION SYSTEMS IN REINFORCED CONCRETE

A Thesis

Submitted by

NAVEEN KRISHNAN

(CE18S027)

For the award of the degree

of

MASTER OF SCIENCE (By Research)

August 2021

This page is intentionally left blank

DEDICATION

This thesis is dedicated to my mother, Geetha, who had taught me that there is no room in the world for living a lazy life.

This page is intentionally left blank

THESIS CERTIFICATE

This is to undertake that the Thesis titled, **FIELD PERFORMANCE ASSESSMENT AND AN ATTEMPT FOR ELECTROCHEMICAL MODELLING OF CATHODIC PROTECTION SYSTEMS IN REINFORCED CONCRETE** submitted by me to the Indian Institute of Technology Madras for the award of **Master of Science (by Research) degree** is a bonafide record of the research work done by me under the supervision of **Dr Radhakrishna G. Pillai**. The contents of this Thesis, in full or in parts, have not been submitted to any other Institute or University for the award of any degree or diploma.

In order to effectively convey the idea presented in this Thesis, the following work of other authors was reprinted in the Thesis with their permission:

- Figure 2.10, page 34: Reprinted from Whitmore et al. 2019 with the permission of the authors.

Chennai, India

Research Scholar

Date: August 26, 2021

Research Guide

This page is intentionally left blank

LIST OF PUBLICATIONS BASED ON THIS THESIS

REFEREED JOURNAL PUBLICATIONS

Published

[1].   **Krishnan, N.,** Kamde, D.K., Veedu, Z.D., Pillai, R.G. and Shah, D., and Velayudham, R. (2021). "Long-term performance and life-cycle-cost benefits of cathodic protection of concrete structures using galvanic anodes", *Journal of Building Engineering, Elsevier.*

[2].   **Krishnan, N.**, Veedu, Z.D., Shah, D. and Liao, H. (2020). "Hybrid anodes for accelerated cathodic protection of corroding concrete structures", *The Indian Concrete Journal*, Vol. 94, No. 11, pp. 101-110.

Draft ready/in preparation

Krishnan, N. and Pillai, R. G. (2021). "Instantaneous performance assessment and electrochemical modelling of cathodic protection in reinforced concrete", to be submitted to Journal of Materials and Structures, Springer.

CONFERENCE PUBLICATIONS

[1].   **Krishnan, N.**, Kamde D.K., Pillai, R.G. (2019) "8 – Year performance of cathodic protection systems in reinforced concrete slabs and life-cycle cost benefits" RILEM SMSS 2019, *Proceedings of the International Conference on Sustainable Materials, Systems and Structures*, Rovinj, Croatia.

[2].   Veedu, Z.V., **Krishnan, N.**, Kamde, D.K., Pillai, R.G. (2018) "Effect of resistivity of the concrete on the performance of sacrificial anode cathodic prevention (SACP) Systems" NIGIS CORCON 2018, Jaipur, India.

[3].   **Krishnan, N.** and Pillai, R.G. (2019) "Understanding the throwing power of galvanic anodes in reinforced concrete structures using numerical simulations" NIGIS CORCON 2019, Mumbai, India (**Won best poster award**).

This page is intentionally left blank

ACKNOWLEDGMENTS

This page is intentionally left blank

ABSTRACT

FIELD PERFORMANCE ASSESSMENT AND
AN ATTEMPT FOR ELECTROCHEMICAL MODELLING OF
CATHODIC PROTECTION SYSTEMS IN REINFORCED CONCRETE

Keywords: Concrete, steel, corrosion, galvanic anode, cathodic protection, life cycle cost, electrochemical modelling

Worldwide, many reinforced concrete structures are corroding well before their design lives and are being repaired to extend their service life as much as possible. However, these repairs fail within a few years due to continued corrosion, which leads to repeated repairs and eventual replacement of structures — resulting in significant reduction in service life and increase in life cycle cost (LCC). Such inadequate and frequent patch repairs (PRs) are also associated with huge loss of existing materials in structures, large use of pristine materials for patch repairs, and high carbon footprint. Service life can be extended and such adverse effects can be minimized by electrochemical treatment of embedded steel, especially for concrete structures contaminated with corrosive elements, which is a need of the hour and focus of this thesis.

First, this thesis focused on the long-term performance and effects of 'cathodic protection strategy using galvanic anodes' (CP strategy, hereafter) in extending the service life and reducing the LCC. The review of literature and practices revealed that most of the repair projects do not consider CP strategy along with conventional patch repairs because of the lack of sufficient long-term field data to substantiate the claim of long-term protection using galvanic anodes and associated wrong perception of adverse financial implications. To address this, two case studies on the long-term performance of CP systems in a coastal jetty and a building close to seashore were performed. The 14-year data indicated that the galvanic anodes could successfully control the chloride-induced corrosion for at least 14 years. It was also found that the additional cost of galvanic anodes is only about 4% of the repair cost for the

jetty structure – breaking the myth of high capital cost of CP strategy. Then, a framework to estimate the LCC of PR and CP strategies was developed and it was found that CP and cathodic prevention (CPrev) strategies are highly economical than the PR strategy in long-term. Also, the LCC analysis of 30 repair projects confirmed that CP strategy can lead to LCC savings of about 90% in about 30 years after the first repair.

Second focus was on assessing the instantaneous performance of CP systems in concrete structures. The standard criteria available for assessing the instantaneous performance of CP systems are based on experiments conducted in the 1940s on metals in low resistive electrolyte systems (e.g., pipeline and offshore). The validity of such criteria for steel in today's highly resistive concrete systems needed to be evaluated. The data collected from two reinforced concrete (RC) buildings over a period of ≈ 750 days revealed that the conventionally used "100 mV criterion" was not suitable in assessing the performance of CP systems, especially when the corrosion rate is less than 2 mA/m^2. Hence, this criterion is found to be not suitable for assessing CP systems in typical RC structures. In addition, this thesis refined the methodology to instal CP systems in concrete and assess their instantaneous performance.

Finally, this thesis also presents a new approach to assess the instantaneous performance of C-S-A systems through finite element modelling of electrochemical processes. It was found that suitable electrochemical models are not available to understand the instantaneous behaviour and assess the performance of concrete-steel-anode (C-S-A) systems. Therefore, an electrochemical model was developed and a parametric study on the variation of the electrical potential along steel rebars and the output current density from anodes in a three-dimensional C-S-A system was studied. The study found that the influence region of anodes is dependent on the resistivity of concrete and the design must take this into account, which is not a practice today. In summary, this thesis covers the long-term and instantaneous performance and the electrochemical modelling of C-S-A systems.

TABLE OF CONTENTS

LIST OF FIGURES

LIST OF TABLES

This page is intentionally left blank

GLOSSARY

The following are some of the commonly used terms in this thesis:

Anode: The electrode where oxidation of metal takes place. The location where electron loss and metal loss takes place.

Calomel electrode: A reference cell with mercury electrode in potassium chloride solution of specified concentration and saturated with mercurous chloride.

Corrosion cell: Electrochemical cell on the metal surface because of chemical or physical differences on the metal surface.

Cathode: The electrode where reduction reaction occurs. The location where the electrode accepts electrons.

Electrode: Electrode is a metallic conductor transporting electricity into non-metallic solid, liquid, gases, vacuums, etc.

Electrolyte: The medium, preferentially conducting in nature, where ions can travel from anode to cathode. In reinforced concrete systems, the concrete pore solution is the electrolyte.

Ohmic drop: Potential drop due to electrolytes such as solution, mortar, or anything between the working electrode and the reference electrode.

Passive film: This is the layer of oxide formed around the steel surface when it is in contact with oxygen and moisture. Ironically, this is the first corrosion product formed

Three-electrode system: The three-electrode system consists of the following electrodes: working electrode, reference electrode, and counter electrode.

Working electrode (WE): Working electrode is the test specimen or the electrode whose behaviour needs to be understood in an electrochemical test. During PDS, LPR, or EIS test, the current is passed through the working electrode to displace the electrode's potential from its equilibrium state because of the resulting overpotential.

Reference electrode (RE): The electrode that has accurately maintained potentials is used as a reference to measure the potential difference of other electrodes.

Counter electrode (CE): The electrode is usually used for polarization studies to pass current to and from the test electrode. It is made of any non-corroding material. It is also known as the auxiliary electrode.

Exchange current density (i_o): Exchange current density is the reaction rate at the reversible potential of an electrode, i.e., it is the current density that flows equally in both cathodic and anodic directions at equilibrium.

Tafel slopes (β_a and β_b): Slope of the anodic or cathodic polarisation curve in E versus log i relationship (Evans diagram). These slopes determine the amount of current flow corresponding to an applied potential.

Limiting oxygen current density (i_{lim}): This is the maximum current density required to achieve oxygen reduction in an electrode reaction.

Potentiostat: It is an electronic device used to obtain the current flow from an electrode reaction by changing the potential of the system in a controlled manner.

On potential (E_{on}): Potential of the steel when it is connected to the anode. This is the mixed potential of the steel and anode system.

Instantaneous-Off potential (E_{i-off}): Potential of the polarised steel after eliminating the voltage drop (*iR* drop) across the cover concrete.

Depolarised potential (E_{24h}): Potential of the steel measured after 24 hours from the time of disconnecting the steel from the anode.

Potential shift: The potential shift is obtained by calculating the difference between the instantaneous-off potential (E_{i-Off}) and the 24-hour depolarised potential of the steel rebars (E_{24h})

This page is intentionally left blank

ABBREVIATIONS

CP   :   Cathodic protection (with galvanic anodes)

CPrev   :   Cathodic prevention (with galvanic anodes)

C-S-A   :   Concrete-steel-anode

CSE   :   Copper-copper sulphate reference electrode

EIS   :   Electrochemical impedance spectroscopy

FV   :   Future value

HCP   :   Half-cell potential

ICCP   :   Impressed current cathodic protection system

LCC   :   Life cycle cost

LPR   :   Linear polarisation resistance

MPY   :   Mills per year

NDT   :   Non-destructive test

NPC   :   Net present cost

OCP   :   Open circuit potential

PDS   :   Potentiodynamic scan test

PR   :   Patch repair (without galvanic anodes)

PS   :   Potentistatic test

PVT   :   Passivity Verification Technique

RC   :   Reinforced concrete

SCE   :   Saturated calomel reference electrode

SHE   :   Standard hydrogen electrode

SSCE   :   Saturated silver-silver chloride reference electrode

This page is intentionally left blank

NOTATIONS

ΔE : Potential shift obtained from the depolarisation test

C : Cost of repair excluding the cost of inspection and anodes

C_{anode} : Cost of manufacturing, supply, and installation of anodes

$C_{CP, j}$: Future value of jth repair with CP

$C_{insp, i}$: Future value of ith inspection

$C_{insp-zero}$: Cost of inspection at the time of 1st repair

$C_{PR, j}$: Future value of jth repair without CP

$C_{total, CP}$: Total cost of repair with CP till n^{th} year

$C_{total, PR}$ Total cost of repair without CP till n^{th} year

E_{24h} : Depolarized potential at 24 hours

E_{i-Off} : Potential of the polarised steel within 0.1 seconds after disconnecting from the anode

E_{on} : Mixed potential of the CP system

i : Identification of individual inspection (i = 1, 2, 3, …)

$i_{applied}$: Current density applied to the rebar by the anodes

i_{corr} :: Corrosion rate of the rebar

i_{lim} : Limiting current density

$i_{n, surface}$: Normal current density on all the concrete surfaces

i_o : Exchange current density

I_{output} : Output current density from anodes

I_{totoal} : Total current density at any point in the electrode surfaces

I_{xj} : Component of the current flowing in xj direction

j : Identification of individual repair (j = 1, 2, 3, …)

j_{max} : Maximum allowable number of repairs

K : Electrochemical equivalence of zinc metal (kg/A-year)

n : Time elapsed from 1st repair (n = 1, 2, 3, …)

n_{max}	:	Maximum service life extension (analysis period)
r	:	Discount rate
SD	:	Steel density ratio
SL	:	Design service life of the CP system
$t_{initiation}$	:	Duration of corrosion initiation phase
$t_{insp,\,i}$	:	Time interval between $(i-1)^{th}$ and i^{th} inspections
$T_{insp,\,i}$	:	Time elapsed between 1st and i^{th} inspection $(i = 1, 2, 3, ...)$
$t_{propagation}$	:	Duration of corrosion propagation phase
$t_{rep,\,j}$	:	Service life of jth repair
$T_{rep,\,j}$	:	Time elapsed between 1st and j^{th} repairs $(j = 1, 2, 3, ...)$
t_{repair}	:	Duration of the entire repair phase (Desired extension in service life)
V	:	Potential inside the concrete domain (Volts)
v	:	Volume of the three-dimensional concrete domain (m^3)
β_a	:	Anodic Tafel slope
β_b	:	Cathodic Tafel slope
$\eta_{efficency}$	:	Efficiency factor of the anode material
$\eta_{utilisation}$	:	Utilisation factor of the anode material
ρ	:	Resistivity of the concrete

1 INTRODUCTION

1.1 PROBLEM STATEMENT

In reinforced concrete structures, patch repairs with localized replacement of contaminated concrete are the usual repair method. However, it has been proven that such partial replacement of contaminated concrete may not arrest corrosion in the structure. It was observed that the rebar locations along the periphery of the patch repair had experienced severe corrosion after a few months of the patch repair. During a patch repair, the chloride-contaminated concrete in the region experiencing corrosion is removed, and fresh chloride-free concrete is placed. As a result, the active rebars in the patch becomes passive by shifting the corrosion potential to a more positive value (say -200 mV). This stops the corrosion of the rebars within the patch. However, the rebars in the adjacent region continue to corrode with a more negative potential (say, less than -350 mV). This variation in the corrosion potential across the steel in the new and old concrete leads to accelerated corrosion around the periphery of the patch repair. This phenomenon is called the halo or ring effect (Chess and Broomfield 2013; Costa 2010; Dugarte and Sagüés 2014; Sergi and Page 2000; Whitmore and Abbott 2003). Figure 1.1 shows a beam that developed corrosion adjacent to a repaired area about six months after the repair. This means that the halo effect can accelerate the rate of corrosion adjacent to the repaired area.
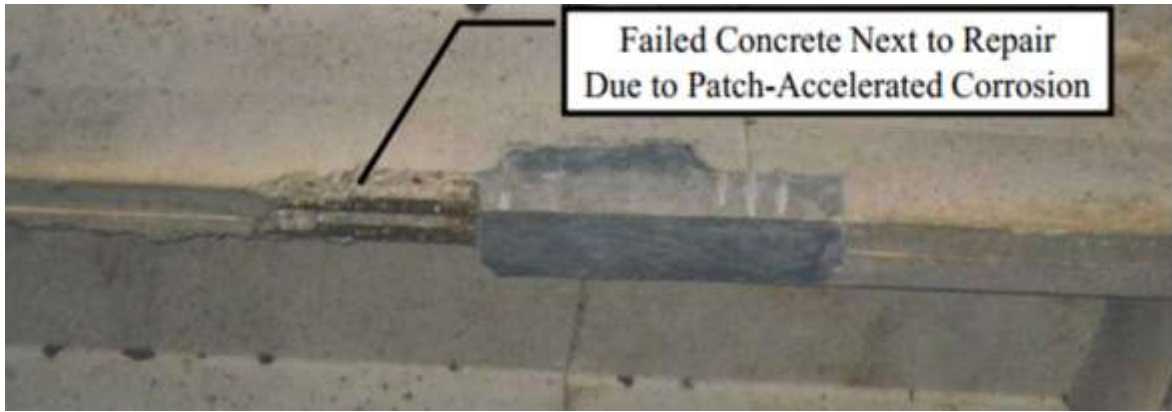
Figure 1.1: Corroded rebars adjacent to a patch repaired area of a beam (Photo courtesy: Vector corrosion technologies, Canada)

Electrochemical repair treatments, such as cathodic protection, must be employed to arrest the corrosion to avoid repeated repairs and continual cost. However, these techniques lack sufficient long-term performance data leading to the omission of using such treatment in a repair tender document. In addition to that, the high initial cost is another reason as many repair works do not consider CP's long-term benefits. Therefore, there is a dire need to obtain the long-term performance data of galvanic anodes to promote such electrochemical repair treatment. Also, it is necessary to understand the service life and the long-term cost benefits of using such repairs.

In the last four decades, the cathodic protection (CP) system with galvanic anodes — say, concrete-steel-anode system (denoted as C-S-A system, hereafter) — is used in many repair projects as an electrochemical treatment. The use of this technology in the concrete sector has grown significantly in recent times as it prevents the formation of incipient anodes in steel rebars (Bertolini et al. 2002; Bertolini and Redaelli 2009; Pedeferri 1996; Polder and Peelen 2018). However, many substandard quality anodes or CP systems without following sound installation practices are implemented in many repair projects. Figure 1.2 shows some photographs of inadequate installation of CP systems in concrete structures.

| (a) Galvanic anodes embedded outside the concrete domain | (b) Loosely tied galvanic anodes around the steel reinforcement | (c) Anti-corrosive chemical coated on the concrete surface |

Figure 1.2: Inadequate implementation of galvanic anode CP systems in RC structures — leading to an incomplete electrical circuit

Most inspection techniques and acceptance criteria available for C-S-A systems are originally made for metals in low-resistive systems (ship in seawater, pipelines in soil, etc.). These cannot be directly used for reinforced concrete systems because the resistivity of concrete is about 1 to 2 orders of magnitude higher than that of soil or aqueous systems. Also, the resistivity of concretes and repair materials used today is much higher than that of concretes used about two decades ago. If such anodes prevail, then there is a danger of CP technology getting a false negative perception. Therefore, there is a need to check the efficiency of the present interpretation criteria' to assess a CP system's performance in RC structures.

The existing inspection methods allow inspection only at pre-defined locations and pose severe implementational and long-term monitoring drawbacks. In addition, there have been many cases where the monitoring boxes were destroyed or damaged due to weathering actions (through wind, rainfall, tides, etc.) or because of vandalism. Because of these, monitoring results from most CP implemented sites are not available after a certain period (say, 10 years). Therefore, there is a dire need to develop new non-destructive methods to assess CP

systems in concrete structures. This requires electrochemical models that can predict the current and potential on the surface of steel and anodes at any time in the future.

1.2 MOTIVATION FOR THE STUDY

Many national academies worldwide have identified cathodic protection (CP) systems using discrete galvanic anode systems as one of the most efficient methods to prevent corrosion. In India, many stakeholders are hesitant to implement CP in their repair projects. This is because of the lack of sufficient long-term performance data and the additional capital cost of galvanic anode cathodic protection systems in the repair work. Also, it was identified that some of the anodes circulating in the Indian market do not meet the required design criteria for a good anode. These anodes may work for a short period (say one year) but fail to provide long-term protection. Furthermore, as there is no specific BIS standard for installing these anodes in concrete, usually, CP installation is carried out by unskilled labours, leading to improper installation. In addition, the currently adopted practice to assess a cathodic protection system in concrete is by installing monitoring boxes at representative locations in a structure. However, this cannot ensure adequate workmanship and monitoring of the performance of all the anodes in large concrete structures.

This study attempts to obtain long-term performance data and analyse the long-term benefits of CP. This will promote the usage of such electrochemical treatments in repair projects, resulting in a durable repair. The methodology of installation and testing procedures of a C-S-A system documented in this study can develop a Bureau of Indian Standards (IS) for CP to ensure proper construction/repair practises using CP. In this way, adequate workmanship for installation and testing can be confirmed in all the repair projects. Also, the study developed an electrochemical model that can estimate the current and potential distribution in a C-S-A system. Such models can assess the instantaneous performance of anodes in a concrete

structure by collecting and analysing the electrical signals against an external electrical perturbation. Later, this can help develop non-destructive testing equipment that can assess the C-S-A system as and when needed, without multiple monitoring boxes throughout the structure. Such testing techniques can enable routine inspection and assess the quality/performance of numerous anodes at random locations inside concrete structures, which are essential to function as a 'watchdog' and ensure the quality of CP products and workmanship.

1.3 RESEARCH QUESTIONS

1. Galvanic anode cathodic protection uses the galvanic action of a sacrificing metal that depends on the microclimate around the anode metal (say, zinc). As this microclimate changes with time due to the formation of zinc corrosion products, will the remaining pristine anode metal provide adequate long-term protection to extend the residual service life of the structure?

2. Implementing cathodic protection in concrete during repair or while constructing the structures incurs an additional cost of the manufacturing, transportation, and installation of anodes. Is this additional initial cost worth investing in galvanic anodes during repair?

3. The existing test method for assessing the performance of the CP system in concrete (EN ISO 12696) relies on the test results from the representative monitoring locations. Are these interpretation criteria reliably assess the performance of galvanic anodes.

4. Numerical methods have been used to assess and optimize the design of galvanic anodes. Can this concept help develop a non-destructive test to assess the performance of galvanic anodes at random locations and at any time in the future?

1.4 OBJECTIVES AND SCOPE

The following are the objectives and scope of this study:

i. To assess the long-term performance and life cycle cost (LCC) benefits of using a cathodic protection system in concrete repair projects.

➢ Two case studies where CP is implemented

➢ Depolarisation and current measurement tests

➢ Cost of various repair heads and LCC savings

ii. To assess the instantaneous performance of a cathodic protection system using existing test methods and evaluate the feasibility of extending these test methods for long-term performance assessment.

➢ Two case studies; a reinforced lime concrete sunshade in a heritage building and a residential apartment complex

➢ Test method as per EN ISO 12696

➢ Three types of galvanic anodes

iii. To prove a concept for electrochemical modelling of steel-reinforced concrete with embedded galvanic anodes (i.e., concrete-steel-anode (C-S-A) system).

➢ Electrochemical characteristics of steel reinforcement and zinc anodes in cementitious systems

1.5   RESEARCH SIGNIFICANCE

In 2016, the overall cost of corrosion for various countries was about 5 to 10% of GDP, of which about 50% is due to corrosion in concrete structures. The conventional patch repairs adopted in many structures fail in about five years and lead to repeated repairs and a significant increase in the cost of corrosion and life-cycle cost (LCC) of concrete structures. Patch repair with cathodic protection (CP) can enhance the life of repairs to about 20+ years, even in aggressive environments. However, many practitioners do not consider cathodic protection using galvanic anodes because of the myth of excessive cost implications. This thesis presents the long-term field data on the performance of galvanic anodes and LCC analysis of patch repairs of RC systems with and without galvanic anodes. The long-term data and possible huge LCC savings (of about 90%) due to cathodic protection presented in this thesis could be an eye-opener. This can build confidence in engineers to use galvanic anodes to achieve durable repairs and extend the service life of concrete structures.

Presently, EN ISO 12696 is used to assess the performance of a CP system in reinforced concrete. This method includes conducting depolarisation tests that use half-cell potential (HCP) measurement of rebars before and after connecting them to the anodes. However, these HCP measurements depend on the resistivity of the concrete structures and may not always represent the actual condition of the rebar surface. Also, previous research on concrete specimens suggested that a relatively lower polarization significantly suppresses macrocell activities than 100 mV (Helm and Raupach 2019). Therefore, the criteria indicated by EN ISO 12696 (in particular the '100 mV potential shift' criteria) needs to be relooked to avoid erroneous estimation of the efficiency of the CP systems in concrete. This study reviews and documents the methodology of installation and testing of galvanic anodes in two concrete structures. Also, this study provides the initial day instantaneous performance data from CP systems installed in two cases studies. This enables the review of the ability of a CP system to

provide the required amount of protection current. Such studies are essential to refine and modify the existing criteria for CP assessment.

Typically, the quality of C-S-A systems is assessed by using monitoring boxes at minimal representative locations (say, about ten anodes when lakhs of anodes are installed in a single structure) and observing if there is a polarization shift of 100 mV. Unfortunately, this criterion may disqualify good anodes (i.e., those that function well in short and long terms) and qualify poor ones (i.e., those that perform well only for a short time and not for the long term). This criterion must be modified to enable the selection of good anodes and the rejection of poor anodes. Also, the repair contractors know that the small number of anodes installed at pre-defined locations can only be tested, and the existing techniques cannot assess the performance of other numerous anodes installed. This study presents the concept for developing an electrochemical (EC) model to estimate the various potential and currents inside a C-S-A system. Such an EC model can aid the development of new non-destructive test methods and acceptance criteria for the routine inspection of C-S-A systems at any random location and work as a watchdog to ensure quality CP products and installations.

1.6   RESEARCH METHODOLOGY

Figure 1.3 shows the methodology adopted to achieve the objectives of this thesis. For objective 1, first, a survey was conducted among various repair consultants and galvanic anode manufacturers to obtain information on the number of repeated repair projects and the usage of galvanic anodes in the repair industry. Then, CP systems in a 14-year old jetty structure and a 4-year-old salt processing plant were assessed to understand CP's long-term performance. After that, a life cycle cost analysis of a repair with and without CP was conducted to understand the long-term cost benefits of CP.
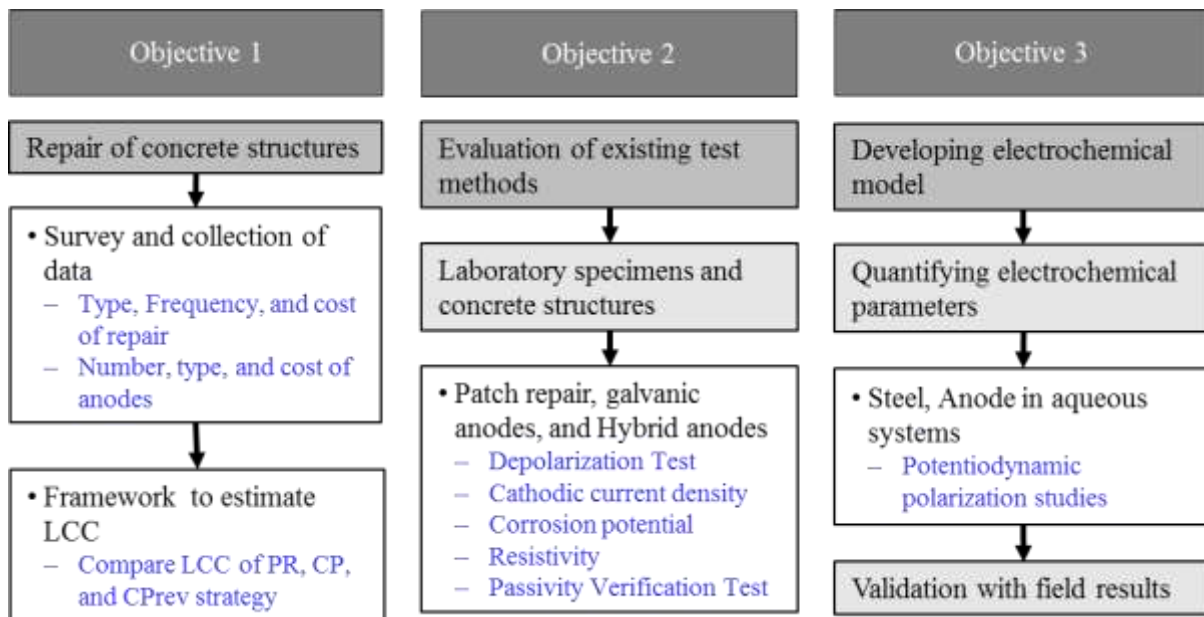
Figure 1.3: Experimental program and methodology

Then for Objective 2, the instantaneous performance of the CP system was monitored for 800 and 400 days, respectively, in a heritage building and residential apartment. The reliability of the present interpretation criteria is assessed using this observed data. Finally, for Objective 3, the concept of numerical simulation was used to develop a new electrochemical model to assess CP systems non-destructively. For this, laboratory experiments on steel and zinc-based anodes are conducted to obtain the necessary kinetic parameters. These parameters are then incorporated in an electrochemical model to estimate a concrete-steel-anode system's current and potential distribution.

1.7   ORGANIZATION OF THESIS

This thesis is organized by using a chapter-subsection format. There are six chapters (first level heading) and several subsections to discuss the identified issues highlighted in Section 1.1 (Problem statement). The outline of the chapters is as follows.

Chapter 1 (Introduction, the current chapter) introduces the problem statement of this thesis, motivation for the study, followed by research questions and formulated objectives. The scientific sectors are summarised in the research significance section, followed by the methodology used for the various studies is explained.

Chapter 2 (Review of literature) provides a literature review describing the corrosion mechanism and its thermodynamic and kinetic properties. Then, some of the test methods to assess corrosion in reinforced concrete is provided. The application of these test methods to evaluate a cathodic protection system is reviewed. Then a brief literature review on CP in concrete and its types are discussed. After that, the drawbacks in the available test methods (in literature and as European standard) to assess the CP system in concrete is critically reviewed. Finally, a brief about various available LCC models to estimate the cost of a repair strategy is provided.

Chapter 3 (Long-term performance and life cycle cost benefits of cathodic protection) presents field studies conducted on reinforced concrete structures that had undergone repair. It consists of a market study of the application of CP in India. Then, the long-term performance of CP systems on a jetty and industrial building structure are presented. After that, an LCC model is proposed to estimate the LCC of repair. Then, the comparison of cost during the 30 years after the first repair is compared. Finally, conclusions from this research are presented.

Chapter 4 (Instantaneous performance assessment of cathodic protection systems — field studies) provides the methodology of installing galvanic anodes, its performance assessment based on instantaneous tests, and a review of the present interpretation criteria of the existing test methods for assessing CP systems in reinforced concrete. First, a pilot study on the reinforced sunshades of a heritage structure built using lime mortar is provided. The details about the CP systems used, the methodology of installing galvanic anodes, and the monitored performance of the CP system based on depolarisation frequent tests are highlighted. Then,

the installation of anodes in an apartment complex is presented. Followed by that, the monitoring and interpretation results from 12 monitoring boxes are delivered. Finally, the drawbacks in adopting the existing test methodology for the modern reinforced concrete system with localized variation in resistivity are provided.

Chapter 5 (Electrochemical modelling of cathodic protection systems in reinforced concrete) contains the preliminary study of developing an electrochemical model for a non-destructive test method. The following section describes the need for electrochemical modelling in the concrete-steel-anode (C-S-A) system. Then, the background knowledge to perform modelling using numerical simulation methods is provided. Then, the experimental program conducted to obtain various corrosion kinetic parameters is provided. Finally, the results obtained from the developed electrochemical model is shown.

Chapter 6 (Conclusions and recommendations) provides the conclusions from each of the studies in the thesis. Also, the recommendation for extending the study to develop an NDT test method to assess the performance of CP in reinforced concrete structures is provided.

Appendix A shows the calculated cumulative future value of repair heads for repairing the jetty structure in Chennai.

Appendix B provides the checklist for installing galvanic anodes and a sample installation procedure — explained with photographs — from Case study I of Chapter 4. Also, the datasheet for recording various potential measurements from a CP system as per EN ISO 12696 is shown in this appendix.

Appendix C discusses the results from a pilot repair project using galvanic anodes conducted at the residential building (discussed as Case study II of Chapter 4).

Appendix D discusses the results from the parametric study conducted using the developed electrochemical model. The preliminary results of potential and current measurements on the surface of various rebars are provided in this appendix.

1.8 SUMMARY

Frist, the problem statement of this thesis is presented. Although CP using galvanic anodes is a proven technique, many galvanic anodes available fail to provide long-term protection. In addition, the limited database on its long-term performance data and the high initial cost of installation curbs their usage in many repair projects; stakeholders are hesitant. In addition, the present testing methods for assessing CP systems in concrete does not address the resistivity of modern concrete. This leads to a possibility of false-negative results when a CP system is evaluated as per EN ISO 12696. The sections on research significance emphasise the lack of reliable testing methods to assess a CP system in concrete. Then, research questions, and the formulated objectives, are summarised in the research significance section, followed by the methodology adopted is briefly explained.

This page is intentionally left blank

2   REVIEW OF LITERATURE

2.1   INTRODUCTION

This chapter presents information on the topic of cathodic protection in reinforced concrete structures mentioned in the literature. First, a general review of the corrosion mechanism is discussed. Then, the kinetics of corrosion and the brief about mixed potential theory are discussed. Then, the existing test methods to assess corrosion are provided. Then a short review of the evolution of cathodic protection systems in reinforced concrete is provided with relevant literature. Then, insight on the existing test methods for assessing the performance of CP systems is provided. After that, the key findings from the literature that discusses the long-term performance of CP systems are provided. Finally, a literature review that reported the benefits of using a CP system considering the life cycle cost is provided.

2.2   CORROSION OF STEEL IN REINFORCED CONCRETE STRUCTURES

2.2.1   Thermodynamics of corrosion

Reinforced concrete (RC) is one of the most successful construction materials invented by humans (Chess and Broomfield 2013). The versatility and ability of moulding reinforced concrete to any shape and size make it the second most used item on earth. However, there are a few factors that can deteriorate a reinforced concrete structure. As iron ore is processed as the reinforcing element, corrosion is one significant deterioration mechanism in RC systems (Popov 2015; Tait 2018).

Steel reinforcement is subjected to corrosion in reinforced concrete when there is an electro-physical interaction between iron, water, and oxygen (Ahmad 2003; Böhni 2005). This involves the flow of electrons through the metals and the transport of ions through concrete (electrolyte). The metal region that loses electrons is called the anodes, and the area where the

electrons are consumed to produce corrosion products is called the cathode. The corrosion

process in concrete can be represented using two equations, Eq. (2.1) and Eq. (2.2). First, the

steel rebar loses two electrons when it is in contact with oxygen and moisture to return to its

thermodynamically stable state. The ferrous ions (Fe^{2+}) migrate through the interconnected

pores in the concrete and reach the cathodic site. Here they react with the freely available

hydroxyl ions to form iron hydroxide and is called the first corrosion product (Abd El Haleem

et al. 2010; Glass et al. 2000). This reaction is shown in Eq. (2.3).

$$Fe \rightarrow Fe^{2+} + 2e^- \text{ (Anodic reaction)} \tag{2.1}$$

$$\tfrac{1}{2} O_2 + H_2O + 2e^- \rightarrow 2OH^- \text{ (Cathodic reaction)} \tag{2.2}$$

$$Fe^{2+} + 2OH^- \rightarrow FeOH \tag{2.3}$$
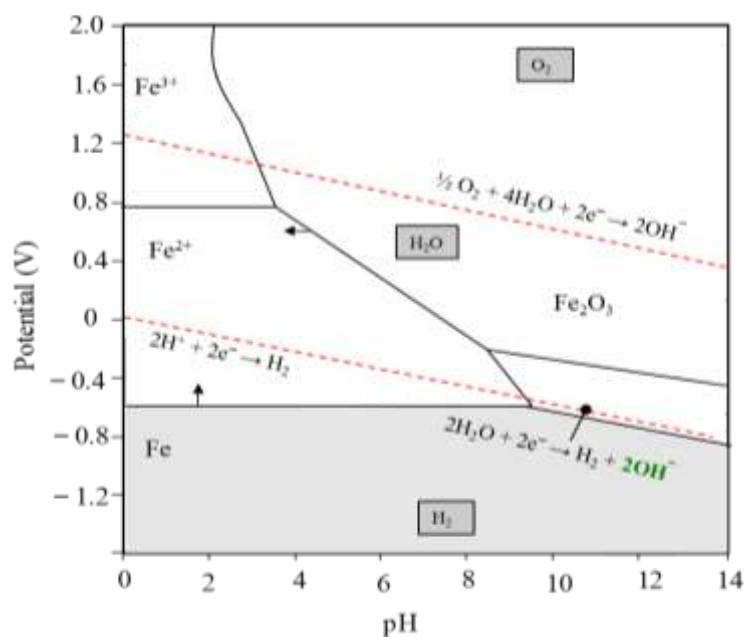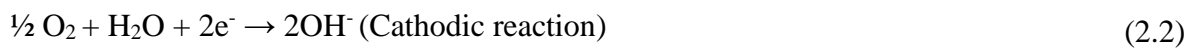
Figure 2.1: Pourbaix diagram of iron corrosion in acqueous media (Pourbaix 1974)

This product reacts with oxygen to form various other corrosion products having higher

volumes than the steel rebars. Thus, these corrosion products exert tensile stress on the adjacent

concrete and eventually crack the cover concrete. The tendency to lose an electron from the steel depends on its thermodynamics properties (Goyal et al. 2018). Figure 2.1 shows the possible corrosion products of iron (Fe) that can develop at various combinations of potential and pH. This graph that shows the relationship between potential and pH is called the Pourbaix diagram (Pourbaix 1974; Poursaee 2016).

2.2.2   Electrode kinetics

The corrosion capability of a metal depends on its thermodynamic properties. However, the rate of corrosion depends on the kinetic properties of the metal. This, in turn, depends on the amount of polarization or the overpotential applied to the system. Generally, the total overpotential comprises three different types of potentials — (i) activation overpotential (η_{act}), (ii) concentration overpotential (η_{act}), and (iii) the ohmic drop (iR). These three potentials are additive, and the total overpotential (η) can be expressed as Eq. (2.4).

$$\eta = \eta_{act} + \eta_{conc} + iR \tag{2.4}$$

Figure 2.2 shows the typical potential versus the current response of steel in concrete during corrosion. The curves (in Figure 2.2) represents an activation polarization condition of the metal because of its corrosive environment. The red line indicates the behaviour of the anodic reaction, while the cathodic response is shown in the blue line. The anodic and cathodic curves can be extrapolated to meet at a common point to obtain the mixed potential of the system (Roberge 2008). In concentration polarization conditions, the cathodic reaction inculcates both the hydrogen evolution and the oxygen reduction reaction. The ordinate axis at the intersecting point of these two curves is the equilibrium potential (E_{corr}) of the metal in the given electrolyte, and the corresponding x-axis intercept is the exchange current density (i_0) (Fontana and Greene 2018; Roberge 2008).

During an activation polarization condition, the rate at which these reactions progress depends on the exchange current density of each electrode (shown as i_o in Figure 2.2). The exchange current density of an electrode refers to the reaction rate at the reversible potential; the overpotential at this time is zero (Ge and Isgor 2007; Pour-Ghaz et al. 2009). This can be experimentally obtained by conducting a potentiodynamic polarization test. The slope of the anodic and cathodic curves is the Tafel slopes, denoted as β_a, and β_c, respectively. However, when the reaction rate is limited diffusion in the solution, it results in concentration polarization.

Typically, in a highly alkaline medium such as concrete, the diffusion rate of oxygen influences the cathodic reaction, and oxygen reduction becomes a possible second cathodic reaction. The rate at which this reaction occurs is called the limiting current density of oxygen (i_{lim}).
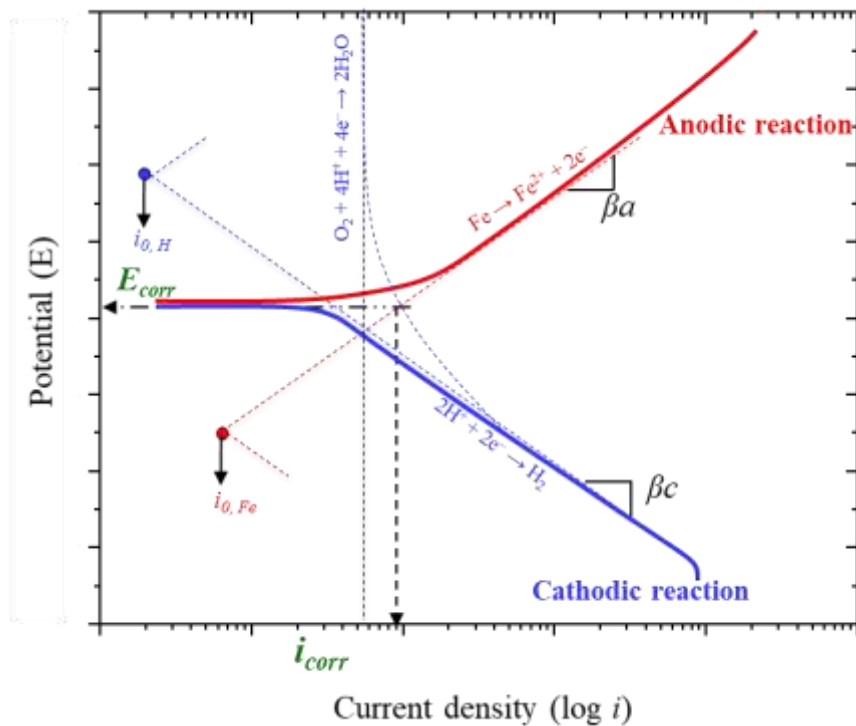
Figure 2.2: Evans diagram showing the polarisation behaviour of steel in a concrete

2.3 CORROSION ASSESSMENT OF STEEL IN CONCRETE

Once corrosion is initiated, it is necessary to understand the regions exhibiting corrosion and the corrosion rate to calculate the residual service life. The following section describes the field and laboratory assessment method to detect corrosion /obtain the corrosion rate.

2.3.1 Open circuit potential

Open circuit potential or the Half-cell potential (HCP) method is one of the most widely adopted corrosion assessment technique for reinforced concrete structures (Elsener 2002; Elsener et al. 2003a). The test measures the corrosion potential of steel rebars by using a reference electrode whose potential at equilibrium is known (Zaki et al. 2015). The probability of corrosion of rebars is interpreted based on ASTM C876 2015, using the measured corrosion potential. Usually, this potential can be measured using a multimeter of 0.001 mV resolution and a reference electrode (Song and Saraswathy 2007). Typically, in concrete, three reference electrodes are used — saturated copper/copper sulphate (CSE), saturated calomel electrode (SCE), and silver/silver chloride reference electrode, KCL (SSCE). CSE has a potential of + 0.318 V with respect to a standard hydrogen electrode (SHE), while SCE and SSCE is + 0.241 V and + 0.199 V, respectively, with respect to SHE (Elsener et al. 2003a).

2.3.2 Corrosion rate

The ingress of chloride or other deleterious species into concrete can lead to the breakdown of the passive film — results in corrosion initiation. Corrosion rate refers to the rate at which the corrosion of a metal system in electrolyte propagates. This is usually expressed in mills (one thousand of an inch) per year (MPY) or A/m^2 or $\mu A/cm^2$. In concrete, if the steel corrosion rate is less than 0.1 $\mu A/cm^2$, then the corrosion level is considered negligible. While a corrosion rate greater than 0.5 $\mu A/cm^2$ could be fatal, and the structure requires immediate attention to

arrest corrosion (Andrade et al. 2007; Andrade and Alonso 2004; Angst et al. 2009). Corrosion rate can be measured in many ways, such as through linear polarization resistance (LPR) measurement, electrochemical impedance spectroscopy (EIS), potentiodynamic polarization (PDS) — each being one step accurate than the previous one. Some of them are discussed in detail in the subsequent sections.

2.4 TEST METHODS/TECHNIQUES TO DETERMINE CORROSION RATE

2.4.1 Linear polarization resistance (LPR)

ASTM standards such as the G59 and G96 describes the standard test procedures for conducting polarisation resistance measurements (ASTM G59 2014; ASTM G96 2009). The working electrode is polarised cathodically and anodically in the LPR technique by supplying a known current quantity and correspondingly measuring its potential. Usually, the amplitude of this applied overpotential potential ranges from 5 to 10 mV (Rengaraju et al. 2019). The slope of the resulting curve gives the polarization resistance of the rebar, and the corrosion rate (i_{corr}) can be obtained using Eq. (2.5),

$$i_{corr.} = \left(\frac{\Delta i_{app}}{2.3\Delta E}\right)\left(\frac{\beta_a\beta_c}{(\beta_a+\beta_c)}\right) \tag{2.5}$$

where, ΔE is the applied overpotential, i_{app} is the applied current density, and β_a and β_c are the Tafel slopes.

The LPR technique assumes that the change in potential from the equilibrium potential is linear over a small range ($\pm\, 5 - 10$ mV). Thus, we can eliminate the nonlinear component in Eq. (2.5), and simply the corrosion rate (i_{corr}) can be expressed in terms of a parameter called the polarization resistance (R_p), represented by Eq. (2.6) (Fontana 1987). The constant value (B) in the equation is called the Stern-Geary constant. This is also known as the Stern-

Geary equation. Typically, these values are considered 120 mV for steel in concrete (Andrade et al. 2007). Thus, by using a small perturbation in the potential and measuring the corresponding current change, we can obtain the polarization curve for the material.

$$i_{corr.} = \frac{B}{Rp} \qquad (2.6)$$

However, there are some errors in assuming this equation and using LPR techniques. A more common argument against using the LPR technique is the incapability of the test to account for the solution resistance. Also, the capacitive current, which develops because of the increase in the scan rate, is not given consideration. This could result in erroneous values.

2.4.2 Electrochemical impedance spectroscopy (EIS)

The EIS techniques try to solve the drawbacks of the LPR technique. The technique is similar to the LPR technique as EIS also relies on perturbation to the system. In the actual case, the perturbation from the equilibrium potential exhibits much more complex behaviour. Therefore, the simple concept of using the linearized method cannot result in accurate measurements. An alternating amplitude potential (in the range ±10 mV) is used for perturbating the working electrode at different frequencies. The impedance data is used to analyze the corrosion rate of the reaction. The frequency-dependent impedance $Z(\omega)$ (is determined by the relation shown in Eq (2.7).

$$Z(\omega) = V(\omega)/i(\omega) \qquad (2.7)$$

where, $V(\omega)$ and $i(\omega)$ are the applied potential and the current as a function of ω.

Obtaining the frequency dependence of impedance for a corroding system can help determine an appropriate equivalent electrical circuit consisting of various components like resistors, capacitors, inductors, etc. Thus, the resistance of each material component can be

obtained individually. The magnitude of the current response can be used to extract information on the corrosion rate of the working electrode. Also, the corrosion behaviour of the metals can be understood by separating the components corresponding to mass transfer-controlled movements.

2.4.3 Potentiodynamic scan (PDS) test

This test is used to understand the polarization behaviour of an electrode in the electrolyte system. Unlike the LPR test, a potentiodynamic scan (PDS) test involves varying the electrode's potential over a relatively large potential ($\pm$ 50 mV) at a selected rate by applying an external current (Bertolini et al. 1996; Moreno et al. 2004; Poursaee 2016). First, the potential of the steel is polarised to the far end of the required cathodic polarisation. Then, the potential is decreased in steps following the scan rate to reach the final polarisation value. The necessary kinetic parameters characterising an anodic and cathodic reaction can be obtained using this test method. These include exchange current density, corrosion potential, Tafel slopes, and the limiting oxygen current density of the cathodic reaction. A typical result from a PDS test is shown in Figure 2.2.

2.4.4 Cyclic potentiodynamic polarisation method

This test method is an extension of the PDS test. This test method is usually used in reinforced concrete to study the steel rebars' chloride threshold and pitting corrosion potential (E_{pit}). In this method, the cyclic-potentiodynamic polarisation measurements are conducted to obtain the relative susceptibility of the metal to localized corrosion. During this test, the potential at which the anodic current increases significantly with the applied overpotential and the potential at which the hysteresis loop is completed during a reverse polarisation scan are measured and is called the protection potential (E_{prot}) (Ormellese et al. 2009; Poursaee 2010). The result can be interpreted such that the material exhibiting a more positive E_{prot} value is less likely to have

localized pitting corrosion. However, the methods have some drawbacks. The experimental values of the breakdown potential are vary depending on the time required to induce pitting corrosion. Also, allowing the potential to exceed beyond the pitting potential can lead to a localized change in the chemistry of the pits.

2.4.5   Potentiostatic method

The drawbacks of potentiodynamic tests are addressed in potentiostatic test methods. Here potential is measured against the time, keeping the current as a constant value. The potential measurements are taken until the change in the potential with time reaches a value equal to 0. Then the forward and the reverse potential-current density plot are extrapolated to the point where zero current density. From this, we can obtain the breakdown potential as well as the E_{prot}. ASTM G100 standard describes the methods for conducting cyclic potentiostatic polarization methods (ASTM G100 2009).

2.5   DETERIORATION MECHANISMS OF PATCH REPAIRS

Patch repairing is the most widely adopted practice in the repair industry to preserve a corroded structure. During a patch repair, the chloride-contaminated concrete in the region experiencing corrosion is removed and the exposed steel rebars are cleaned to remove any loose corrosion products. Then, fresh chloride-free concrete is placed to prevent further exposure of steel rebars to the atmosphere or other deleterious substances. However, though this practice prevents steel corrosion underneath the patch, it has been reported that the region adjacent to the patch experience accelerated corrosion (Chess and Broomfield 2013; Costa 2010; Dugarte and Sagüés 2014; Sergi and Page 2000; Whitmore and Abbott 2003). Figure 2.3 shows this mechanism of corrosion during a patch repair.

After removing the chloride contaminated concrete, the rebar in the patch – that was previously active – becomes passive by shifting the corrosion potential to a more positive value

(say, −200 mV CSE). This stops the corrosion of the rebars in the patch. However, the rebars in the adjacent region continue to corrode with a more negative potential (say, –350 mV CSE). Subsequently, formation of incipient anodes in adjacent regions occurs due to the variation in corrosion potential of the rebar in the new and old concrete. This phenomenon is referred to as the halo effect or ring effect in the literature. Raupach, in 2013, measured the distribution of electric current from the rebars in patch repaired RC specimens (Raupach 2006). It was observed that the electric current from the rebars near the patch repaired area increased significantly in the anodic region that was acting as a cathode before the repair. The studies by Dugarte and Sagues in 2014 suggest adequate electrochemical treatment to address the halo effect during the repair of a reinforced concrete structure (Dugarte and Sagüés 2009).
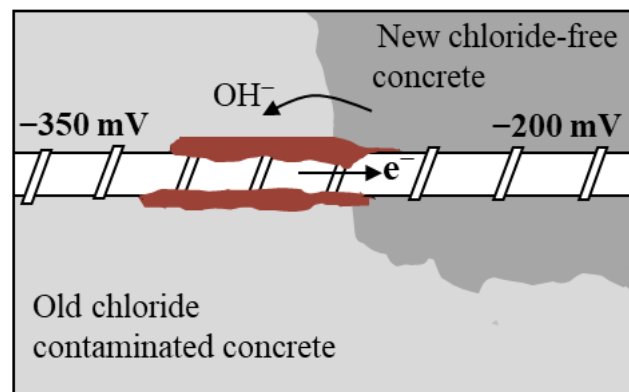
Figure 2.3: Patch repair leads to corrosion in adjacent regions due to the halo effect (Adapted from Krishnan et al. (2021))

2.6 ELECTROCHEMICAL REPAIR TREATMENT

There are many methods to protect the steel rebars from corrosion in reinforced concrete structures. Conventional methods include using corrosion inhibitors during concrete casting, applying coatings such as the fusion bonded epoxy coating, cement polymer composite coating, galvanised zinc coating, or using stainless steel rebars (Joseline et al. 2019b; Kamde and Pillai

24

2020a; b). These methods can be used to protect a structure that is about to construct. Nevertheless, the application of these methods during repair is limited. In such cases, electrochemical techniques have to be implemented as a protective treatment for reinforcement rebars to arrest corrosion during the repair of a concrete structure.

Cathodic protection, electrochemical re-alkalization, and electrochemical chloride extraction are common electrochemical repair strategies used in the repair industry (Bertolini et al. 2008; Chess and Broomfield 2003; González et al. 2011; Ihekwaba et al. 1996; Orellan et al. 2004; Pedeferri 1996). Electrochemical re-alkalization and electrochemical chloride extraction are temporary treatments given to the concrete in which a very high current is supplied to increase the alkalinity around the rebars or remove the chloride ions from the concrete (Bertolini et al. 2008). CP systems are permanently installed in concrete, can positively arrest ongoing corrosion, and have been widely used in RC structures for more than two decades. As the focus of this thesis is CP, the following section describes the principle and type of cathodic protection systems in concrete.

2.6.1 Cathodic protection in reinforced concrete

The basic principle of CP is to force the steel rebars to be protected by becoming the cathode of a galvanic cell when it supplies additional electrons (Berkeley and Pathmanaban 1990; Chess and Broomfield 2003; Pourbaix 1974; Stratfull 1974). The current supplied to the steel by an external source prevents the current flow from the metal, thus preventing ions' discharge to the electrolyte (Popov 2015). Kinetically this can be described using Figure 2.4. It can be observed that the green line represents the anodic and cathodic behaviour of the steel in concrete, whereas the red line indicates the reactions of more electronegative metal, i.e., zinc. When they are electrically connected, the mixed potential of the system shifts by the amount of applied

25

polarisation shift (ΔE) to $E_{corr, Fe/Zn}$, and the corresponding corrosion rate of the steel rebar reduce to $i_{Fe(Fe/Zn)}$. This means that the corrosion rate of the steel can be decreased by polarising the steel to its cathodic direction.
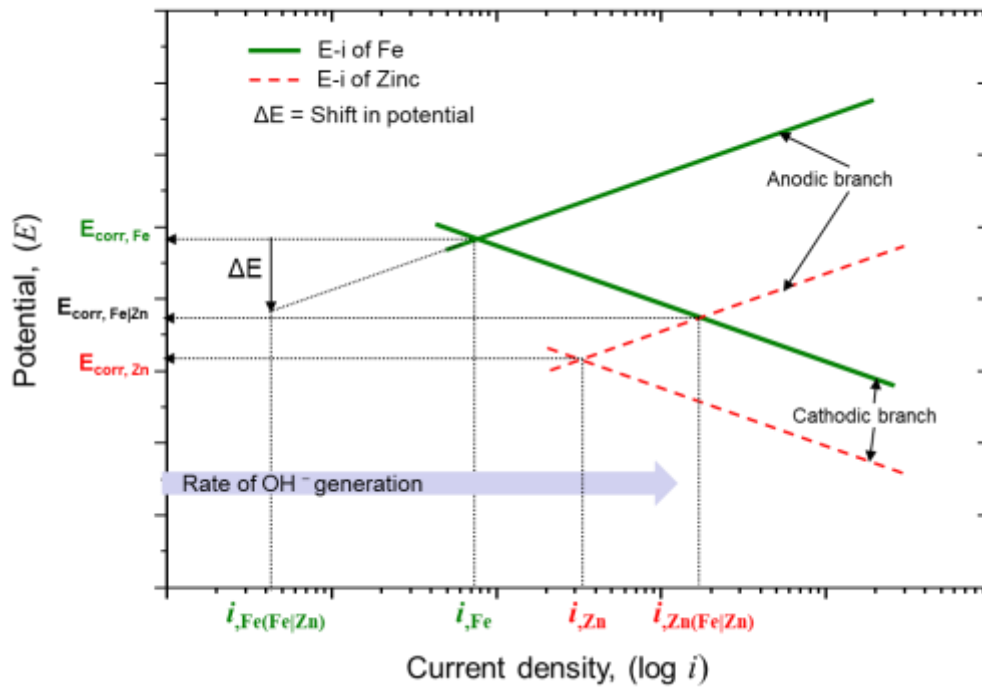
Figure 2.4: Change in mixed potential due to the application of CP

Ideally, the steel must be polarised to a potential less than the immunity potential (no reversible reaction at this potential). However, in concrete, the development of hydroxyl ions (OH$^-$) at the cathodic interface increase the alkalinity near the cathodic surface and reduce the chloride ion content at the level of steel (Angst 2019; Davison et al. 2003; Pedeferri 1996). Figure 2.5 shows the behaviour of steel in concrete when a known overpotential polarises it. In atmospherically exposed concrete with steel rebars, a protection current to modify the micro-environment at the steel-concrete interface to inhibit pitting corrosion is sufficient (Pedeferri 1996). The presence of the additional cathodic reaction increases the formation rate of hydroxyl (OH$^-$) ions near the rebar surface (see Figure 2.5) – leading to the re-passivation of

rebars in concrete. In addition, the negative chloride or sulphate ions are repelled from the negatively charged steel rebars (Bertolini et al. 2009; Pedeferri 1996).
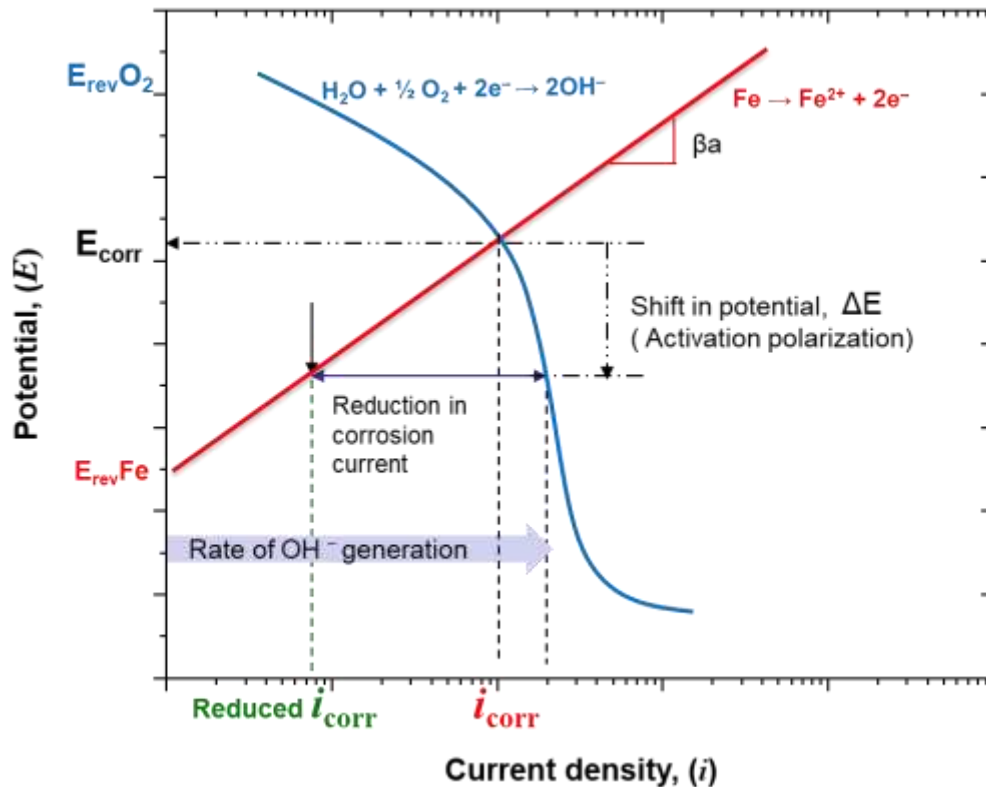
Figure 2.5: Principle of cathodic protection shown with the help of Evans diagram

In India, the application of CP in concrete started in the early 2000s (Krishnan et al. 2019). Usually, galvanic anodes contain metal with a reduction potential more negative than steel rebars (mostly zinc alloy) embedded in a highly alkaline mortar disk (pH > 14). The alkaline mortar ensures the continued corrosion of the zinc metal in a galvanic anode. When installed in a concrete patch, Galvanic anodes supply a permanent current to the steel system that prevents the formation of the corrosion cell. When a metal of higher corrosion potential (say –1100 mV_{CSE}) than steel is installed in reinforced concrete, the metal acts as a positively charged electrode and becomes the anode of the galvanic cell (see Figure 2.6). Correspondingly, the steel rebars become the negatively charged electrode and become the

cathode of the galvanic cell. This suppresses the escape of ferrous ions (Fe^{2+}) from the steel

rebars and prevents the formation of any corrosion cell at the interface of the new and existing

concrete.
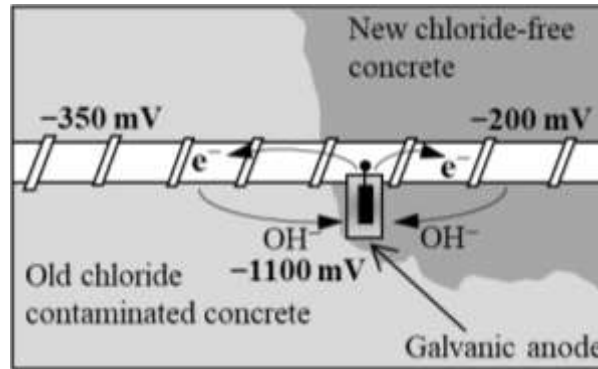
Figure 2.6: Prevention of halo effect – when CP is used

Typically, in concrete, CP is implemented by installing an anodic metal inside or on the

surface of the concrete and electrically connecting it to the rebars to achieve a continuous

supply of a small current (1 to 200 mA/m^2) with or without using a rectifier unit (Highways

Agency 2002). Then, the steel rebar becomes the cathode, and the electrically connected

sacrificing metal becomes the anode.

If CP is implemented during the construction of the structure, the applied current

density for protection can be in the range of 0.2 to 2 $mA/m^{2,}$ and the technique is termed

cathodic prevention and denoted as CPrev, herein (ISO 12696 2016). Because of less

maintenance, monitoring, ease of installation, and protection against vandalism, the use of

galvanic anodes for the electrochemical repair of the RC systems is gaining acceptance in the

last two decades (Christodoulou et al. 2013; Sergi 2011; Sergi and Page 2000). The technique

involves applying a permanent current through galvanic anodes in the range of 0.2 to 20 mA/m^2

to the steel rebars (Christodoulou et al. 2013; Wilson et al. 2013a). Zinc is a widely used

galvanic metal because of its high oxidation potential against steel (Sandron et al. 2005). The

corrosivity of the zinc metal is ensured by embedding it in a high pH (13 to 14.5) or halide-activated environment (Genescà Ferrer and Juárez 2000; De Rincón et al. 2018; Schwarz et al. 2016). In the case of alkali-activated zinc anodes, zinc anodes can get passivated if the pH of the embedding mortar is in the range of 12 to 9 (Whitmore and Abbott 2003). Then, zinc oxides start accumulating in the mortar pores, hindering the ion transport from the zinc to the steel (Christodoulou et al. 2014a; Dugarte and Sagüés 2009). Therefore, a frequent inspection needs to be conducted on the installed CP system to ensure these galvanic anodes' continuous functioning until the desired service life of anodes (say, 20 to 25 years).

2.6.2 Types of cathodic protection/prevention in concrete

CP can be implemented in concrete either using a galvanic anode cathodic protection system or through impressed current cathodic protection (ICCP) system. The following section describes the various types of CP systems in detail.

2.6.2.1 Impressed current cathodic protection (ICCP) system

In the impressed current cathodic protection system (ICCP), a large surcharge of current (20 to 100 mA/m^2) is supplied to the steel to polarise the steel rebars towards the cathodic region (Lambert and Atkins 2005). ICCP can control corrosion at any level because of its ability to control the output current from the system (Kean and Davies 1981; Wilson et al. 2013b). However, long-term exposure of steel to high currents can lead to the risk of hydrogen-induced cracking (SP0290 2007; Yehia and Host 2010). The installation of ICCP is expensive as it requires complex design strategies and constant monitoring throughout the service life of the anode. In addition, in many cases, the installed monitoring boxes and rectifier units were found to be destroyed due to vandalism (Vukcevic 2010). The cathodic polarization due to the impressed current shifts the steel potential towards a more positive value, and corrosion does not initiate immediately after the discontinuation of the impressed current (Broomfield and

Tinnea 1993; Presuel-Moreno et al. 2005). However, it is to be noted that there is no guarantee that the steel rebars will remain in a passive state once the current supply to the steel is discontinued. Therefore, there is a need to install a CP system that can supply the current to passivate the steel as early as possible and maintain the steel passivity for a long-term (say, 30 years) with minimal maintenance requirements. This can be achieved using hybrid anodes that combine the advantages of both the ICCP system and the galvanic system.

2.6.2.2   Galvanic anode cathodic protection system

In a galvanic anode CP system, a lower amount of current is supplied to the steel using a sacrificial anode metal that is electrochemically more active compared to the steel. Installing galvanic anodes in concrete is easy and requires minimal monitoring throughout its service life. Also, lower installation cost and the negligible chance of vandalism makes galvanic anodes widely popular in the concrete repair industry. Galvanic anodes supply current based on the cathodic current density demand of the steel. Figure 2.7 shows the schematic representation explaining the working mechanism of galvanic anodes in concrete.
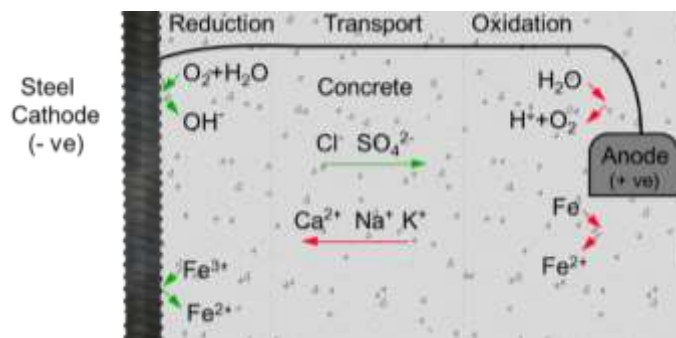
Figure 2.7: Working mechanism of galvanic anode CP system in concrete

Galvanic anodes can supply the current density required to prevent corrosion when the steel is in a passive state. This is the case of new construction when the galvanic anodes are

used as a cathodic prevention method. In such cases, a constant current density of $0.2 - 2$ mA/m^2 is required to maintain the passivity of the steel (Bertolini and Redaelli 2009; ISO 12696 2016). The desired current density or the anodic charge supply can be achieved by varying the number and spacing of the anodes. The long-term efficiency of galvanic anodes in controlling the corrosion has been proven previously by many research works by the monitored results from various structures (Christodoulou et al. 2014b; Hans Van Den Hondel et al. 2018; Krishnan et al. 2019; Pistolesi and Zaffaroni 2018; Polder and Peelen 2018; Sergi 2011). The galvanic anodes are self-regulating in nature and supply output current based on the corrosion rate of the steel rebars. Therefore, galvanic anodes take a longer time to passivate the steel as the current density supplied by the anodes is first used to arrest the corrosion and then to passivate the steel (Whitmore et al. 2019). **This thesis focuses on galvanic anode CP systems and is denoted hereafter as 'CP systems'.**

2.6.3 Two-stage hybrid anodes

Two-stage hybrid anodes combine the advantages of both impressed current cathodic protection systems and galvanic anode cathodic protection systems. Hybrid anodes contain an integrated self-powered ICCP anode and an alkali-activated galvanic anode (zinc metal). Figure 2.8(a) shows a photograph of a two-stage hybrid galvanic anode. Figure 2.8 (b) shows a schematic of the different components in two-stage hybrid anodes. Hybrid anodes do not require any external D.C. power source as they are self-powered. The protection process is categorised into two stages:

- Stage 1 - the application of a high current to make the steel passive, and
- Stage 2 - the supply of the current by the residual galvanic anodes to maintain passivity.

    Figure 2.9 shows a schematic of the working of a two-stage process. Active corrosion in the reinforcing steel rebars occurs because of the ingress of chlorides or due to carbonation

(Figure 2.9(a)). When hybrid anodes are installed and connected to the steel rebars, the integrated self-powered ICCP unit activates and provides a high current in the range of 20 to 40 mA/m^2 to the steel. This is considered as the Stage 1 process (Figure 2.9(b)). The high current supply during the Stage 1 can lower the corrosion potential of the steel to values equal to or lower than the equilibrium potential of steel in a short time and also increase the rate of the cathodic process (usually oxygen reduction and hydrogen evolution) near the steel surface. The high negative polarity of the steel tends to drive the negative ions in the direction opposite to the current. Therefore, in chloride contaminated concrete, the chloride ions near the steel rebars are repelled away. The increased rate of the cathodic process increases the production of hydroxyl (OH$^-$) ions near the rebars, increasing the pH around the steel surface. Once the integrated ICCP system stops supplying the current, the galvanic anode gets activated and starts providing the current in the range of 0.2 to 2 mA/m^2 – the required current for cathodic prevention. This is considered as the Stage 2 process (Figure 2.9(c)). However, the repulsion of negative ions and the formation of hydroxyl ions continue.
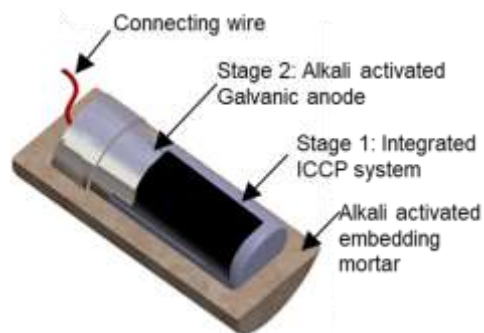
(a) Photograph (b) Schematic representation showing integrated ICCP and galvanic system (courtesy Vector Corrosion Technologies)

Figure 2.8: Two-stage hybrid anodes (Adapted from Krishnan et al. 2020)

| (a) Active corrosion of steel rebars due to chloride ingress or due to carbonation. | (b) Stage 1: Passivation of steel by the integrated ICCP due to the formation of OH- ions around steel (increase in pH). Also, repulsion of negatively charged chloride ions. | (c) Stage 2: Maintaining passivation by the active galvanic anode with continued current supply. Continuous repulsion of chloride ions. |
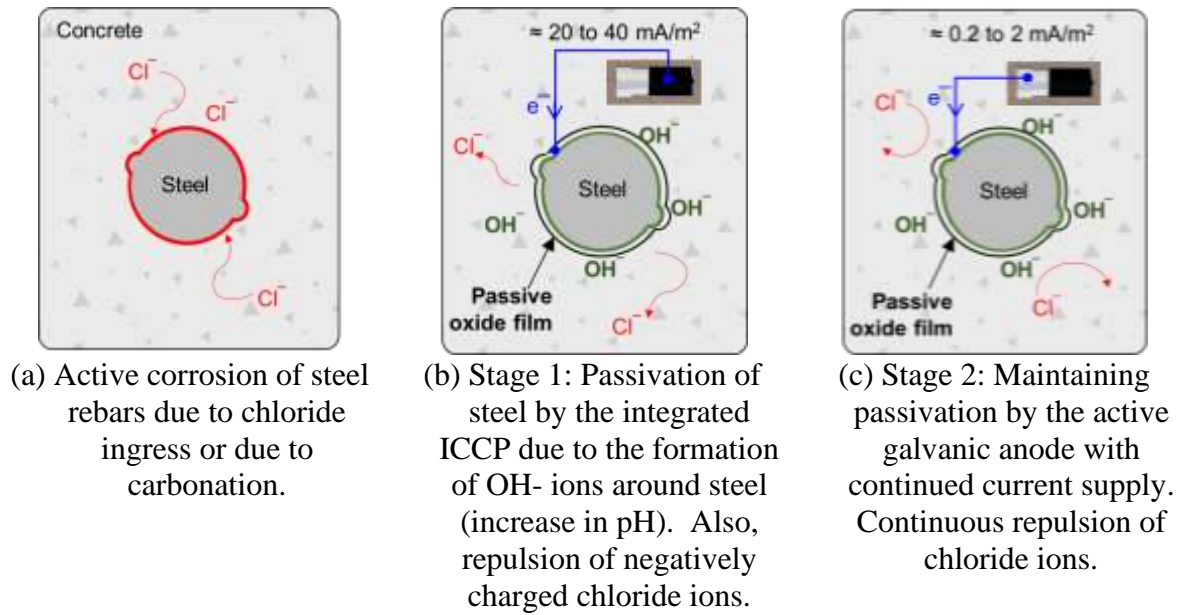
Figure 2.9: Schematic of the working of the two-stage hybrid anodes (Adapted from Krishnan et al. 2020)

One of the main advantages of a two-stage anode is that it can be easily implemented in areas where a full-fledged ICCP system is complex. These systems eliminate the requirement of external power supply and additional electrical equipment and can be connected discretely to the steel rebars like the galvanic anodes (Dodds et al. 2018b; Rathod et al. 2018; Whitmore et al. 2019). Previous studies on cathodic protection of steel rebars in various concentration of chloride-containing mortars has reported that a mean supply of $60\,\text{mA/m}^2$ can control the ongoing corrosion and re-passivate the steel (Rathod et al. 2018). This was achieved without any physical crack or delamination on the mortar specimens. A few other studies reported that a charge in the order of $50\,\text{kC/m}^2$ of steel surface area is sufficient for passivation (Dodds et al. 2018a; Holmes et al. 2013; Polder et al. 2011). However, the exact amount of charge varies depending on the bulk resistivity of concrete, level of corrosion, chloride contamination etc. In another study, the monitored output current density delivered by nine hybrid anodes installed in a concrete slab was in the range of 20 to $35\,\text{mA/m}^2$ for the first 45 days (see Figure 2.10)

(Whitmore et al. 2019). After 45 days, the output current density decreased to a range of 0.2 to 2 mA/m^2 – indicating discontinuation of ICCP current and activation of galvanic anodes. This is in adherence to the current requirement criteria for cathodic prevention as stipulated in BS EN ISO 12696:2016 (ISO 12696 2016).
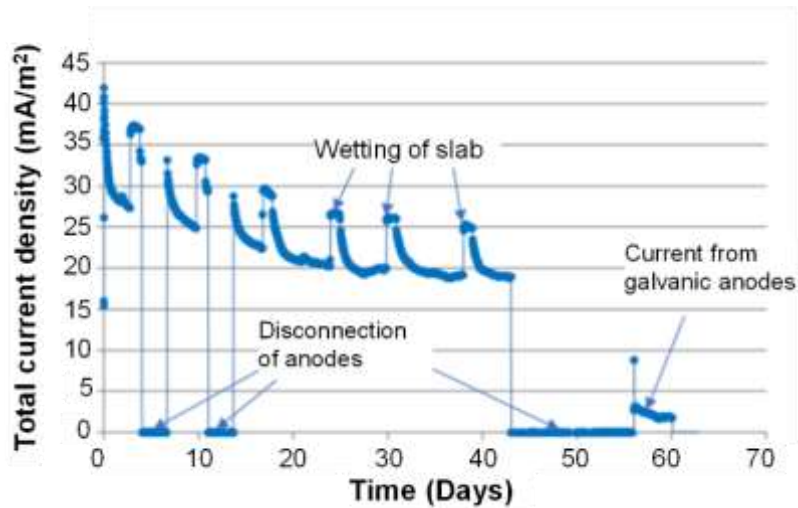
Figure 2.10: Variation in output current density from nine fusion anodes
(Whitmore et al. 2019)

Previous studies on hybrid anodes suggest that, once the steel has become passivated, a smaller current of 0.2 to 2 mA/m^2 would be sufficient to keep the steel in the passive state throughout the service life of the galvanic anode in Stage 2 (Bertolini and Redaelli 2009; Rathod et al. 2008). However, at present, there is limited field data available to validate the passivation ability of the hybrid anodes in a short time.

2.7 ASSESSMENT OF CATHODIC PROTECTION SYSTEMS

2.7.1 Depolarisation tests

EN ISO 12696 (2016) and NACE SP0290 (2007)(ISO 12696 2016; NACE SP0290 2007) are used for assessing the performance of CP in RC structures. The test methods suggested in these standards mandate external electrical connections from the anodes to the steel through a monitoring box with a resistor and switch assembly. One of the most widely adopted assessment criteria for CP in concrete is verifying a 100 mV shift in the potential of steel rebar by the influence of the galvanic anodes in 24 hours (Barlo 2001; Ewing 1940). Figure 2.11 shows the sequence of potential measurements to be obtained to conduct the depolarisation test. The $E_{i\text{-}Off}$ is the potential of the polarised steel within 0.1 seconds after disconnecting the anode (ISO 12696 2016). The E_{24h} of the steel is the potential measured after 24 hours from the time of disconnecting the steel from the anode. The potential shift is obtained by calculating the difference between the instantaneous-off potential ($E_{i\text{-}Off}$) and the 24-hour depolarised potential of the steel rebars (E_{24h}). Engineers arrived at the '100 mV shift criteria' through experimental studies on the corroding pipes buried in soil (Barlo 2001; Ewing 1940; Gummow and Eng 2007; NACE SP0408 2014). However, in RC systems, the polarisation shift depends on environmental conditions such as atmospheric temperature, relative humidity inside the concrete, steel corrosion rate, and chloride contamination level (Muehlenkamp et al. 2005). Also, after the installation of CP and once the steel is protected/passivated, the use of the 100 mV criteria is not appropriate for in-situ assessment because the steel being protected at that stage may not necessarily shift its potential by 100 mV if disconnected from the anode (Helm and Raupach 2019; Rathod et al. 2019). This is because the potential shift demand or current demand for protection is less at that stage.
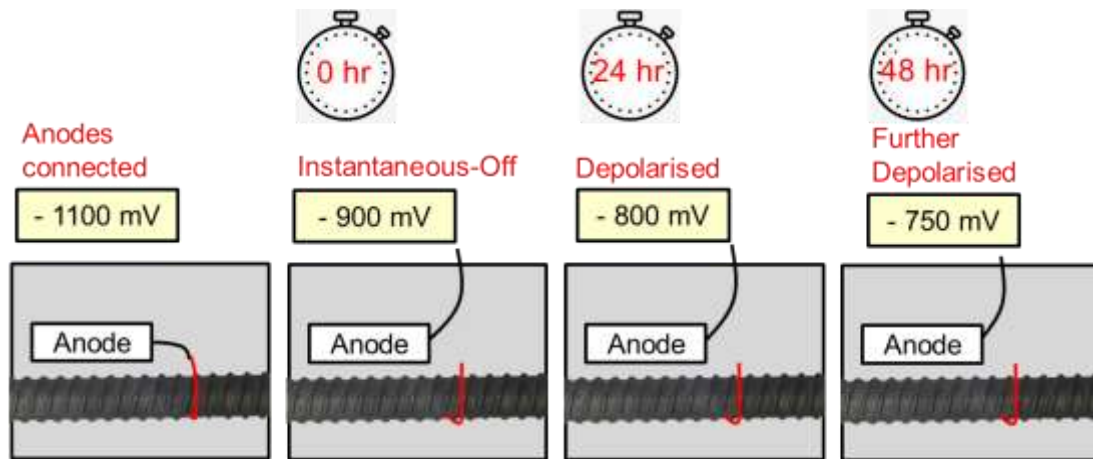
Figure 2.11: Schematic representation of various potential measurements

In short, no conclusive empirical justification is reported to adopt '100 mV shift criteria' for continuous assessment of CP in RC systems (Bennett and Mitchell 1990). An alternative approach to assess CP systems is disconnecting the system for 24 hours and checking the depolarised potential, which is essentially the half-cell potential (HCP) of the steel disconnected from the anode. These HCP values can be compared with protected/passive rebars on the same structure, and the active/passive states can be defined.

2.7.2 Passivity verification test (PVT) method

Linear polarization resistance (LPR) and electrochemical impedance spectroscopy (EIS) techniques have been used to assess the performance of CP systems in concrete. (Martínez and Andrade 2008) developed a test method that can be performed at any time to assess the instantaneous performance of embedded galvanic anodes without disconnecting them from the steel rebar system, called the passivity verification test (PVT) method. Impedance spectra show changes in its shape and associated parameters when the steel is protected or unprotected. Cathodically polarized steel exhibit a reduction in maximum phase angle value compared to unprotected steel at higher frequencies. The efficiency of the CP system is measured in terms of percentage of protection depending on the formation of a semi-circular impedance spectra

in the frequency range of 0.1 to 0.001 Hz. Based on the obtained phase angle value, the technique interprets the results as "Well protected", "Moderately protect" or "Not-protected". This technique was developed based on studies on one type of low resistivity concrete. Further research to rationalize this technique based on the underlying science and to enable its applications to various anode-concrete systems is not reported.

2.7.3 Numerical modelling methods

Attempts were made to model the CP system in steel-concrete systems using finite element methods (Bertolini and Redaelli 2009; Bruns and Raupach 2010; Goyal et al. 2019), finite difference methods, and boundary element methods (Muharemovic et al. 2008). These models predicted the corrosion rate of CP systems and interpreted the results to assess the adequacy and the functionality of the installed anodes. The Butler Volmer formula and measurements on polarization induced by a known applied current density were used to evaluate the corrosion rate. However, the available database on the time-dependent polarization behaviour of reinforcement steel is very limited to assess all long effects for similar geometric specimens (Helm and Raupach 2016). The correlations between the numerical models and electrical responses from a C-S-A system mimicking various site conditions, especially when the resistivity of concrete changes, are not well-developed for enabling quality assessment of CP systems in concrete structures.

2.8 LONG-TERM PERFORMANCE OF C-S-A SYSTEMS

Much literature is available to validate the short-term working of galvanic anodes for RC systems through laboratory studies (Bennett and McCord 2006; Bertolini et al. 2002; Bertolini and Redaelli 2009; Dugarte and Sagüés 2009; Presuel-Moreno et al. 2003). Also, consistent performance (for 4 years) of submerged anodes exhibited a 100 mV potential shift in RC column specimens (Bertolini et al. 2002; Bertolini and Redaelli 2009). Another study

suggested that the galvanic anodes can supply a current of ≈ 0.4 to 0.6 mA after about a year

when the initial output current densities were 1.5 to 2.0 mA/m^2 (Dugarte and Sagüés 2014).

The galvanic anodes made in the 1990s and 2000s were designed to function for 10+ years

(Sergi 2011). Later, based on 20-year data from a CP system in a bridge in the UK, it was found

that the anodes could protect the structure for about 15 years until the encapsulating mortar was

saturated with alkali (Sergi et al. 2020). Today, many anodes with encapsulating mortar

exhibiting fine pore structure, long-term and high pH buffer, and better ion-exchange system

capabilities are available. In support of this, much literature concludes that an adequately

designed galvanic anode CP system could extend repair life for more than 25 years; thereby, a

repeated repair can be avoided (Helm and Raupach 2016; Sergi 2011; Whitmore 2018).

2.9   COST OF REPAIR USING GALVANIC ANODES

There is a myth that the cost of anodes can significantly increase the cost of repair. However,

such a myth arises because of the lack of consideration of life-cycle cost (LCC). Ideally, such

cost comparisons should be made between the LCC of repair instead of the capital cost of

repair. The LCC of a repair depends on the frequency of repeated repairs and the maximum

number of possible repeated repairs during the desired service life (Wilson et al. 2013a). The

use of galvanic anodes can prevent the halo effect and help in decreasing the frequency of

repeated repairs.

Life-cycle costing can be used as a reliable tool to decide on a repair strategy (Polder

et al. 2013; Val and Stewart 2003) and to assess the performance of various repair strategies

during the service-life, in terms of costs incurred for its acquisition, operation, maintenance,

and disposal (Feliu et al. 1990). Typically, the LCC of infrastructure is calculated by the

discounted cash flow method that involves calculating the net present cost (NPC) to account

for the time value of money (Purvis et al. 1994). However, this requires the knowledge of the

cash flow of every operation at each instance in the future. Unfortunately, such information is not available (Lee et al. 2020; Younis et al. 2020). A comparative LCC can be conducted by obtaining the future value (FV) of all operations using Eq. (2.8) and some assumptions on future cost parameters.

$$FV = \sum_{n=0}^{N} (1+r)^{n} \times C_{1}$$

(2.8)

where, C_1 is the total cost at 1st year (can be a constant), N is the analysis period (say, desired life extension), and 'r' is the discount rate. The number of repairs within the N years of life extension could be different for different repair strategies. For example, N of 30 years can be achieved either by adopting a repair system with a life of five years for six times or another repair system with a life of 15 years for two times. LCC in these two cases would be different and must be considered before making the choices. The discount rate, r, accounts for both the nominal interest and inflation rates (Lee and Lee 2017). The LCC of infrastructure can then be calculated using Eq. (2.9) (Younis et al. 2020).

$$LCC = C_D + C_C + C_R + C_{DD}$$

(2.9)

where, C_D is the cost of the design of the structure, C_C is the cost of construction (acquisition and operation), C_R is the maintenance and repair cost, and C_{DD} is the cost for demolition and decommissioning of infrastructure.

A few deterministic and probabilistic models are available to evaluate the LCC of RC structures exposed to various environments in a holistic manner (Lee et al. 2020; Li and Madanu 2009; Stewart and Val 2003). Peng and Stewart used deterministic LCC by considering the number of maintenance instances and the efficiency of the material to compare the economic viability of various repair materials for surface repairs on RC structures deteriorated due to corrosion (Peng and Stewart 2016). In another study, Younis et al. compared probabilistic and deterministic cost models for carbonation corrosion and showed

that after 100 years, the repair cost is reduced by 50 % compared to a deterministic LCC model (Younis et al. 2020).

Polder et al. (2014) proposed a probabilistic cost model for estimating the LCC of ICCP systems in concrete by using failure data from 105 case studies. The frequency of the global failure of the ICCP system was excluded from the model as it was scarcely reported within the analysis period (Polder et al. 2013). The model used the average time for replacement of ICCP systems as $\approx$ 15 years. This replacement can be considered as a minor repair because it does not involve the major structural repairs, which is the advantage of any cathodic protection system (including the galvanic anodes, which is the focus of the current study). Note that a statistically significant database on the failure period of the repair strategies is required to evaluate the probabilistic maintenance time and its cost. This is not available in the case of repair using galvanic anodes. Therefore, deterministic approaches are a way forward to determine the LCC of repair of RC systems using galvanic anodes. Therefore, a deterministic approach is adopted in this study. This study proposes a model for analysing the life-cycle cost and benefits of patch repair with and without CP for concrete structures.

2.10 SUMMARY AND RESEARCH NEEDS

Corrosion of reinforcement is one of the major durability problems in concrete. The problem requires efficient repair treatment to avoid the massive cost of repair and maintenance — the cost of corrosion is 2.4% of the global GDP as per the NACE Impact report 2014. Therefore, a critical study was required to understand corrosion mechanisms and other complex electrochemical processes in concrete. The ability of the steel to corrode when embedded in concrete depends on the thermodynamics of the steel. However, the rate at which the electrodes corrode depends on their kinetic behaviour in a specified microenvironment. The factors and parameters that can characterise the corrosion kinetics are discussed. Corrosion of steel has to

be detected early to provide adequate protective treatment and extend the structure's service life. Some test methods that can quantitatively assess corrosion and obtain the corrosion rate are the LPR, EIS, PDS, and PS test methods. Once corrosion is initiated, these assessment tests can provide an overview of the areas to be protected.

Conventional patch repair cannot efficiently arrest the corrosion of CP in concrete; instead, it leads to accelerated corrosion due to the halo or ring effect. Cathodic protection using galvanic anodes could be a promising technique to achieve durable repairs. Among the various types of CP, the galvanic anode cathodic protection system is widely adopted for repair works because of its limited monitoring requirements and the lower installation cost than ICCP systems. Newer technologies such as two-stage hybrid anodes that incorporate the advantages of both ICCP and galvanic anode systems have excellent prospects for the future. However, these techniques lack long-term performance data due to failure in monitoring systems after a few years. This cause hesitation in the minds of the stakeholders in adapting CP in a repair project. Thus, the long-term performance of these systems has to be obtained to understand the average extended service life of a repaired structure.

In addition, it was discussed that the monitoring methods as per EN ISO 12696 are directly adopted from the metallic system in a low resistive system. Therefore, there is a dire need to assess the methods of the existing test method to assess the performance of CP. In addition, it was discussed that these monitoring results are from representative locations, which cannot guarantee the performance of all the galvanic anodes in the CP system. Therefore, newer techniques that use the electrical response from the concrete-steel-anode (C-S-A) system are analysed. However, these techniques use test methods conducted on aqueous systems and cannot be directly adopted in concrete. Therefore, a review on the electrochemical modelling technique used numerical methods to simulate cathodic protection was conducted. From the review, it was understood that electrochemical models to estimate time-dependent changes in

the electrochemical kinetics at the steel-cementitious interface are not available. However, more information on the polarization properties of the metals (steel and zin anode) in the electrolyte is required to develop a time-dependent model which can correlate measurable parameters from a CP system with the polarisability of the galvanic anodes. Thus, there is a need to understand the parameters that affect the electrochemical kinetics of zinc anode and steel cathode.

3   LONG-TERM PERFORMANCE AND LIFE CYCLE COST BENEFITS OF CATHODIC PROTECTION

3.1   INTRODUCTION

This chapter presents field studies conducted on reinforced concrete structures that had undergone repair. The following section consists of a market study of the application of CP in India. Then, the long-term performance of CP systems on a jetty and industrial building structure are presented. After that, an LCC model is proposed to estimate the LCC of repair. Then, the comparison of cost during the 30 years after the first repair is compared. Finally, conclusions from this research are presented. Most of the content in this chapter is adapted from Krishnan, N., Kamde, D. K., Doosa Veedu, Z., Pillai, R. G., Shah, D., and Velayudham, R. "Long-term performance and life-cycle-cost benefits of cathodic protection of concrete structures using galvanic anodes." published in *Journal of Building Engineering*, Elsevier Ltd, 42 (February 2021), 102467, in particular the figures and tables.

3.2   REPAIR OF CONCRETE STRUCTURES

The effectiveness of a repair can be evaluated by estimating the service life of repair, frequency of inspection or maintenance, the time required to execute the repair, aesthetics after the repair, and life cycle cost (LCC) of repair. Patch repair (PR) using cementitious materials is one of the widely adopted repair strategies for reinforced concrete structures. However, their application on reinforced concrete structures decreases the residual service life of the structures. This results in the repeated repair of the structure and significantly increases the life cycle cost of the structure. Over the past two decades, a gradual trend towards implementing electrochemical repair techniques such as cathodic protection (CP) was observed in the concrete repair industry. Among the different methods to implement CP in concrete, the

galvanic anode CP strategy has gained widespread acceptance in developing countries. The strategy involves connecting galvanic anodes to the cleaned steel rebars and the subsequent patch repair with cementitious material. However, less literature is available to substantiate the long-term performance of these anodes. Also, the wrong perception of the possibly high initial cost of repair with galvanic anodes is another factor that hinders the implementation of CP in concrete. It is high time that LCC is given due consideration while selecting repair strategies. This chapter focuses on comparing the long-term performance and LCC of patch repairs with and without CP.

3.3 STATE OF CONCRETE REPAIR INDUSTRY

3.3.1 Collection of data from the field

An interview was conducted between few Indian distributors of galvanic anodes for concrete structures. Following questions were asked during the interview: (i) What is the interval between the repeated repairs in structures without CP systems? (ii) How many projects do they know where the repair has been done using CP systems? (iii) What is the approximate number of anodes used in each project? (iv) What was the age of the structure at the time of the first repair? (v) Which infrastructure sector (jetty, buildings, etc.) does the concrete structures under repair belong to? (vi) Whether the installed electrochemical repair is a CP or CPrev? (vii) Whether monitoring results from CP are available? And (viii) If monitoring results are available, can results be shared for analysis and publication? The collected data was analyzed to understand (i) the number and frequency of patch repairs without CP systems, (ii) the number of projects undertaken as CP and CPrev, and (iii) the number of anodes supplied to various infrastructure sectors.

3.3.2 Frequency of concrete repairs

As reported in the literature, the patch repair without CP does not arrest corrosion or address the root cause (Christodoulou et al. 2013; Raupach 2006; Sergi 2011). Figure 3.1 shows data from 20 structures without CP and indicate that more than 70% of the structures were re-repaired within five years after the first repair. About 30% of them were re-repaired about 4 years after the first repair – causing a huge economic burden. Maybe because of this, the number of usages of galvanic anodes has risen significantly in recent times. Another reason for this rise is the increase in the communication about CP and its benefits among the CP manufacturers, practitioners, researchers, and consultants. However, this practice of patch repair (without CP) continues in many parts of the world, and one way to change this is by obtaining field data through pilot studies.
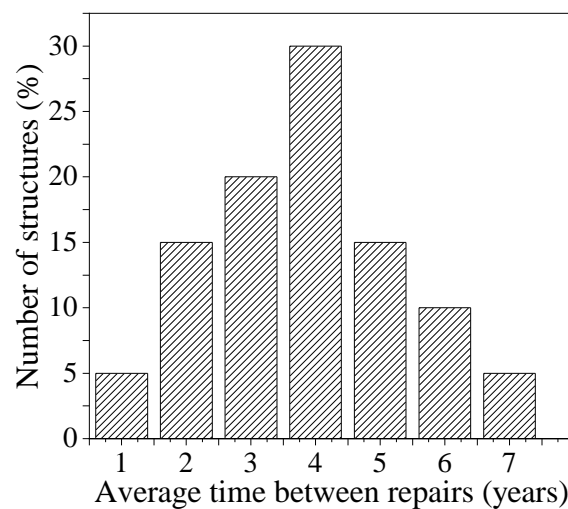
Figure 3.1: Frequency of repeated repairs experienced by about 20 structures considered in the study (Adapted from Krishnan et al. (2021))

3.3.3 Indian experience with cathodic protection

Figure 3.2 shows the sector-wise growth in the usage of galvanic anodes in India from 2003 to 2020 – with a total usage of ≈ 60,000 anodes in reinforced concrete structures in India. About 60% of these anodes (33,000) were used in 2020 – exponential growth in the usage of galvanic anodes. The usage of CP systems varies from sector to sector. For example, from 2003 to 2020, the industrial buildings, jetties and ports used ≈ 20,000 anodes each. The highway and bridge sectors consumed the least number of anodes (about 400 were used in two projects in 2016). This indicates that significant efforts are needed to promote the use of CP systems in highways and bridges. This is of utmost importance because the Indian Bridge Management Systems (IBMS) has recently identified about 6000 bridges for immediate repair (Dash 2017). The LCC of those bridges can be significantly reduced if CP systems are used while repairing the bridges with corrosion as a root cause of distress.
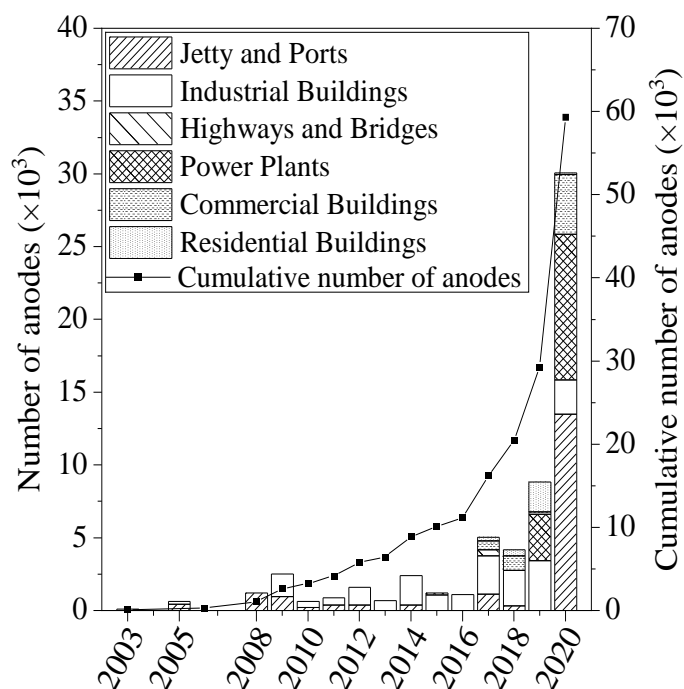
Figure 3.2: Acceptance of galvanic anodes to repair RC systems from 2003 to 2020.

Overall, only about 70 projects in India have used galvanic anodes in the repair work, which is minuscule considering the huge number of ongoing repair projects across the country. Similar could be the case in many parts of the world – highlighting a dire need to promote CP technology and save structures from deterioration. It has been reported that the use of galvanic anodes in RC systems was/is limited because of the following: (i) lack of experienced CP professionals in the construction sector, (ii) wrong belief that the introduction of CP in repair industry could reduce the market share of repair chemicals, and (iii) lack of knowledge of the life-cycle benefits of CP.

Even today, only a few firms in India practice the use of good galvanic anodes for concrete repair. About more than a decade ago, a few practitioners in India started pilot studies with CP in concrete repair projects. In these, a minimum number of galvanic anodes was determined using an approximate calculation and without considering the actual surface area of the steel, concrete resistivity, exposure condition, etc. For example, a standard practice of one anode per m2 of concrete surface area was considered, which may not be sufficient to passivate the steel rebars, but adequate to suppress ongoing corrosion. Also, in India, one recently constructed port facility has used cathodic prevention systems, which is a very positive signal indicating that engineers now realize the importance of CP and CPrev technologies for concrete structures.

3.3.4 Worldwide experience with cathodic protection

Figure 3.3 shows the sector-wise distribution of CP usage worldwide from 2003 to 2018. Figure 3.3(a) shows that 62% of cathodically protected structures belong to industrial facilities with aggressive environments (e.g., chemical manufacturing plants and industrial effluent treatment plants). Other buildings (e.g., government, heritage, and institutional buildings, public parks, and shopping complexes) and jetties and ports used about 15% of the total anodes

used. Figure 3.3(b) shows the sector-wise distribution of various repair projects with cathodic prevention (CPrev). It is observed that 28%, 25%, and 18% of structures with CPrev are residential, industrial, and commercial buildings, respectively. However, cathodic prevention and protection are least employed in power plants, highways, and bridges (about 4 to 10%.).

In general, the long-term performance data of CP systems from many of these structures are not available because the clients hesitate to facilitate field measurements. Based on the available documentation, data collected, site visits, and possible access to the structure, two of the infrastructure (a finger jetty and an industrial building) were selected to present CP systems' long-term performance.

(a) Cathodic protection   (b) Cathodic prevention
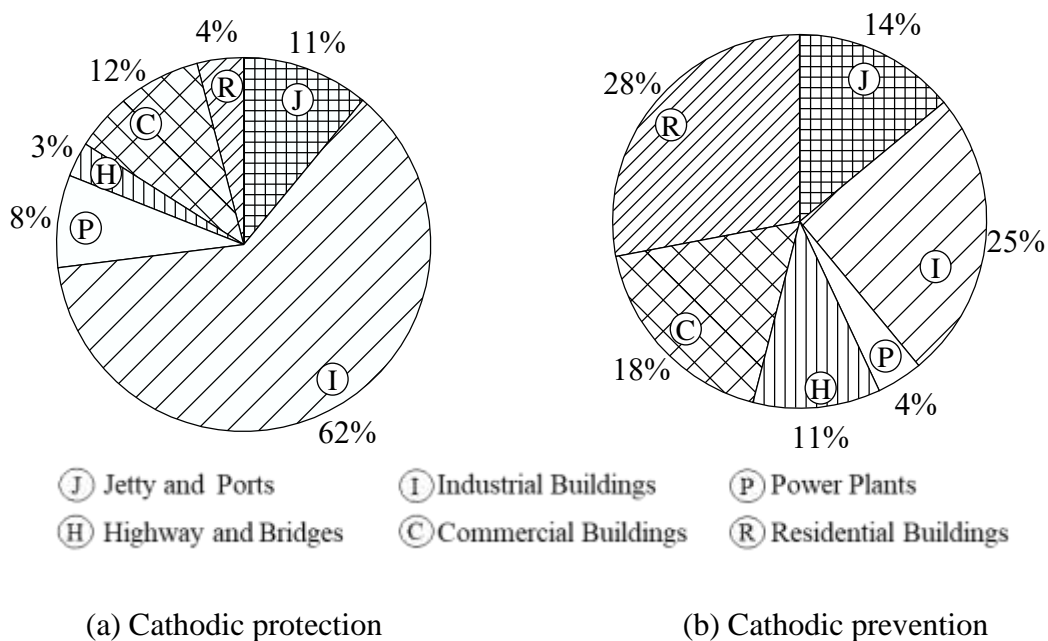
Figure 3.3: Distribution of usage of the galvanic anodes in various repair works worldwide from 2003 to 2018 (Courtesy: Vector Corrosion Technologies, Canada).

48

3.4 CASE STUDY 1 - FINGER JETTY IN CHENNAI, INDIA

3.4.1 Field investigation

Figure 3.4 shows the photograph, schematic, and layout of the finger jetty constructed in 1992 and located at Chennai city on the East Coast of India. As shown in Figure 3.4(b), the typical tidal variation is 0.7 m, and the mean sea level (MSL) is below the pier cap, indicating that the top portion of the pier and pier cap experiences severe wet-dry exposure to seawater. After about 14 years of service, although M35 concrete was used, significant corrosion of rebars was observed in the piers at the splash zone (see Figure 3.5(a)). In 2005, the jetty structure was visually investigated, and chloride tests were conducted — as per ASTM C1152 — on the cylindrical concrete core samples extracted from the structure. An average chloride concentration in concrete at the rebar level was greater than 0.6% by weight of the binder, which is significantly higher than the chloride threshold of the uncoated steel rebar in concrete (Kamde and Pillai 2020a). Based on the visual inspection and determined chloride concentrations, it was decided to immediately repair and strengthen the piers and pier caps.

(a) Repaired piers of finger jetty (Photograph taken in 2019)
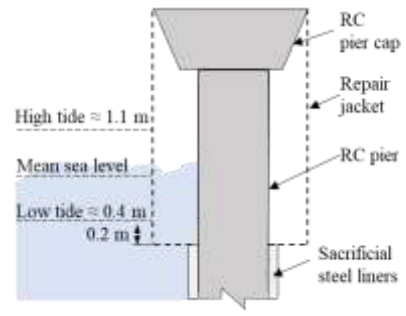
(b) Elevation of the piers and jacket repair
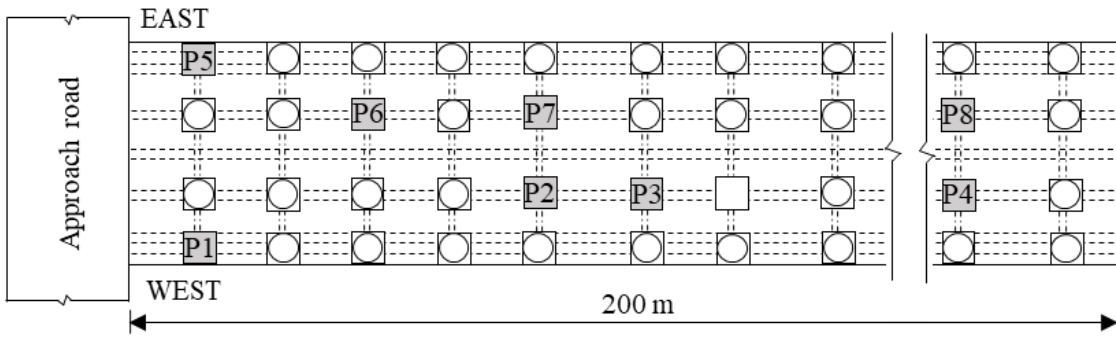
(c) Layout of the finger jetty (Monitoring boxes were installed on the shaded piers only)

Figure 3.4: Repaired finger jetty in Chennai, India

3.4.2 Methodology of the repair and subsequent inspections

Figure 3.5(b) shows the photograph (taken in 2005) of a pier under repair. The sacrificial steel liners were removed up to ≈ 0.2 m deep from the bottom of the pier cap. The rebars were coated with anticorrosive zinc coating. Also, one anode was installed for every 1 m^2 of concrete surface. About 10 m^3 of prepackaged repair concrete (denoted as 'microconcrete', herein) was used for repair. Also, about 10 tons of additional reinforcing steel was used. An epoxy-based polymer adhesive was applied to the existing concrete surface – to enhance the bond between the microconcrete and substrate concrete. Considering the high chloride contamination at the rebar level and significant loss of steel cross-section, the repair using galvanic anodes was implemented. For this, the continuity of all the rebars in the piers was

checked using a high impedance multimeter to ensure the functioning of CP systems. About 1400 galvanic anodes were installed in various structural elements (pier, pier cap, longitudinal beams, and slabs). Figure 3.5(b) shows the additional reinforcement and galvanic anodes installed in one of the piers. Figure 3.5(c) shows the piers after repair using the CP. To monitor the performance of galvanic anodes, monitoring boxes were installed in eight piers [see the shaded piers in Figure 3.4(c)].

From 2005 onwards, the depolarized potential of steel and output current from the anodes (I_{output}) were obtained from the piers. During depolarisation tests, the anode-steel circuits are disconnected and allowed to depolarize for 24 hours, then HCP of the steel rebars are measured (as per ASTM C876 procedures) and defined as the depolarized corrosion potential (E_{24h}). After obtaining the E_{24h}, the steel-anode circuits are reconnected for the CP system to resume its function. The E_{24h} of steels were monitored about every six months until 4 years after the installation of anodes. After that, frequent visual inspections were carried out. In 2019, after 14 years from the 1st repair with CP, the monitoring boxes were found to be degraded and even missing in some cases; and hence, E_{24h} could not be measured, and only I_{output} was measured.

| (a) Piers with corroded rebars (with circular cross-section) | (b) Setup for concrete jacketing with additional rebars and galvanic anodes | (d) Piers after repair (with rectangular cross-section) |
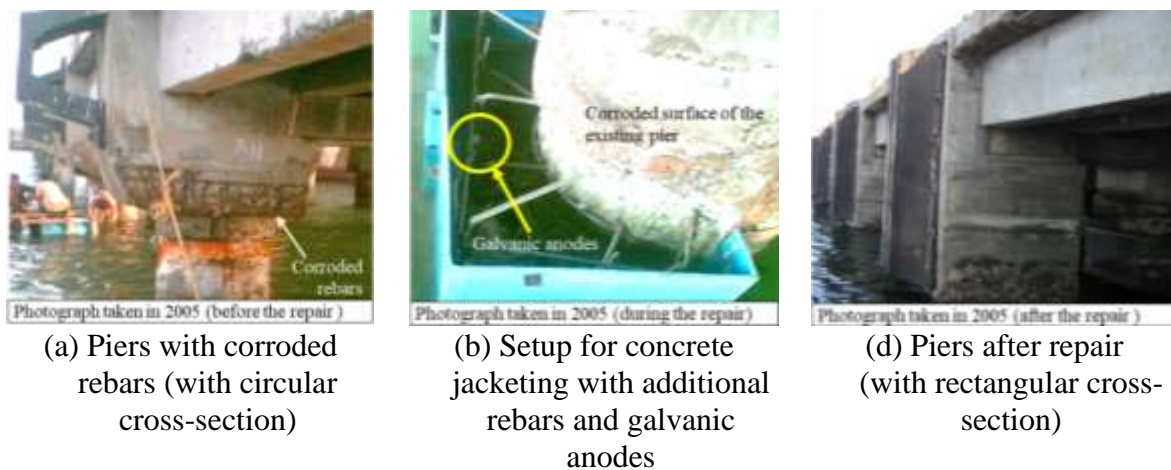
Figure 3.5: Repair of finger jetty using galvanic anodes

3.4.3   14-year long performance of galvanic anodes

Figure 3.6(a) shows the E_{24h} of steel rebars in the piers before and after the repair. Note that the starting data point (inside the ellipse) of each curve is the HCP of the steel rebars before installing anodes and are more negative than −350 mV, which indicates a high probability of corrosion. After six months of repair, E_{24h} were more positive than −100 mV, indicating re-passivation of rebars within about six months of installing galvanic anodes. E_{24h} were monitored for about four years and were found to be more positive than –270 mV. This indicates that the probability of corrosion was less than 10% (ASTM C876 2015). Due to contractual agreements and other constraints, regular monitoring was possible only until 4 years after the installation of anodes. Later, after 14 years of the first repair, a visual inspection was conducted, and no significant corrosion-induced cracks were observed on the concrete surfaces. Figure 3.6(b) shows a photograph of one of the pier caps with cracks 14 years after the repair - indicating good protection of embedded steel for more than 14 years.
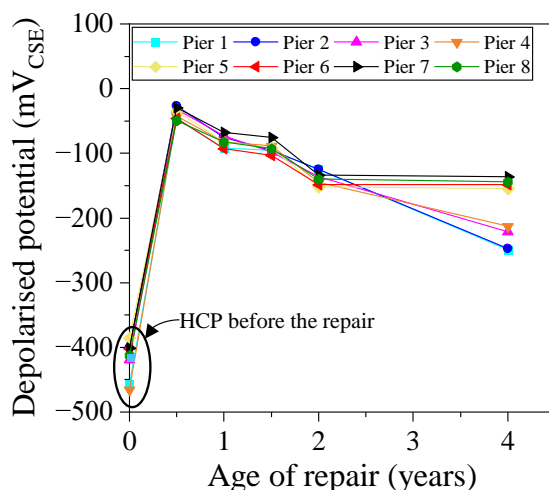
(a) Depolarized corrosion potentials obtained from piers of finger jetty

(b) CP protected pier after 14 years

Figure 3.6: 14-year long performance of repair using galvanic anodes in Finger Jetty.

During the 2019 visit, it was found that all the monitoring boxes and lead wires were naturally damaged/degraded (see Figure 3.7(a) for a typical scenario). Also, many of the monitoring boxes and lead wires were missing (say, degraded/damaged and fallen into the seawater below). Hence, E_{24h} could not be measured, and only the I_{output} was obtained from Piers 1 to 8 (see Figure 3.7(b)). The I_{output} from a galvanic anode in Piers 1 and 5 were 0.25 and 0.42 μA, respectively, which are significantly higher than the I_{output} from galvanic anodes in other piers. Piers 1 and 5 are located in the outer wing of the finger jetty and experience the incoming tides to a higher level than the internal piers. Also, the outer piers have been experiencing higher temperatures (during summer) and more severe splashing, whereas the inner piers always experienced lower temperatures (under shade) and less severe splashing. Therefore, the I_{output} required for the outer piers could be higher than that for the inner piers. Figure 3.6(a) shows that the rebars are passivated within the first six months after the installation of anodes; also, the I_{output} would be less for the anodes connected to the passivated steel, which is the case for Piers other than P1 and P5.
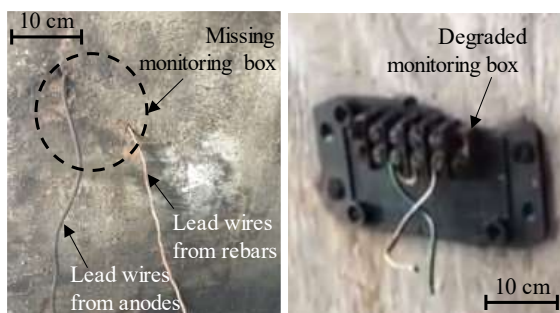
(a) Missing, naturally degraded/damaged monitoring boxes
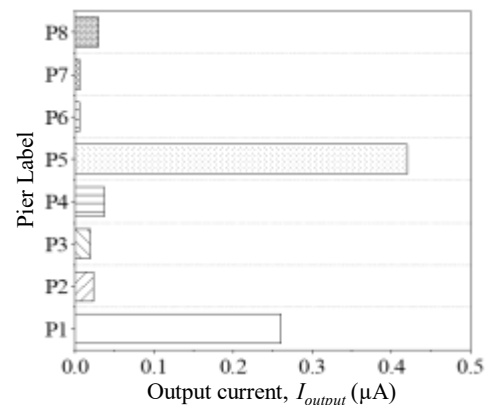
(b) Output current data collected in 2019

Figure 3.7: Condition of monitoring boxes and the output current of anodes at the end of 14 years after repair.

In the case of P1 and P5, the I_{output} required to protect the steel is high, the same is provided by the anodes, and no corrosion-induced cracks were visible – hence, it can be concluded that the steel is protected from corrosion. Due to the high I_{output}, the anodes in P1 and P5 have shorter residual life than in other piers and may have to be replaced soon. Frequent monitoring (say, once every 2 years) of I_{output} from the Piers 1 to 8 can help develop a preventive maintenance strategy and protect the steel inside the piers for as long as desired – with minimal life cycle cost implications.

3.5   CASE STUDY 2 - INDUSTRIAL BUILDING

3.5.1   Methodology of repair and subsequent inspections

Figure 3.8 shows the photograph of a four-storey industrial building (salt processing unit) built in the early 1990s near a seashore in Tamil Nadu, India. Due to the high chloride and humidity levels, significant corrosion and concrete spalling were observed in about 15 years of service (see Figure 3.8(a)). Because of these severe and visible corrosion conditions, the various columns, slabs, and beams were cathodically protected using a total of about 2,800 anodes. Figure 3.9(a) shows the layout of the structural frame of the building. Monitoring boxes were installed at the following members in various floors: (i) Ground floor: Beams B5-C5, and A3-B3, (ii) 1st floor: Column C4, (iii) 2nd floor: Column C1, Beam B2-B3, and (iv) 3rd floor: Beam C2-C3. At these locations, E_{24h} was measured every six months until four years after installing anodes.

One of the columns with severe corrosion-induced cracking

| (a) Before repair | (b) After repair |
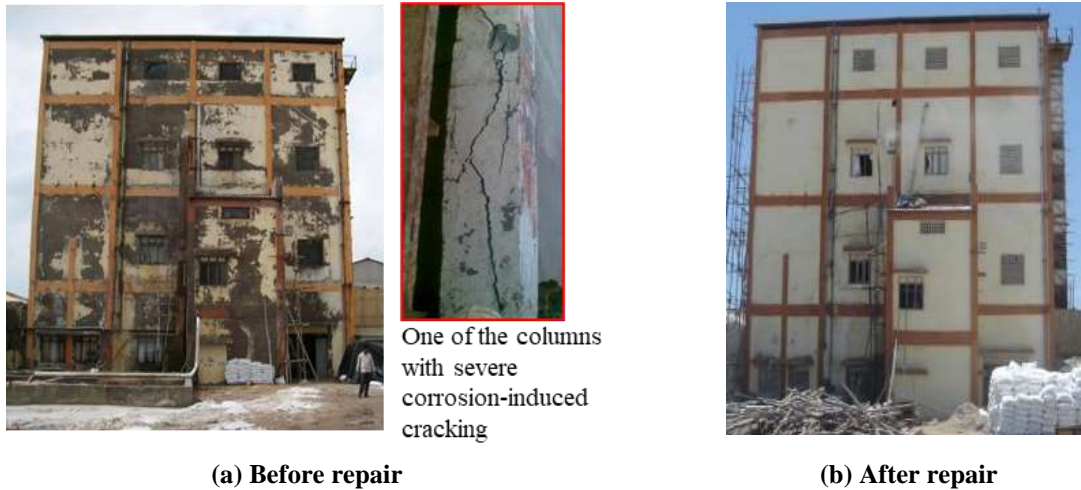
Figure 3.8: Industrial building (salt processing unit) before and after the repair in 2008

3.5.2   4-year long performance of galvanic anodes

Figure 3.9(b) shows the variation of the E_{24h} of steel rebars after the installation of anodes. At the end of six months, E_{24h} was about –50 mV, which indicates that the galvanic anodes have passivated the steel rebars. At the end of 4 years, the E_{24h} reached from about –50 mV to about –200 mV, indicating that the steel rebars were still in a passive state. Due to contractual agreements and other constraints, regular monitoring was possible only for 4 years after installing anodes. However, to check the long-term performance of galvanic anodes, a visual inspection of the industrial building was conducted at the end of 10 years after repair. It was observed that the structural elements did not exhibit any corrosion-induced cracking. However, in 2018, the salt processing procedure was changed, and the building was demolished. But this is a very good case study showing that galvanic anodes can protect the steel rebars from corrosion for more than 10 years, even in chloride-rich environments. However, clients are hesitant to adopt repairs using galvanic anodes due to the myth of the high cost of anodes instead of considering the effect of galvanic anodes on the LCC of the structure.
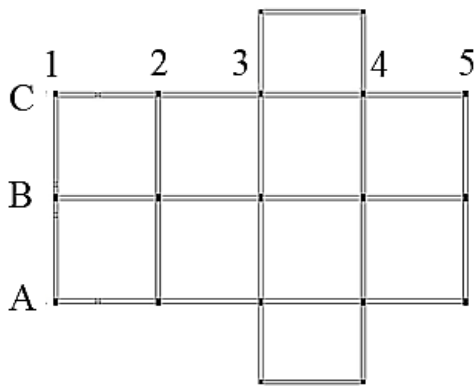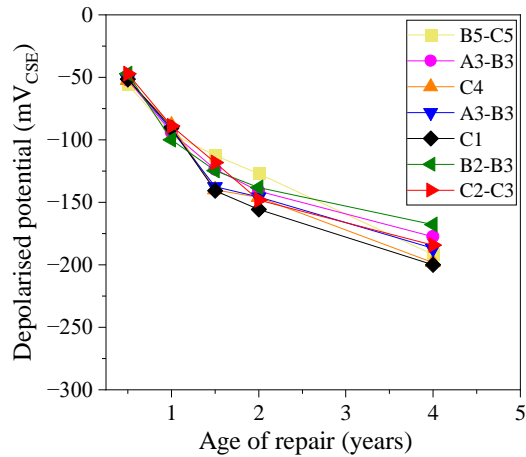
(a) Layout of the structural members   **(b) Variation of depolarized potential**

Figure 3.9: Depolarized potential (E_{24h}) obtained from the industrial building elements.

3.6 EFFECT OF REPAIRS WITH AND WITHOUT GALVANIC ANODES

Figure 3.10 shows the difference between the patch repairs with and without galvanic anodes. In case of repair without CP, the steel rebars can corrode due to two mechanisms: (i) new corrosion due to the halo effect and (ii) continued corrosion due to the possible residual chlorides in the residual corrosion products (say, residual chloride effect; if rebars are not undercut and cleaned well, which is usually the case in many repair projects). The former results in an increase in the length of the corroding region on the rebars and the area of the repair region. The latter results in a reduction in the cross-sectional area of rebars in the already corroded portions. Use of CP can arrest corrosion due to both these mechanisms, which is depicted in the schematics in Figure 3.10.

Figure 3.10 (a) shows that when patch repaired without anodes, the length of the corroded regions of rebars and the area of the repair region continues to increase. The structural capacity of the RC systems continues to decrease during the life of patch repair without CP; necessitating more frequent repairs with increasing areas of repair region. Also, as shown in the last schematic in Figure 3.10 (a), this can lead to severe ongoing corrosion in short period (say, n_1 years after first repair) requiring the addition of even splice rebars. These will have

significant impact on the LCC after 1st repair. On the other hand, Figure 3.10 (b) shows that when an RC system is repaired with galvanic anodes, the corrosion due to both the halo effect and residual chloride effect is arrested or controlled.
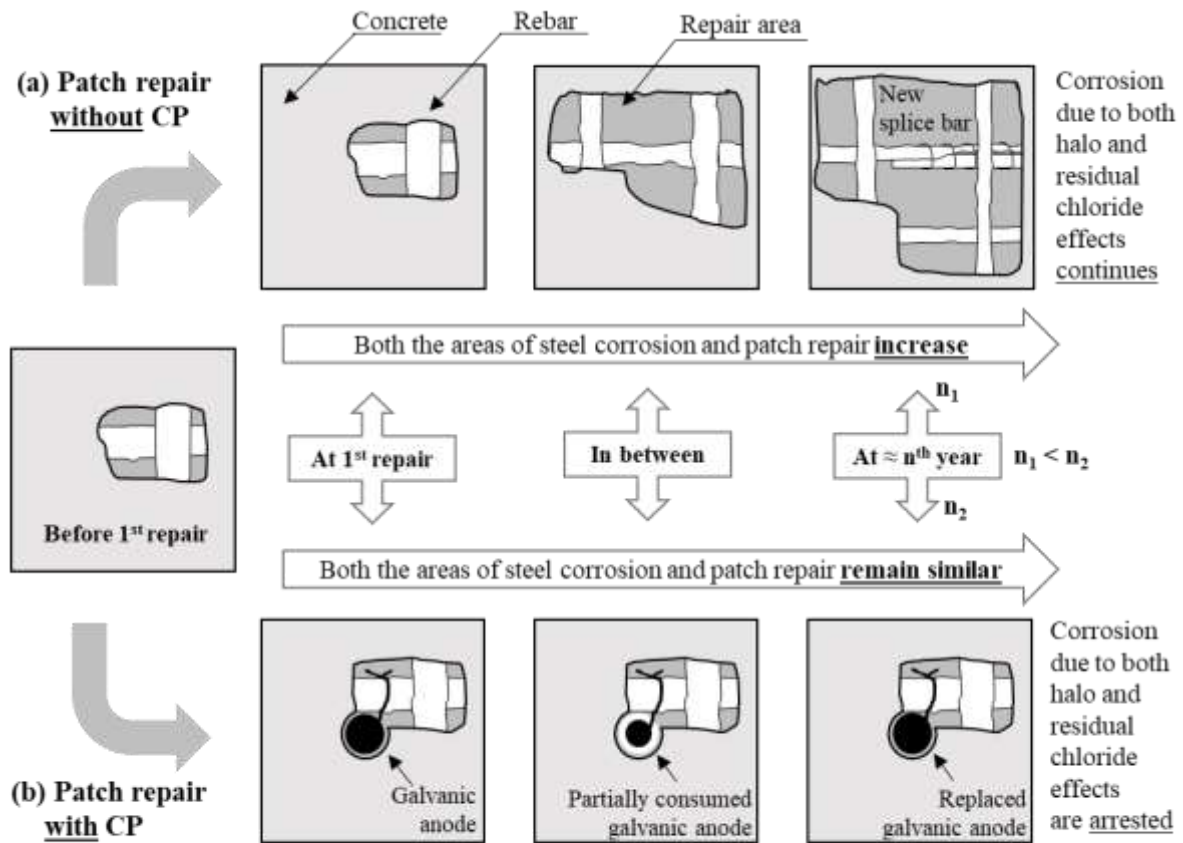
Figure 3.10: Differences in the areas of repair region and steel corrosion in case of patch repairs with and without CP

The schematics corresponding to "in-between" indicate that the repair region do not increase (anodes prevent halo effect), cross-sectional area of rebars do not decrease (anodes stop corrosion due to the residual chloride effect). When the anode is found to be consumed completely (say, after n_2 years after the 1st repair; $n_1 < n_2$), they can be replaced with new

anodes at a lower cost than the repair cost in the case of patch repair without CP. However, it should be noted that the locations of all anodes must be identified to enable easy replacement.

3.7 LIFE-CYCLE-COST (LCC) ANALYSIS OF REPAIRS

To compare the life-cycle-cost (LCC) of conventional patch repair with and without galvanic anodes, the individual costs associated with the various repair materials/systems/activities are required. Hereafter, the patch repair without and with cathodic protection are denoted as "PR" and "CP", respectively.

3.7.1 Framework for estimating the LCC of repairs

The LCC of the repair is calculated considering the costs associated with all the possible future repeated repairs and inspections during the repair life; the costs of construction and demolition are not included. Figure 3.11 shows a flowchart showing the framework for estimating the LCC of repairs in the following four major steps: (S1) Capital cost of repair, (S2) Future value (FV) of subsequent inspections, (S3) FV of subsequent repairs, and (S4) Cumulative FV of repairs and inspections, which is LCC of repairs. Following is a discussion on these major steps.

      S1: Capital cost of repair is the sum of the cost of the first repair work and the cost of inspection before that ($C_{insp\text{-}zero}$). For example, the cost of 1st repair for PR and CP strategies are calculated using Eq. (3.1) and Eq. (3.2), respectively (see S1 in Figure 3.11).

Capital cost of PR, $C_{total,\ PR} = C + C_{insp\text{-}zero}$

$$(3.1)$$

Capital cost of CP, $C_{total,\ CP} = C + C_{anodes} + C_{insp\text{-}zero}$

$$(3.2)$$

where, C is the sum of the cost of all the repair heads, such as (i) cleaning and preparation of the surface of steel and concrete at the repair region, (ii) additional steel, (iii) formwork,

(iv) bonding agent for concrete surface, (v) repair concrete, (vi) other costs (if any), and C_{anodes} is the cost of anodes (including shipment, installation, and monitoring).

S2: FV of subsequent inspections until the End of Life (EoL) or the 'LCC analysis period' are calculated using Eq. (3.3) (see B2 in Figure 3.11).

$$C_{insp,\,i} = (1+r)^{T_{insp,\,i}} \times C_{insp\text{-}zero};\; i = 1, 2, 3, \ldots \tag{3.3}$$

where, r is the discount rate, $T_{insp,\,i}$ is the time elapsed from the 1st to ith inspection. Frequency of inspections of infrastructure varies based on the suggested duration prescribed by the governing code of practice or client.

S3: FV of subsequent repairs are calculated using Eq. (3.4) and Eq. (3.5), respectively (see S3a and S3b in Figure 3.11).

$$C_{PR,\,j} = (1+r)^{T_{rep,\,j}} \times C_{PR,\,1};\;\; j = 2, 3, 4, \ldots \tag{3.4}$$

$$C_{CP,\,j} = (1+r)^{T_{rep,\,j}} \times (C_{anodes} + C_{insp\text{-}zero});\; j = 2, 3, 4, \ldots \tag{3.5}$$

where, $C_{PR,\,j}$ is the sum of the various head-wise costs of jth patch repair and the inspection costs, whereas $C_{CP,\,j}$ is the sum of the cost of anodes and the inspection before the jth repair. Note that in the case of CP strategy, the patch repair is needed only once and hence, the repair costs (for $j > 1$) include only the cost of anode replacement and not the cost of patch repair; this significantly reduces the LCC of CP strategy. $C_{PR,\,1}$ and $C_{CP,\,1}$ are calculated in S1.

C ; C_{anodes} ; $C_{insp\text{-}zero}$; $t_{insp,i}$; $t_{rep,j}$; r ; j_{max}

S1 Capital cost of repair
$$C_{total,\,PR} = C + C_{insp\text{-}zero}$$
$$C_{total,\,CP} = C + C_{insp\text{-}zero} + C_{anodes}$$

$i = 1$; $n = 1$; $j = 2$; $T_{rep,j} = t_{rep,j}$; $T_{insp,i} = t_{insp,i}$

$n = n + 1$

No — If $n = T_{insp,i}$ — No — If $n \geq T_{rep,j}$ — $T_{rep,j} = T_{rep,j-1} + t_{rep,j}$

Yes

Yes

S2 FV of inspection at n^{th} year
$$C_{insp,i} = (1 + r)^{T_{insp,i}} \times C_{insp\text{-}zero}$$

Total cost of repair till n^{th} year
$$C_{total,\,PR} = C_{total,\,PR} + C_{insp,i}$$
Or
$$C_{total,\,CP} = C_{total,\,CP} + C_{insp,i}$$

$i = i + 1$
$n = n + 1$

$T_{insp,i} = T_{insp,i-1} + t_{insp,i}$

$i = i + 1$
$j = j + 1$

S4 Total cost of repair till n^{th} year
$$C_{total,\,PR} = C_{total,\,PR} + C_{PR,j}$$
Or
$$C_{total,\,CP} = C_{total,\,CP} + C_{CP,j}$$

No — If repair is with CP — Yes

S3a FV of jth repair
$$C_{PR,j} = (1 + r)^{T_{rep,j}} \times C_{PR,1}$$

S3b FV of jth repair
$$C_{CP,j} = (1 + r)^{T_{rep,j}} \times (C_{anodes} + C_{insp\text{-}zero})$$

If $(j - 1) \geq j_{max}$
or
$n = n_{max}$ — No

Yes

$$LCC = C_{total,\,PR}\ or\ C_{total,\,CP}$$

Symbols: C : Cost of repair excluding the cost of inspection and anodes; C_{anodes} : Cost of manufacturing, supply, and installation of anodes; $C_{insp\text{-}zero}$: Cost of inspection at the time of 1st repair; $C_{insp,i}$: FV of ith inspection; $C_{PR,j}$: FV of jth repair without CP; $C_{CP,j}$: FV of jth repair with CP; $C_{total,\,PR}$: Total cost of patch repair till n^{th} year; $C_{total,\,CP}$: Total cost of patch repair with CP till n^{th} year; i : Identification of individual inspection; j : Identification of individual repair; j_{max} : Maximum allowable number of repairs; n : Time elapsed from 1st repair; n_{max} : Maximum possible service life extension; r : Discount rate; $t_{insp,i}$: Time interval between $(i\text{-}1)^{th}$ and i^{th} inspections; $t_{rep,j}$: Service life of jth repair; $T_{insp,i}$: Time elapsed between 1st and i^{th} inspection; $T_{rep,j}$: Time elapsed between 1st and j^{th} repairs

Figure 3.11: Generalized framework to calculate LCC for repair with and without CP

S4: Cumulative FV of repair is obtained by adding all the $C_{PR, j}$ costs until the number of repairs is equal to the maximum allowable number of repairs (say, $j = j_{max}$) OR until the end of 'LCC analysis period', whichever is shorter. This cumulative C_{PR} is defined as $C_{total, PR}$ and is the LCC of the PR strategy. The $C_{total, CP}$ for the CP strategy can also be calculated in a similar manner (see S4 in Figure 3.11). Using this framework, the LCC of the various repair strategies can be compared for selecting a suitable repair strategy. The next section demonstrates this through the case study of the CP repair of a jetty structure in Chennai, India.

3.8   COMPARISON OF LIFE CYCLE COST OF REPAIR STRATEGIES

3.8.1   Input data for estimating life cycle cost of repair of finger jetty

As discussed earlier, in 2004, the finger jetty in Chennai was repaired using CP strategy (i.e., patch-repaired with anodes) and was one of the early CP pilot projects in India. Figure 3.12 shows the distribution of various costs associated with this CP repair work. Repair concrete (microconcrete) used for patch repair constitutes a significant majority (about 66%) of the repair cost. On the other hand, the total cost of the CP system (galvanic anodes and monitoring boxes) was only about 3% of the total cost of repair and is negligible considering the cost of microconcrete. This disproves the myth that the use of CP would add significantly to the cost of repair and also emphasizes that the LCC (instead of capital cost) should be considered for selecting a repair strategy.
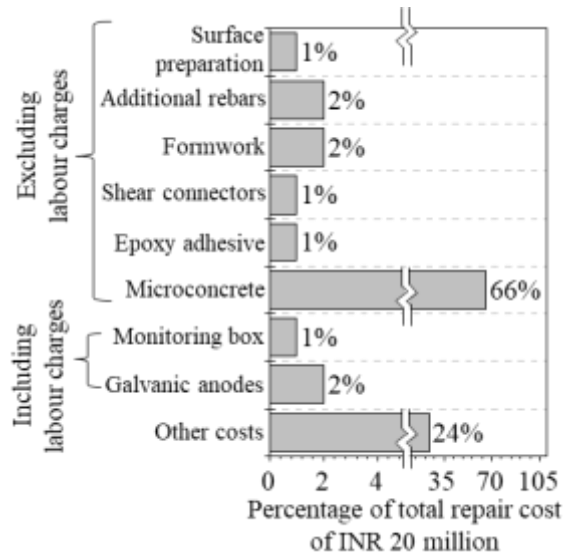
Figure 3.12: Head-wise cost of repair with CP at finger jetty, Chennai, India

3.8.2   Life cycle cost of repairs of finger jetty

The LCCs of the following three repair strategies for the jetty in Chennai, India was compared:

- **PR strategy** - Patch repair without CP and repeated every 5th year (see Figure 3.1)

- **CP strategy** - Patch repair with galvanic anodes and repeated replacement of galvanic anodes at every 15th year (see Case Study 1), and

- **CPrev strategy** – Installation of galvanic anodes at the time of construction and repeated replacement of anodes at the end of the design life of the galvanic anodes, i.e., 30 years.

Note that the CP strategy was actually adopted for the structure and the PR and CPrev strategies are hypothetical in this discussion. In these three strategies, the LCC was stopped if one of the following two conditions were satisfied: (i) maximum number of repairs are five ($j_{max} = 5$) and (ii) LCC analysis period is 75 years. For LCC calculation, the discount rate, r, is assumed to be 7% (International Monetary Fund 2020). Figure 3.13 shows three cash flow diagrams (step

function) showing the variation of the cumulative FV for PR, CP, and CPrev strategies (i.e., $C_{total, PR}$, $C_{total, CP}$, and $C_{total, CPrev}$). For the ease of comparison, the LCC at each year is normalized to the maximum cumulative cost spent for CP repair ($C_{total, CP}$ at 90th year (i.e. 75 years after 1st repair). Note that the first repair in both the PR and CP strategies was done 15 years after construction. Each unfilled square marker along the step function graph represents the repeated patch repair. Each unfilled circular and triangular marker along the step function graph represents the repeated replacements of galvanic anodes in CP and CPrev strategies, respectively. The calculated FV of the repairs at each 5th year is shown in Appendix A.

This paragraph compares the capital cost of PR, CP, and CPrev strategies (see S1 in Figure 3.11). Note that the hypothetical CPrev is assumed to be implemented at the time of construction, and the cost was about 0.2% more than the cost of PR or CP repair (see Close-up A in Figure 3.13). At the time of 1st repair (in 15 years after construction), the cumulative cost of PR and CP repairs were about 25 times more than the FV of CPrev – indicating a significant advantage of choosing CPrev option in the long term. However, engineers often tend to cite the constraints associated with construction budgets and do not opt for CPrev strategy, leading to significant repair costs later. For the jetty structure in the study, the cost of 1st CP repair was obtained and is about 4% more than the cost of the hypothetical PR repair (see Close-up B in Figure 3.13). Therefore, the capital cost of CPrev < PR < CP. However, this is not a correct comparison to base the selection of repair strategy. The comparison of repair costs should be made based on LCC during the analysis period or the desired extension of service life.

In this paragraph, the LCCs at 45 and 90 years of service are discussed. The PR strategy would require six repeated patch repairs until 45 years of service (i.e., 30 years after the first repair). The structure may experience significant deterioration during this time because of the continued steel corrosion (due to halo effect and residual chloride effects) until End of Life

(EoL). At 45 years of service, if CP strategy is adopted for repair, the anodes need to be replaced twice; if CPrev strategy is adopted, then anodes need only one replacement. Also, compared to the FV of PR strategy, the adoption of CP and CPrev strategies can reduce the cumulative FV (at 45 years of service) by 90 and 98%, respectively. In addition, it is estimated that the cumulative FV (at 90 years of service) of CP strategy is about twice that of CPrev strategy. This indicates that the longer the LCC analysis period, the more will be the LCC of CP strategy when compared to CPrev strategy. Also, note that the PR strategy cannot provide a total service life of more than about 45 years, whereas both CP and CPrev strategies can provide a total service life of more than 90 years.

In other words, the adopted CP strategy in the jetty structure is expected to provide 45+ years of additional service with about half the LCC of PR strategy; and further life extension is possible with repeated replacement anodes for as long as needed. Ideally, if the galvanic anodes are replaced as required and repeatedly, the CP and CPrev strategies can arrest steel corrosion for as long as needed. However, it should be noted that the CPrev strategy is possible only for structures that are yet to experience corrosion. For corroding structures, CP is the only appropriate option - among the PR, CP, and CPrev strategies under study. This detailed study on LCC shows that the adoption of either CP or CPrev can lead to huge savings in terms of LCC, see Figure 3.13. Further examples of such huge savings in LCC are shown next.
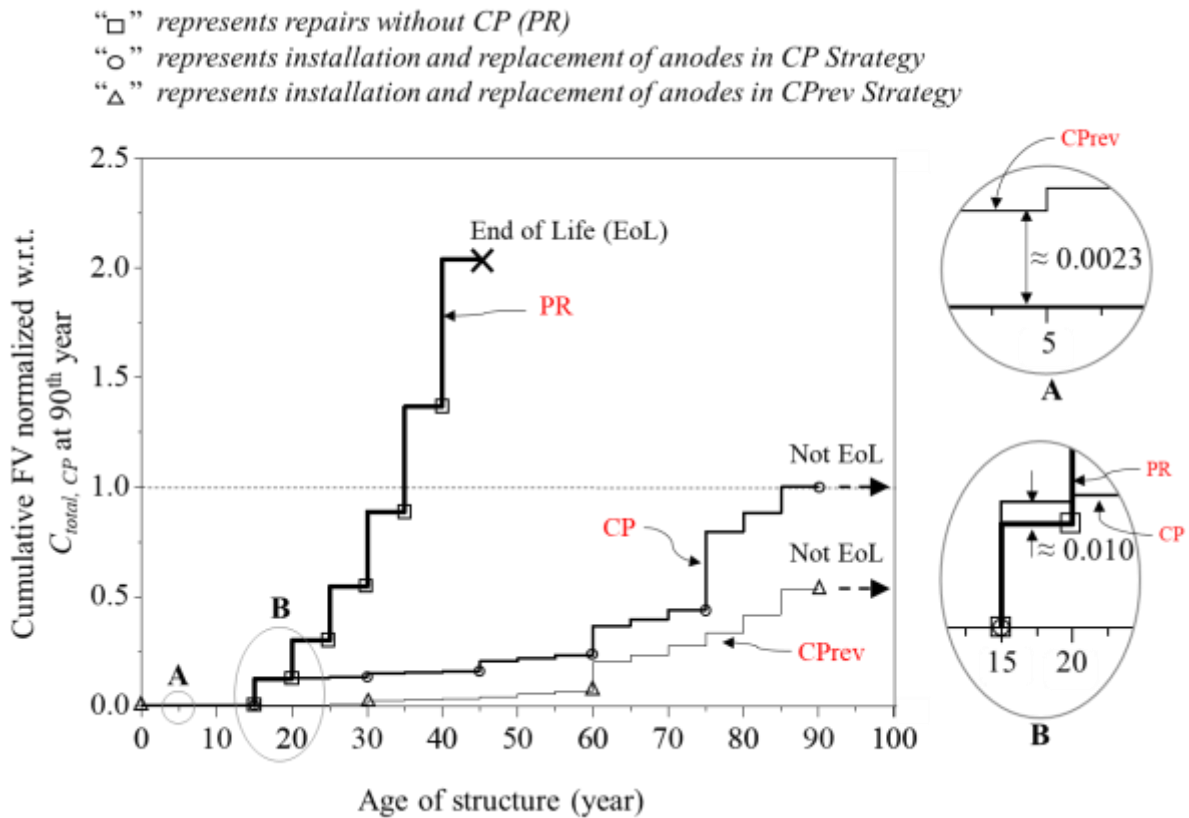
Figure 3.13: LCC of PR, CP, and CPrev strategies for the repair of Jetty in Chennai, India.

3.9   SAVINGS IN LIFE CYCLE COST

Table 3.1 shows the cost data for the 30 repairs with CP strategy in various sectors, such as jetty and ports, highway and bridges, industrial building. Using these data, LCCs of the 30 structures were calculated as per the framework proposed in Figure 3.11. Figure 3.14 shows the time-variant saving in LCC with the adoption of CP strategy over PR strategy for the 30 case studies. It shows that at the end of first repair, employing a CP strategy instead of PR strategy would lead to ≈7% more capital cost (mainly due to the additional cost of the anodes). Most often, engineers tend to decide against the CP strategy because of this small increase in capital cost. Considering only capital cost is not a suitable approach; and the decision on repair strategies must be made based on LCCs.

As shown in Figure 3.14, at the end of 5, 10, 15, and 30 years from 1st repair, the LCC saving with adoption of CP strategy is about 55, 75, 80, and 90%, respectively. After 20 years of repair, the rate of increase in LCC saving decreases and LCC saving becomes asymptotic to the time axis. Note that the LCC beyond 30 years after first repair is not calculated because the structures with PR strategy experience multiple patch repairs without arresting corrosion and reach their End of Life typically at about 30 years after first patch repair. After that, they get either demolished or replaced. Therefore, for corroding infrastructure, the CP repair strategy is clearly more economical than the PR strategy. Also, the present study discusses only the direct costs; if the indirect costs are considered, then the advantages of adopting CP or CPrev strategies over PR strategy would be further enhanced. However, data to estimate indirect costs were not available, hence kept out of scope of this study.

Table 3.1: Various cases studies on concrete structures with repair using CP in India

Type of structure	Location (State/Union Territory)	Year of anode installation	Number of anodes	Total cost of anodes at the time of repair (INR)
Jetty 1	Lakshadweep islands	2005	440	264,000
Jetty 1	Tamil Nadu	2008	1390	959,100
Jetty 2		2008	790	545,100
Jetty and approach bridge	Maharashtra	2009	1200	1,050,000
Jetty 3	Lakshadweep islands	2009	500	345,000
Jetty 4		2009	460	317,400
Jetty and fender columns	Gujarat	2010	225	249,975
Jetty deck slab beams 1	Goa	2011	400	376,800
Water treatment plant	Maharashtra	2014	1500	1,350,000
Industrial building 1	Gujarat	2015	40	52,000
Industrial building 2		2016	210	220,080
Staircase in a building	Puducherry	2016	86	193,500
Bridge 1	Gujarat	2017	240	289,920
Residential building		2017	453	449,829
Bridge 2		2017	61	61,000
Industrial building 3		2017	250	300,000
Public building		2018	180	199,980
Office building 1	Maharashtra	2018	910	1,274,000
Pipe rack 1	Gujarat	2018	600	720,000
Industrial building 4		2018	220	225,060
Industrial building 5		2018	200	220,000
Wastewater treatment tank		2019	131	236,455
Office building 2	Tamil Nadu	2019	50	50,000
Pipe rack 2	Gujarat	2019	500	600,000
Industrial building 6		2019	1316	2,500,400
Industrial building 7		2019	200	220,000
Water-treatment plant		2019	2837	6,388,924
Cooling tower		2020	9000	15,138,000
Jetty deck slab beams 2		2020	10000	12,000,000
Office building 3		2020	60	181,740
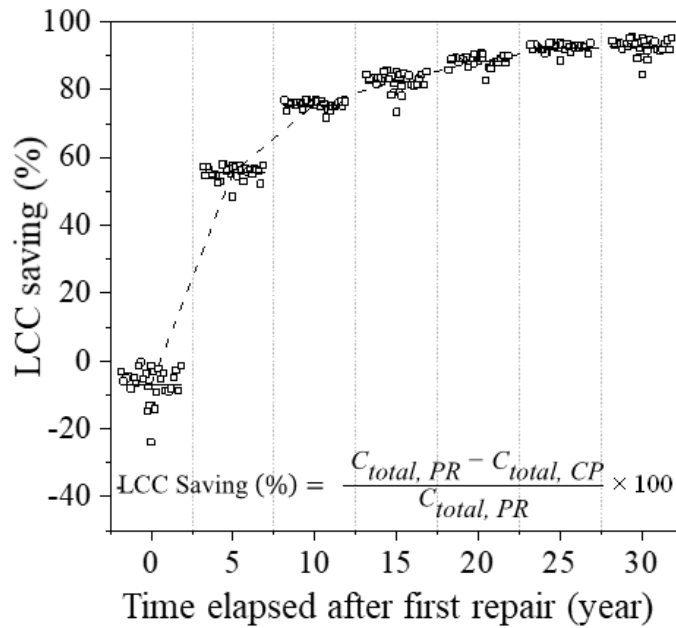
Figure 3.14: LCC saving due to CP strategy

3.10 SUMMARY AND WAY FORWARD

Conventional PR strategy alone may not arrest the corrosion due to halo effect and residual chloride effects – resulting in continued corrosion of structures leading to multiple and less durable repairs and eventual replacement of structures in a few decades. Adopting CP strategy (patch repair with galvanic anodes) is a viable and cost-effective option to extend the service life for multiple decades. Based on the experience in India, the following as the way forward for promoting CP strategy in the concrete repair industry: (i) to perceive galvanic anodes as a product that augments the performance of other concrete repair products rather than as a competitor, (ii) emphasize on the electrochemical advantages of CP strategy in stopping further corrosion/damage and the possibility of enhancing service life to as long as needed by less expensive replacement of anodes (iii) give more emphasize on the LCC benefits of CP strategy over the capital cost benefits alone of PR strategy, (iv) allow pilot studies on CP strategy in concrete repair works with provision for long-term monitoring of performance,

(v) incorporation of good performance-based specifications for CP strategy in the documents governing repair activities, especially in the public sector, and (vi) enable industry-supported academic research on CP strategies and use the performance data of anodes to enhance the codal specifications, in addition to the scholarly publications.

This page is intentionally left blank

4 INSTANTANEOUS PERFORMANCE ASSESSMENT OF CATHODIC PROTECTION SYSTEMS — FIELD STUDIES

4.1 INTRODUCTION

During the application of CP in concrete, controlling corrosion propagation and the subsequent formation of dense passive film in rebar depends on its effectiveness during the initial days of installation. This depends on many secondary electrochemical processes inside the concrete, which can be identified by obtaining the instantaneous performance of galvanic anodes in their early stage after installation.

This chapter provides the methodology of installing galvanic anodes, its performance assessment based on instantaneous tests, and a review of the present interpretation criteria of the existing test methods for assessing CP systems in reinforced concrete. First, a pilot study on the reinforced sunshades of a heritage structure built using lime mortar is provided. The details about the CP systems used, the methodology of installing galvanic anodes, and the monitored performance of the CP system based on depolarisation frequent tests are highlighted. Then, the installation of anodes in an apartment complex in Kolkata made of present-day reinforced concrete is presented. Followed by that, the monitoring and interpretation results from 12 monitoring boxes are shown. Finally, the drawbacks in adopting the existing test methodology for the modern reinforced concrete system with localized variation in resistivity are provided. Some of the content in this chapter is adapted from Krishnan, N., Veedu, Z.D., Shah, D. and Liao, H. "Hybrid anodes for accelerated cathodic protection of corroding concrete structures", published in *The Indian Concrete Journal*, (November 2021)Vol. 94, No. 11, pp. 101-110, in particular the figures and tables.

4.1.1 Factors affecting the design of CP systems in concrete

The performance of a CP system using galvanic anodes depends upon the resistivity of the concrete, corrosion rate of the steel rebars, output current density from the anodes, the geometry of the structure to be protected, and the corrosive environment in the encapsulating mortar. Figure 4.1 (b) shows the schematic of a typical galvanic anode with the encapsulating mortar. The pore structures, the alkalinity, and the buffer capacity of the anodes affect the rate of passivation and, of course, the long-term performance. A CP system has to be designed considering these factors. Therefore, there is no generalized design philosophy for implementing a CP system using galvanic anodes. In addition, a sound CP system demands proper installation and connection practices. The connection to the steel rebars should be such that there is no gap between the tying wire and the rebars (Figure 4.1 (b)). Also, the continuity of all the rebars and the connections to the anodes must be checked before placing the overlay material. In other words, the efficiency of a CP system to arrest corrosion, the time to achieve passivation of the steel, and its long-term performance cannot be accurately predicted with the available performance database.

More studies to understand the performance of the anodes during their initial days of installation have been conducted. To understand how CP systems work in various concrete environments, galvanic anodes are installed in two structures; a heritage structure in New Delhi, India, and an apartment complex in Kolkata, India. The test method as per the guidelines in ISO 12696: 2016 is used to assess the installed CP systems in these two structures. The details of these two cases studies are provided next.

| (a) Schematic of a galvanic anode with encapsulating mortar | (b) Proper connection between the anode and the steel rebars |
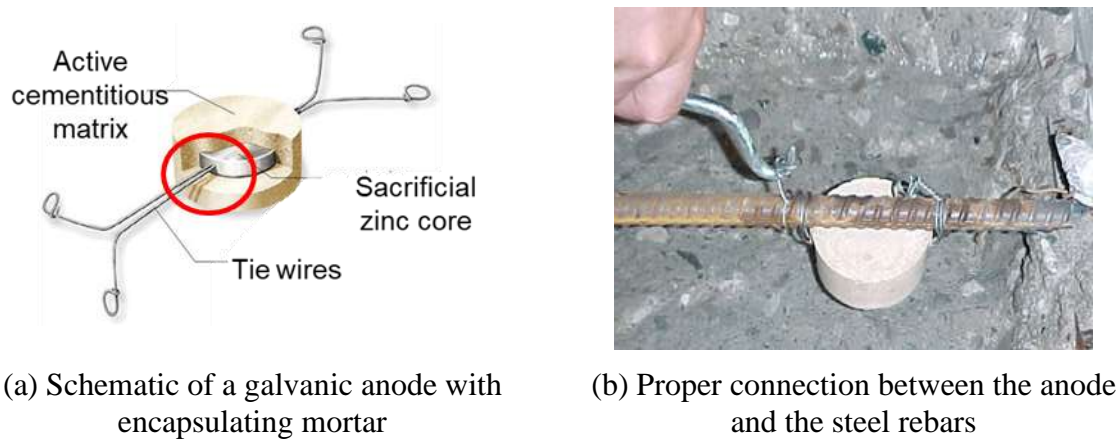
Figure 4.1: Factors affecting the performance of a CP system in concrete (Photo courtesy: Mr Haxie Liao)

4.1.2 Performance assessment of CP systems in concrete

Presently, the BS EN ISO 12696 standard is commonly used to assess CP systems in concrete. The assessment is based on different measured potentials from the CP installed concrete system, such as 'on' potential (E_{on}), 'instantaneous-off' potential ($E_{i\text{-}off}$), and depolarised potential (E_{24h}). The steel's corrosion potential (native half-cell potential) was measured using the installed reference electrode and a high impedance voltmeter before closing the circuit between the rebars and the anodes. The system is then switched 'on' (using the toggle switch in the monitoring box) to allow the current flow from the anode — the current passes through the resistor and the switch to reaches the rebars. After the system is stabilized, the output current from the system is measured by obtaining the potential difference across the resistor using a high impedance voltmeter. The output current density (in mA/m^2) is then calculated using Eq. (4.1).

$$\text{Output current density} = \frac{\text{Measured potential across the resistor}}{\text{Resistance} \times \text{Total surface area of all the rebars}} \qquad (4.1)$$

Figure 4.2 shows the schematic of a circuit system inside a monitoring box. The 'E$_{on}$' potential is the potential of the steel-anode system when the anodes are connected to the rebars. To obtain this, the potential difference between the Terminal 'S' and Terminal 'R' is measured while the circuit is closed. It is typically a more negative value than the 'Off' potential (corrosion potential of steel when the anodes are disconnected from the steel). One of the widely adopted criteria of protection specified in ISO 12696 (2016) is the 100 mV potential shift criterion. This is based on the ability of anodes to polarise the steel. The criterion is specified in terms of depolarisation of steel achieved within 24 hours. Potential shift refers to the amount of over potential applied to the steel by the anodes after eliminating the voltage drop across the concrete cover.
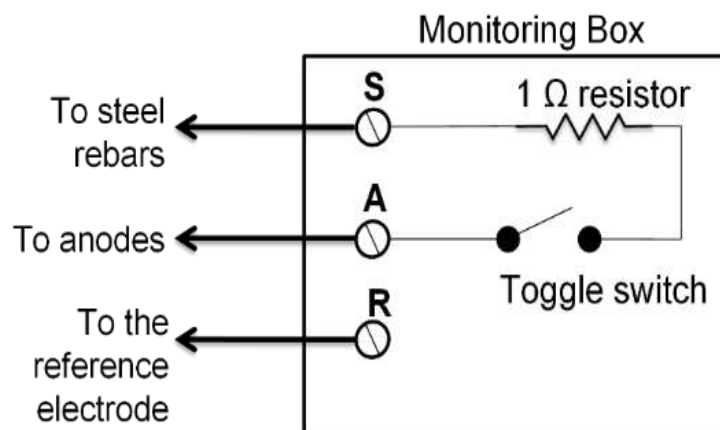
Figure 4.2: Schematic of the circuit inside a monitoring box

To eliminate the voltage drop across the cover concrete, the 'instantaneous off' potential is measured. This is obtained by measuring the potential of the steel immediately (within 0.1 s) after breaking the anode-steel circuit. In this case, the 'instantaneous off' potential is obtained by switching off the system and capturing the immediate drop in the potential difference between the Terminal 'S' and Terminal 'R' using a datalogger assembly.

The system is left in switch 'off' condition for 24 hours. The potential difference measured between the Terminal 'S' and Terminal 'R' after 24 hours in switch 'off' condition is considered the 24 h depolarised potential. Depolarisation tests were carried out at different intervals after the installation of the anodes.

4.2   CASE STUDY I – 100-YEAR-OLD HERITAGE BUILDING IN NEW DELHI

The heritage building considered for the study is the Rashtrapati Bhavan, the official residence of the President of India. Figure 4.3 shows the photograph of the $\approx$ 100 years old heritage structure. The building is located in New Delhi, the capital city of India. The structure is categorized as a Grade-I heritage structure and was previously built for the British Viceroy in 1919. The primary building materials used were the locally available brick and sandstones. However, the sunshades — $\approx$ 1.2 km around the periphery of the structure — were built using reinforced lime concrete with mild steel as reinforcement. Floral patterns were provided at the bottom of the weather shade for aesthetic purposes. Over the years, the steel reinforcement deteriorated due to corrosion and heavy spalling of the weather shade's cover concrete. Adequate electrochemical repair treatment was necessary to protect and preserve the structure (Joseline et al. 2019a).

Figure 4.3: Pilot Project site at the heritage structure in New Delhi (Photo courtesy: CPWD, Rashtrapati Bhavan)

4.2.1 Description of the weather shade

Figure 4.4(a) shows the photographs of the sunshade of the heritage building constructed in 1919. Unlike modern concrete, the sunshade is made of lime mortar with mild steel reinforcement. There are layers of plaster at the top and bottom. Grooves are imprinted both at the top and bottom to generate the appearance of stone slabs (Figure 4.4(a)). The sunshade is painted brick in colour, and the floral patterns as yellow. In the past, there has been corrosion of reinforcing bars and delamination of plaster or concrete. However, repairs with mortar or micro-concrete have been undertaken and failed prematurely, leading to repeated repairs of the sunshade (Figure 4.4(b)). Therefore, a cathodic protection system was proposed to implement on the sunshades to mitigate repeated repairs. However, there has been no evidence of the effectiveness of galvanic anodes CP systems on lime mortar. A pilot study on a representative location was conducted using various galvanic anode systems. The details of the pilot study, such as condition assessment before repair work, the methodology for installing galvanic anodes, and the assessment conducted after the repair, are provided in the subsequent section.

(a) Corroded and spalled weather shade indicating the failure of earlier repair.

(b) Past repair interventions with polymer-modified cementitious mortar was not successful

Figure 4.4: Photographs showing the condition of the weather shade and the petals before repair.

4.2.2 Condition assessment of the sunshade

4.2.2.1 Visual inspection

The sunshade was exhibiting severe corrosion in the corners of the building. This was attributed to the presence of a water fountain at the terrace in these locations. Since there has been a history of many repair interventions, many locations that may be corroding were not appropriately identified. Figure 4.5 (a) shows the photograph of the sunshade during the site inspection. The concrete looked intact, and the painted petals were visible. However, some regions of the sunshade showed a level difference. Therefore, a few areas were chipped/chiselled to see the condition of the rebars inside. Surprisingly, when concrete was removed from few places, it was observed that all the rebars were corroding (Figure 4.5 (b)). This is because of the hidden corrosion due to the halo effect. Hence, a full-fledged condition assessment was conducted on the sunshades.

| (a) Before removing the cover concrete, the sunshade looked neat and clean from the outside | (b) After removing the cover concrete, all rebars were corroded — a classic example of hidden corrosion in a patch repaired area of concrete. |

Figure 4.5: Condition of the sunshade immediately before and after removing the cover concrete — indicating that visual observation alone may not always capture the ongoing steel corrosion

4.2.2.2   Half-cell potential measurement from the sunshade

Half-cell potential (HCP) measurements were carried out at representative locations to assess the probability of corrosion in the weather shade (Elsener et al. 2003b). A grid of 0.15×0.15 m is marked on the surface of the weather shade, and a commercial half-cell potential recorder (see Figure 4.6(a)) is used to map the potential of the steel from a grid A copper-copper sulfate (CSE) reference electrode was used to obtain the potential of the rebars in most locations. In addition, saturated silver chloride (Ag/AgCl) KCl (SSCE) reference electrodes were embedded in the concrete at a few locations; these electrodes can eliminate most of the IR drop between the cover concrete and more accurate potential corresponding to the actual open circuit potential (OCP) of the steel rebars can be obtained.

It is evident from the frequent spalling of the cover concrete that corrosion has already been initiated at most locations. Therefore, the corrosion rate of the rebars was measured at random locations to understand the extent of corrosion. For this, a commercial instrument that works on the linear polarisation technique, such as Gecor 8 (see Figure 4.6(b)), is used (Andrade and Alonso 2004). The Gecor 8[TM] works use the guard rings technique to confine the perturbation current within a certain critical length and obtain the resistance to corrosion at that confined area. Then, the corrosion rate is found using Tafel extrapolation methods (Feliu et al. 1990). Furthermore, the resistivity of the concrete was obtained using a Wenner-four probe machine.

| (a) Half-cell potential meter and reference electrode (Canin +) | (b) Corrosion rate meter and sensors (Gecor 8 TM) | (c) Resisitivity meter (Wenner four probe) |

Figure 4.6: Instruments used for condition assessment of the sunshades

4.2.2.3   Results from condition assessment

Figure 4.7 shows the results of the HCP test plotted as a contour of the corrosion potential from a 10 m stretch at the North-East corner of the structure. It was observed that the structure exhibited heavy corrosion in the selected 10 m stretch. The region where concrete was found to be intact showed a potential more negative than –350 mV_{CSE}, which corresponds to the greater than 90% probability of corrosion. Also, a few places with more positive potential — in the range of –100 to –150 mV_{CSE}. However, further investigations on the more positive potential revealed that the cover concrete at these regions is cracked — leading to a discontinuity in the electrolyte and a more positive corrosion potential.
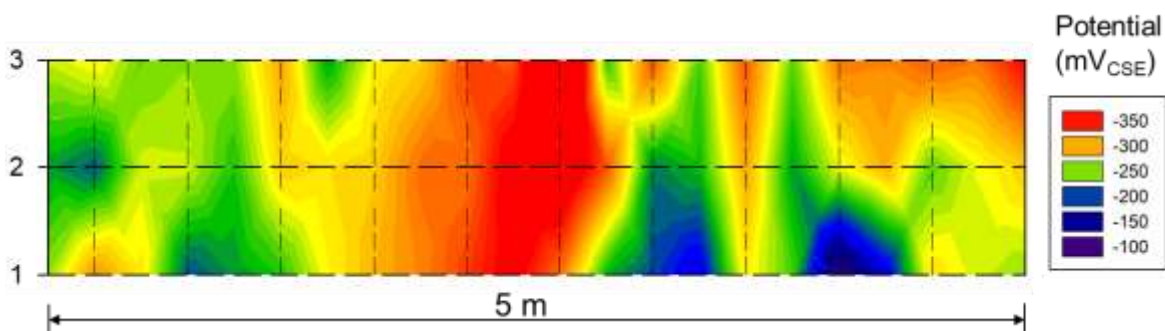
Figure 4.7: Corrosion potential of the rebars before the installation of galvanic anodes

Additionally, the corrosion rate measurements from the steel show that the rebars are corroding with a whooping corrosion rate of ≈ 5 mA/m^2 in most locations. However, the resistivity of the concrete was measured to be ≈ 100 kΩ·cm, which is significantly high for concrete. In other words, corrosion can be due to the change in the microclimate around the steel rebars inside the concrete; a change in pH can be a possible reason for corrosion in this case. Therefore, a more detailed analysis of the concrete samples is performed in the laboratory and is described next.

4.2.2.4   Evaluation of mortar samples

Mortar samples of lateral dimension 3 cm and thickness 1 cm were collected from various parts of the sunshades. Carbonation studies were conducted on these samples by spraying phenolphthalein indicators (Joseline et al. 2019a)(Gopal and Sangoju 2020). Figure 4.8 shows that no change in the colour of the mortar samples was observed after spraying the phenolphthalein indicator. In contrast to the common cases of chloride or carbonation-induced corrosion, the adverse condition of the steel rebars was due to the low pH (less than 9.5) of the embedding concrete. Also, Joseline et al. (2019) conducted an X-ray diffraction (XRD) test on the collected samples and observed that hydraulic peaks are absent in the XRD patterns. Thus, the non-compatibility of lime concrete with mild steel could be the reason for the carbonation of the material.

| Freshly fractured piece of concrete | Phenolphthalein test being performed |
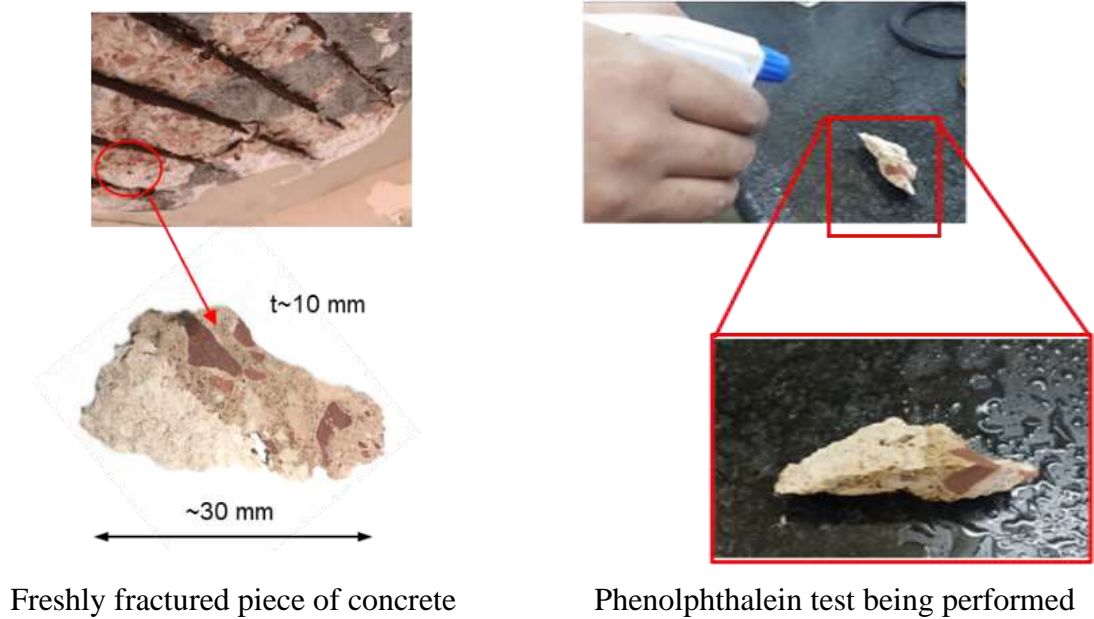
Figure 4.8: Initial corrosion assessment tests on mortar samples

4.2.3 Cathodic protection of reinforced lime concrete weather shade

The following sections of the chapter present the detailed methodology of installing anodes and interpretation of monitored corrosion potential measurements. The results based on the calculated corrosion rate indicate that two of the systems experimented with could re-passivate the embedded steel and can be adopted to protect the entire sunshades.

4.2.4 Pilot study using galvanic anodes

Previous repair interventions such as conventional patch repair had been carried out in the past. This accelerated the corrosion at the adjacent areas, and the spalling of cover concrete became more severe after repair. Because the structure is of national importance, it was necessary to passivate the steel and control corrosion immediately. Implementing an impressed current cathodic protection (ICCP) system was not practically possible because of the limited accessibility for periodic inspection in all the repair areas in the structures. Therefore, CP using

galvanic anodes was installed to control corrosion in the sunshades. After the preliminary inspections and condition assessment using various corrosion assessment instruments, a pilot study on cathodic protection (CP) of weather shade was conducted as this is the first of its kind of application of CP in lime-based concrete. The pilot study was conducted on a 10 m long stretch of the reinforced lime concrete. The objective of the study was to understand the feasibility of implementing a full-scale cathodic protection (CP) system as a corrosion mitigation technique for sunshades. The performance of four anode systems (combinations of two types of anodes and two configurations) was assessed.

4.2.5 Design of cathodic protection systems for the sunshades

A representative location of 10 m $\times$ 2 m (length $\times$ width) was selected for installing a monitoring box to assess the performance of the anodes. During the visual inspection of the deteriorated weather shade, it was observed that the rebars in the weather shade have a spacing of about 50 to 70 mm. The steel density ratio (ratio of the surface area of steel to the surface area of concrete) of the sunshades was ≈ 0.75. Two types of galvanic anodes were used to check the efficiency of CP in lime concrete — (i) conventional zinc-based anode and (ii) a two-stage hybrid anode (see Figure 4.9). For representation purposes, these anodes are denoted as Type I and Type II, hereafter.

(a) Type – I (Conventional galvanic anode)

(b) Type – II: (Two-stage hybrid galvanic anodes)

Figure 4.9: Types of galvanic anodes used in the pilot project

To design the CP system using these anodes, it is assumed that the zinc metal in the Type I anodes should be supplying a cathodic current density of 4 mA/m^2 for 20 years. In contrast, the output current density from the Type II anodes varies during the initial days of installation and in the long term. Therefore, a cathodic current density of 20 mA/m^2 is assumed for the initial days (three months) and 2 mA/m^2 for 19.7 years. Then the required net mass of the anode metal is calculated using Eq. (4.2).

$$\text{Required total mass of zinc (kg)} = \frac{K \times \text{SD} \times I_{output} \times 1000 \times \text{SL}}{\eta_{efficency} \times \eta_{utilisation}} \tag{4.2}$$

where, K is the electrochemical equivalence of zinc metal, kg/A-year; SD is the steel density (ratio of the area of the curved surface area of steel rebars and surface area of concrete); I_{output} is the design cathodic current output from the anodes; SL is the design service life of the anodes/repair; $\eta_{efficency}$ is the efficiency factor, and $\eta_{utilisation}$ is the utilisation factor. Anode efficiency factor accounts for the inefficient distribution of the protection current in the concrete. The utilization factor accounts for anode material consumed when the remaining

material cannot deliver the required current. The number of anodes and the spacing between them is then obtained by dividing the total required mass of the zinc by the mass of the zinc metal in the hybrid anode.

4.2.6 Installation of galvanic anodes in the weather shade

A total of 44 numbers of Type I anode and 28 numbers of Type II anodes were installed in the 10 m stretch of the weather shade. Altogether, four CP systems (System 1, 2, 3, and 4) are experimented on the 10 m stretch of the weather shade using the two types of anodes varying the spacing between them. Table 4.1 summarises the types of CP systems used in the pilot project. System 1 and 2 constitute the Type I anodes with maximum spacing between the anodes as 750 mm and 550 mm, respectively. Conversely, System 3 and 4 consists of Type II anodes with maximum spacing between the anodes as 700 mm and 600 mm, respectively. Figure 4.10 shows the installation of galvanic anodes on the weather shade using the obtained layout as per the design of the CP system.

A checklist document containing the procedures to be followed during the repair was prepared before the repair start. This checklist was helpful to follow the progress of the repair and enabled accessible communication between the researchers and site engineers. The same is provided in Appendix B of this thesis. The anodes were connected in series and are installed in the designated saw-cut chases on top of the weather shade. These chases are then covered with a low resistive repair mortar with anodes embedded to ensure adequate ionic movements. Detailed procedures of repair and the installation of anodes are provided in Appendix B of this thesis.

Figure 4.10: Installation of galvanic anodes in saw-cut pockets on the weather shade

Table 4.1: Types of systems used in the pilot project

System No.	Span (m)	Type of anode used	Number of anodes	Spacing	
				Vertical (mm)	Horizontal
System 1	3.0	Type I	20	500	12 anodes @ 500 mm c/c
					8 anodes @ 750 mm c/c
System 2	2.0	Type I	24	500	14 anodes @ 333 mm c/c
					10 anodes @ 500 mm c/c
System 3	2.6	Type II	11	700	5 anodes @ 500 mm c/c
					6 anodes @ 750 mm c/c
System 4	2.4	Type II	17	700	7 anodes @ 400 mm c/c
					10 anodes @ 600 mm c/c

4.2.7 Testing and monitoring of the cathodic protection system

Figure 4.11 and Figure 4.12 show the galvanic anodes' layout and the various electrical connections extended to the monitoring box from Systems 1, 2, 3, and 4. All the steel rebars

in the 10 m stretch are interconnected using external wires to ensure electrical continuity between rebars. All the connections from the anodes and the steel rebars are then extended to the monitoring boxes. A saturated silver/silver chloride (Ag/AgCl) KCl reference electrode was embedded in the concrete to enable potential and current measurements. The lead wire from the reference electrode is also extended to the monitoring box. After establishing all the connections, a thixotropic repair mortar is placed on the top of the weather shade to embed the anodes entirely in concrete.

Based on the observations from previous laboratory and field studies, it is understood that switching from Stage 1 to Stage 2 for the Type II anodes occurs in about three months. The time at which the shift from Stage 1 to Stage 2 occurs depends upon the number of anodes installed and the current demand. Therefore, to capture the stage switch shift of the Type II anodes, more frequent tests were carried out during the first 100 days. Later it was limited to one in every six months. The potential measurements were obtained using the Ag/AgCl reference electrode. However, the E_{on}, E_{24h}, and $E_{i\text{-off}}$ are expressed in millivolt copper/copper sulphate reference electrodes (mV_{CSE}) for representation purposes. A datasheet for recording the various potential measurements from the site is prepared and is provided in Appendix B of this thesis.

Two monitoring boxes were set-up in near the pilot project site. Inside one monitoring box, a one-ohm resistor and a switch were connected in series — between the wires from anodes and steel — to monitor the current output from the anodes and the various potential values. Figure 4.13(a) shows the photograph of one of the monitoring boxes installed at the site, and Figure 4.13(b) shows a schematic of the various connections inside the monitoring box. The lead wire from the interconnected rebars is connected to the Terminal 'S'. Similarly, lead wires from all anodes are connected to Terminal 'A', and the wire from the reference electrode is connected to the Terminal 'R' in the monitoring box.
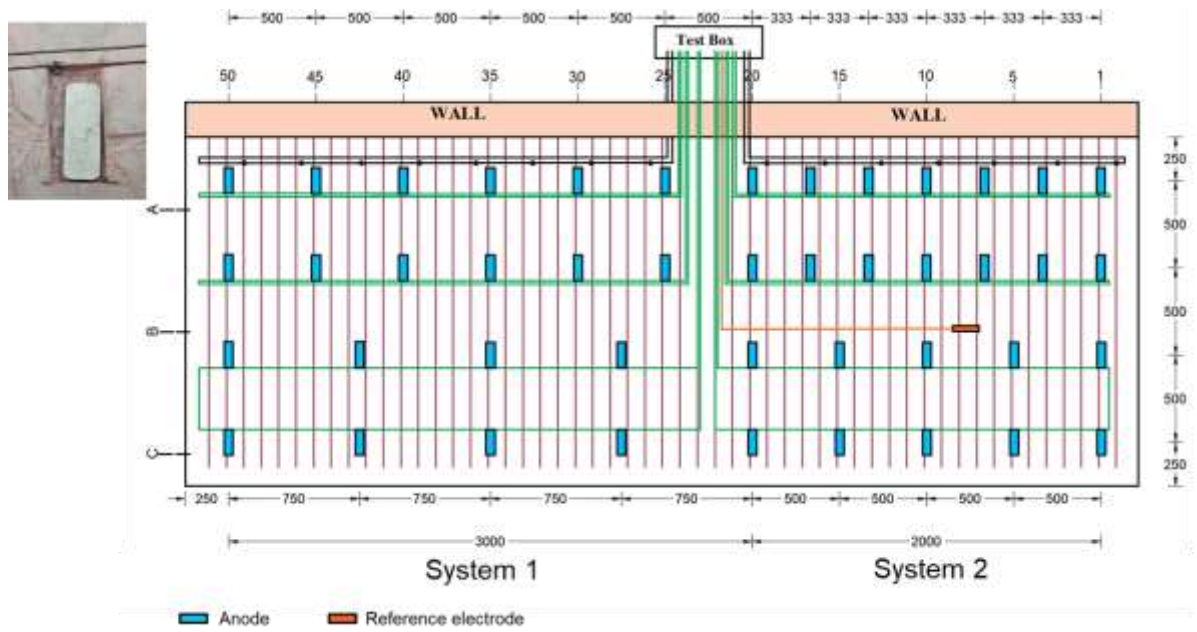
Figure 4.11: Layout of systems 1 and 2 with Type I anodes
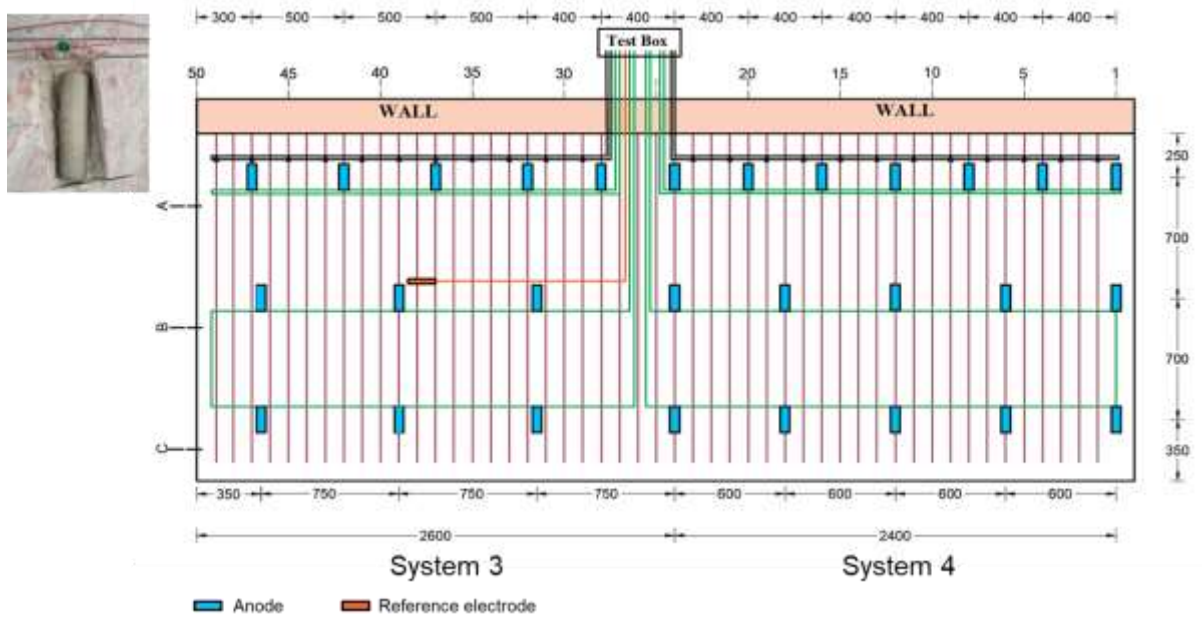
Figure 4.12: Layout of systems 3 and 4 with Type II anodes

(a) Photograph of the monitoring box
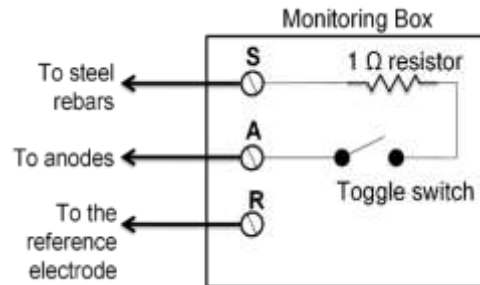
(b) Schematic of the circuit connection inside the monitoring box

Figure 4.13: One of the installed monitoring boxes on the inside face of the parapet wall

4.2.8 Results and discussions

Figure 4.14(a) and (b) show the E_{on} potential variation as a function of time for Systems 1, 2, 3, and 4 during the first 100 days of installation. In this period, the E_{on} of the Type I anodes remained almost the same at ≈ -1200 mV$_{CSE}$ for System 1 and ≈ -700 mV$_{CSE}$ for System 2. Whereas the E_{on} in System 3 and System 4 increased to a more positive value with time. The E_{on} of the Type II anodes dropped from ≈ -2500 mV$_{CSE}$ to ≈ -1500 mV$_{CSE}$ and ≈ -1500 mV to ≈ -800 mV in System 3 and System 4, respectively, within 100 days after installation. When the depolarisation tests were extended to another two years, the drop in E_{on} was significant, and all the Systems exhibited a potential ≈ -100 mV. Figure 4.15(a) shows the variation in E_{on} potential from one location in the Type I and Type II anodes.
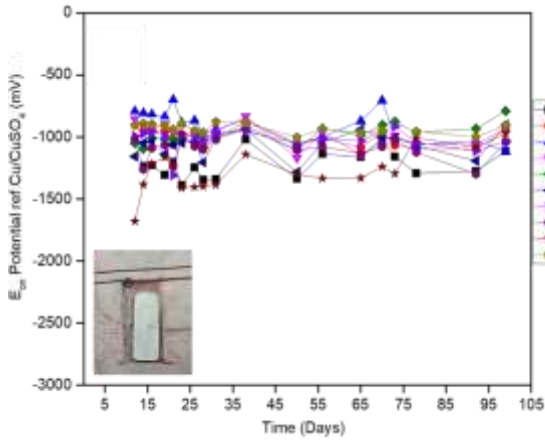
(a) E_{on} of Type I and anodes at various locations.
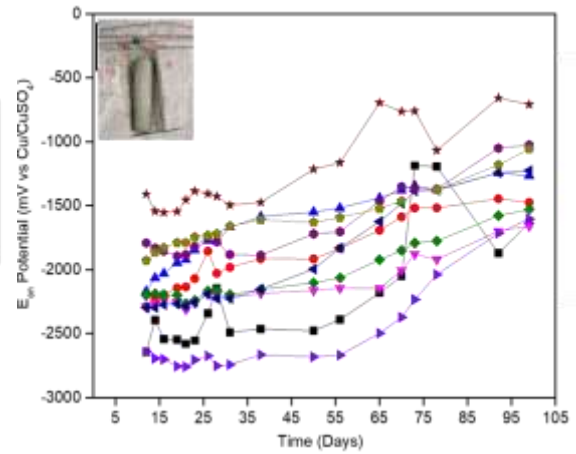
(b) E_{on} of Type II anodes at various locations.

Figure 4.14: Change in E_{on} potential with time (till 100 days). Legends in the graph represent the test locations (see Figure 4.11 and Figure 4.12)

Correspondingly, a falling trend in the output current density from the anodes was observed during this period (see Figure 4.15(b)). The output current density from Type I anodes decreased from ≈ 5 mA/m^2 to ≈ 0.3 mA/m^2, whereas Type II anodes decreased from ≈ 12 mA/m^2 to ≈ 0.3 mA/m^2 by the end of 800 days. As the anodes continue to polarise the steel rebars, the secondary effect of CP causes passivation of rebars and hence the demand for cathodic current density decreases. Here the value of resistance used in the monitoring box was one-ohm, and the total surface area of the steel was obtained as 2.665 m^2.
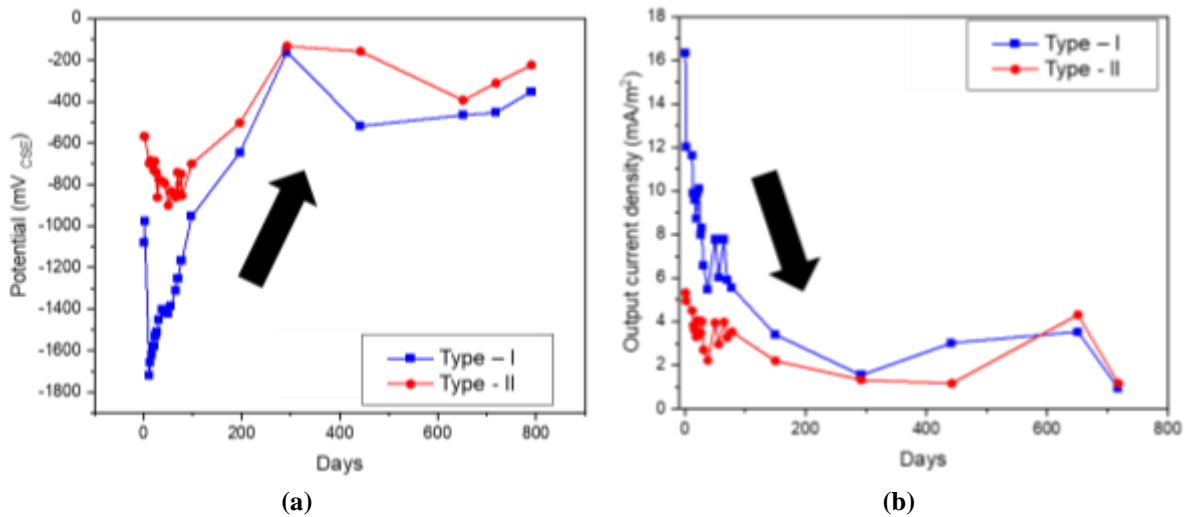
Figure 4.15: (a) Change in Eon potential with time (b) Change in output current density with time

Here, an important observation is the variation in output current density from Type II anodes (see Figure 4.16). Type II anodes are designed to provide an output current density of 20 mA/m^2 during the first three months, and the remaining time the galvanic anode system in the Type II anodes supply a current of 4 mA/m^2. After about 150 days, the current density from the Type II anodes starts decreasing to less than 4 mA/m^2. This indicates a possible stoppage of the ICCP system in the Type II anodes. However, since the output current density is the cumulative effect from all the installed anodes, it is difficult to capture the exact time the stage shift takes place in a specific Type II anode. For instance, even if the ICCP in one set of anodes has stopped, the effect of a working ICCP system in the anodes connected in series with the previous anodes will contribute to high output current density.
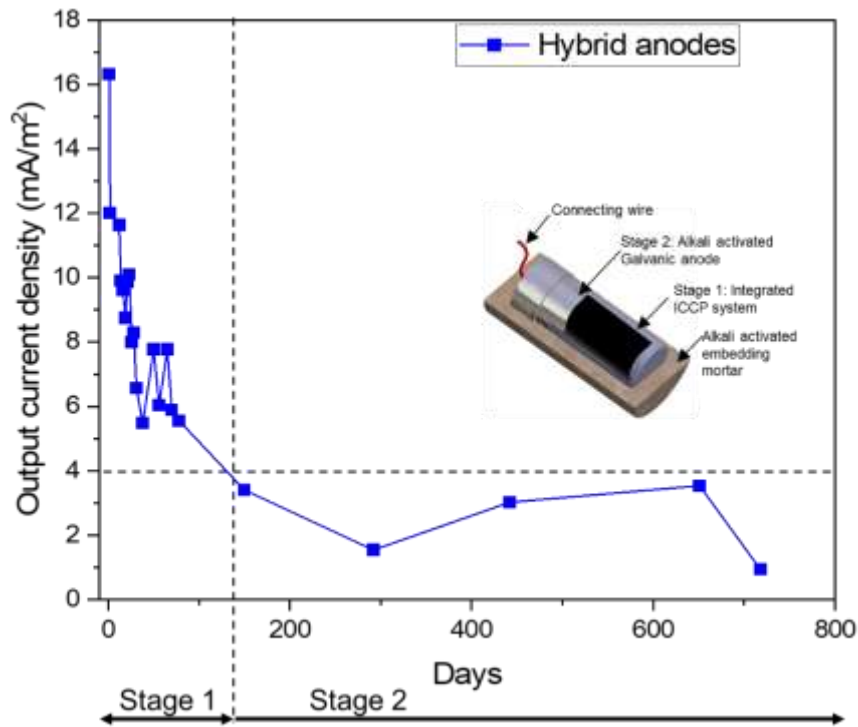
Figure 4.16: Output current density from the Type II anodes — stage shift occurred around 150 days after installation

Figure 4.17 (a) shows the variation of the obtained depolarised potential after every depolarisation test. An increasing trend (towards the more positive direction) was observed in the 24-hour depolarised potential of the steel rebar obtained at different time intervals from both the anode types. In Type I anodes, the 24 h depolarised potential of the steel increased from −225 mV on the 30th day to −295 mV on the 200th day. The corresponding change in Type II anodes was −315 mV on 30th day to −455 mV on the 200th day. After that, the depolarised potential started to decrease and remained as a more positive value. At the end of the 200th day, E_{24} decreased to less than −350 mV_{CSE} for both types of anodes; −350 mV_{CSE} is the cut-off value for 90% probability of corrosion as per ASTM C876 [27]). The high negative potential during the initial days can be due to the lack of attainment of complete depolarisation in these rebars during this period. The anodes work efficiently during their early installation period that more time is required for the complete depolarisation. The fact that the E_{24}

91

decreases to less than –350 mV substantiates the statement on the steel passivation in the CP installed area.

(a)   (b)
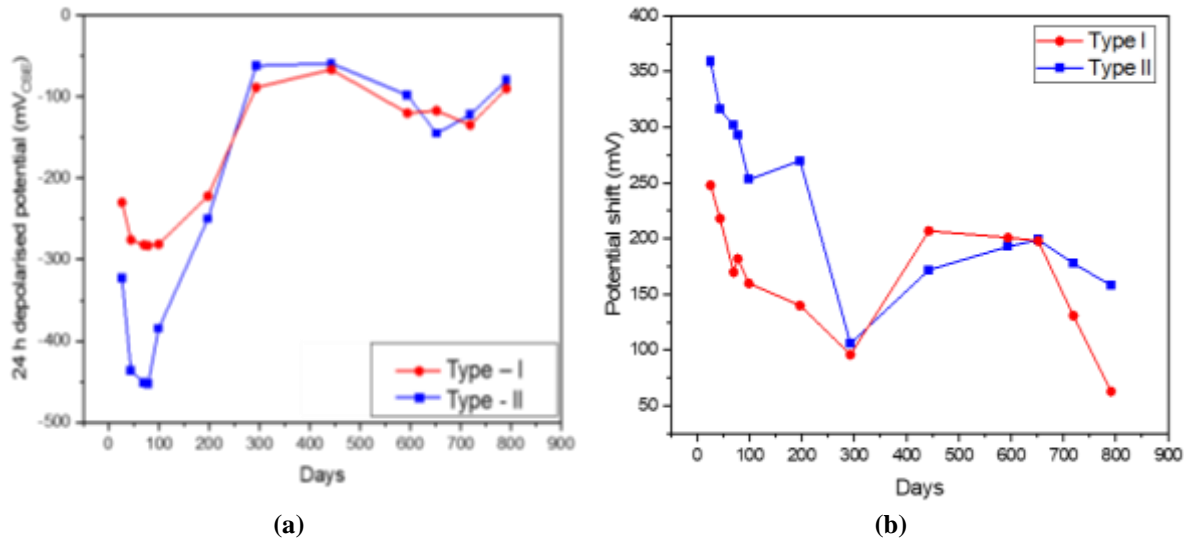
Figure 4.17: (a) Change in E₂₄ potential with time (b) Change in potential shift with time

Further, to understand the polarizability of the anodes on steel, the potential shift is obtained. Figure 4.17 (b) shows the variation in potential shift obtained at different intervals. For the Type I anodes, the potential shift varied from $\approx$ 250 to 165 mV during the initial days of installation (till 100th day), while for Type II anodes, the values were 350 on the 30th day and 250 mV. A sudden increase in the potential shift was observed on the 100th day for Type II anodes because of the more positive 24 h depolarised potential (-201 mV) obtained during this period (see Figure 4.17 (a))). After 300 days, it was observed that the anodes were still able to provide the 100 mV potential shift — recommended minimum potential shift by the ISO 12696 standard. This indicates that the installed CP system can protect the steel rebars throughout the testing period (till 650 days). Also, the 100 mV potential shift is obtained even though the output current density is in the range of $\approx$ 2 mA/m². This again confirms the passivity of all the steel rebars because of the lower current demand from the anodes. It is noted that, in a

recent site inspection, it is observed that no new crack or spalling of concrete has occurred in the CP installed areas since the installation of the CP system. This confirms the efficiency of the installed hybrid anodes in the RC structure.

The results show that the CP systems with Type II anodes performed better than the CP systems with Type I anodes. Therefore, the Type II anodes — that works on the two-stage process — can be used for the actual repair. Nevertheless, the design optimisation of the installed anodes was not conducted because of the lack of real-time monitoring results. Also, the variability in the potential measurements was not considered in this study as the potential measurements are obtained using a single embedded reference electrode. More data points need to be obtained to statistically analyse the variability in the measured potentials (E_{on}, $E_{i\text{-}off}$, and E_{24h}, etc.); these potential values vary depending on the atmospheric temperature, humidity, and steel corrosion rate. Numerical simulation of the cathodic protection can be a useful tool to optimise the design. This requires more understandings of the thermodynamic and kinetic properties of the two-stage galvanic anodes.

4.3 CASE STUDY II – FIVE YEAR RESIDENTIAL BUILDING IN KOLKATA

4.3.1 Description of the site

Figure 4.18 shows the photograph of a residential building (Case study II) cast using an M30 concrete mix in Kolkata. The complex houses nine towers denoted as Tower A, B, C, D, E, F, G, H, and J. The buildings were constructed during the period 2008-2013. They have reinforced concrete framed structures with masonry walls, consisting of buildings with varying heights, and connected with a common basement. Within five years after the construction, structural deterioration such as corrosion-induced delamination, an inadequate cover of concrete, leakage of water and dampness, and cracks on structural members were observed at many buildings. It is reported that the repairing work in the form of restoration of RC members at various floors using micro concrete technique was conducted in the past. However, cracks were observed at many locations adjacent to the completed repair works — indicating hidden corrosion throughout the structure.

Figure 4.18: Apartment complex in Kolkata (constructed during 2008 – 13)

4.3.2 Condition assessment of the apartment complex

From the visual inspection, rampant corrosion was observed throughout the structure. Figure 4.19(a) shows the condition of a staircase ceiling on the 3rd floor of one of the buildings. Figure 4.19(b) shows the photograph of the structure when the cracked concrete from a column was completely removed. Here, despite being an interior column on the 6th floor of the building, the rebars are corroding – which is very unlikely for a 5-year-old structure. Also, during the visual inspection, it was observed that the thickness of the cover concrete is inadequate in many locations, especially on the basement floor of all the towers.

The half-cell potential of the rebars was obtained from representative random locations of the structure. Figure 4.20 shows the HCP map of Column 7 at the basement of Tower D. Moreover, similar contour plots are obtained from all the locations wherever corrosion potentials are mapped. In addition, concrete samples are taken to analyse the presence of chloride in the concrete. For this, the standard method to obtain the chloride content in concrete as per the SHRP 330 was used (SHRP-S-330 1993).

| (a) Spalled concrete from a ceiling slab on the 3rd floor of Tower D | (b) Rebars were corroded when the cover concrete of a cracked RC column –on the 6th floor of Tower E – is chipped off. |

Figure 4.19: Observations during visual inspection

The half-cell potential data and the water-soluble chloride content test show a high probability of corrosion and a high chloride content (more than the threshold limit). More than 25% of the representative samples tested for chloride content showed results beyond the ACI 318 in 2014 (Holland 1998) permissible limit of 0.6 kg of Cl^- per m^3 of concrete. In addition, carbonation tests were also conducted on the collected concreter samples. The depth of carbonation seems less than about 5 mm in most cases. This means that the actual cause of corrosion is the ingress of chloride. Since chloride-induced corrosion can lead to a localised cross-sectional loss in rebars, there was an immediate need to passivate/arrest the corrosion to preserve the structure.
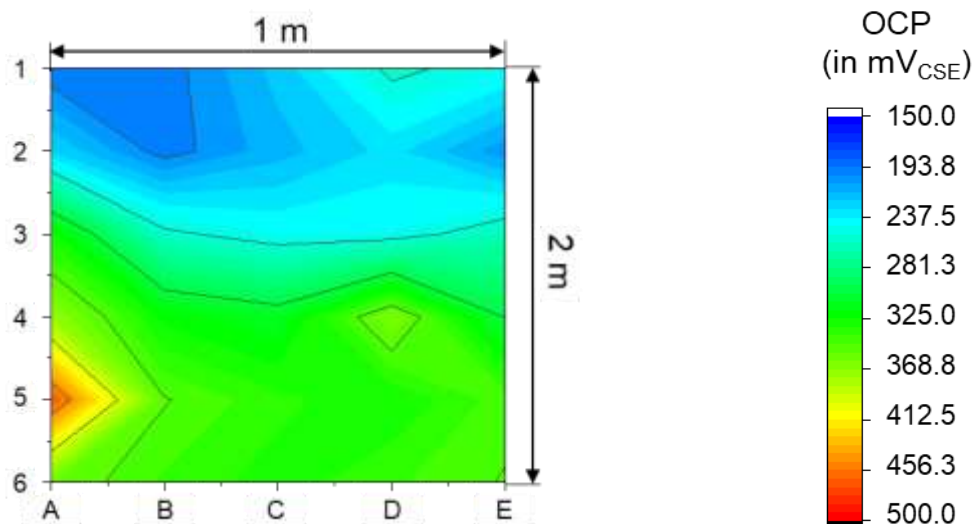
Figure 4.20: E_{on} potential obtained from the surface of a rectangular concrete column in Tower D

The best repair approach would be to remove the chlorides from the concrete (say, chloride extraction technique). However, this poses serious practical difficulties. Also, it is practically impossible to keep all the structural members free from moisture (sources of moisture could be wet ground, rain, bathroom, drainage pipes, etc.). The application of corrosion inhibiting coatings on all the rebars (in cracked and uncracked regions) may not be feasible at this stage. Also, coatings may not arrest further corrosion of the rebars in the regions

without cracks and spalling but with hidden corrosion. Considering all these scenarios, it was decided to implement cathodic protection (CP). Because these members have a high probability of corrosion, an impressed current cathodic protection (ICCP) system is preferable. However, considering the requirement of skilled personnel for monitoring the performance and maintaining the system, ICCP may not be viable for the long-term protection of housing units, where the maintenance staff may not be skilled and may keep changing. Therefore, galvanic anodes were installed in these structures to arrest further corrosion. However, since the structure is constructed with significantly high resistive concrete (constructed in 2012), three types of anodes are tested for their effectiveness. The methodology of installation of galvanic anodes and monitoring boxes are discussed next.

4.3.3   Installation of galvanic anodes in the apartment complex

A galvanic anode cathodic protection system was used for the installation based on the conclusion from a pilot project. The details of the pilot project and the obtained performance data are presented in Appendix C. Figure 4.21 shows the Type III galvanic anode used for the study. The study was conducted to determine whether the spacing provided is adequate to prevent further corrosion of the rebars. Also, the present testing method was evaluated using the monitored data from these anodes. The installation of the monitoring boxes and recording the measurements were carried out in three phases.

Figure 4.21: Type III galvanic anode used for Case study II

(a) Tower 8	(b) Between tower 6 & 7	(c) Between tower 3 & 4	(d) Tower 3	(e) Tower 1

(f) Tower 8	(g) Tower 8

(h) Between towers 3 & 4	(i) Between towers 3 & 4	(j) Between towers 8 & 9	(k) Between towers 3 & 4

Figure 4.22: Photographs of the locations where monitoring boxes were installed

In the first phase, monitoring boxes were installed on three columns (C1, C2, and C3), three retaining walls (RW1, RW2, and RW3), and three slabs (S1, S2, and S3) during September 2019. In the second phase, monitoring boxes were installed in five additional columns (C4, C5, C6, C7, and C8) during October 2019. The observations from the monitoring boxes installed during the first and second phases (excluding C4, C5, C6) are recorded and analysed to understand the efficiency of the installed CP system in the buildings. Figure 4.22 shows the locations where the monitoring boxes are installed. The points wherever an anode is installed are highlighted in the respective images of the structural members.

Figure 4.23 shows the circuit diagram (typical) for assessing galvanic anodes in this case. The monitoring box has terminals that house the wires from the anodes, rebars (cathodes), and the embedded reference electrode. In each structural member, five adjacent anodes are connected (series connections) using external wires to be sent to the monitoring box. The half-cell potential values were measured using a portable copper/copper sulphate reference electrode instead of an embedded reference electrode. Also, the wire from the rebars and anodes are connected to the resistor without any toggle switch in between. Switch OFF and ON of the system is carried out by unscrewing the wires from the terminal manually. In addition, the efficiency of the installed CP systems was assessed using the passivity verification test (PVT), and the results of the same are presented in Appendix C. In addition, some of the photographs that shows misplaced anodes during the time of installation are shown in Appendix C.
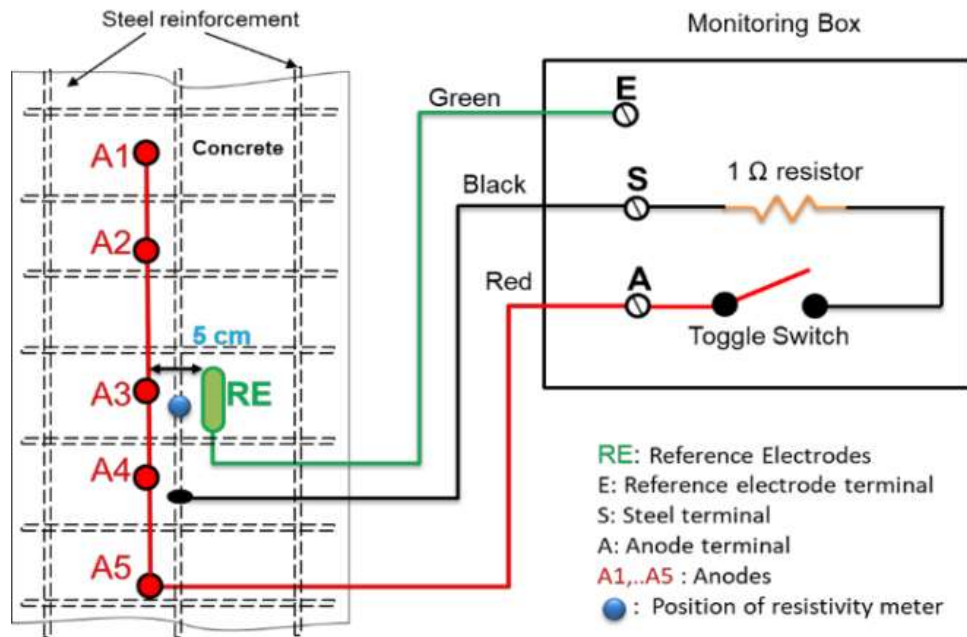
Figure 4.23: Circuit diagram for monitoring the performance of anodes

4.3.4 Results and discussion

The test method as per EN ISO 12696 was used to understand the efficiency of the installed anodes at distinct locations in the site using monitoring boxes. Locations where structural member/element exhibited a corrosion potential of –200 mVCSE or more negative, are selected to install these monitoring boxes. More than 30 monitoring boxes were installed and are being monitored. Here, the results obtained from a selected 12 monitoring boxes are used for assessing the installed anodes. The base potential of each test location was recorded before switching the CP system 'ON'. The data obtained from the monitoring boxes include the mixed potential of anodes and rebars (E_{on}), the 'Instant Off' potential and 'Depolarised potential', and the output current from the connected anodes. E_{on} potentials are recorded once every seven days from all the installed monitoring boxes. Figure 4.24 and Figure 4.25 shows the E_{on} potential reading from monitoring boxes in phase-I and phase-II.

(a) Column 1, 2, and 3

(b) Slab 1, 2, and 3
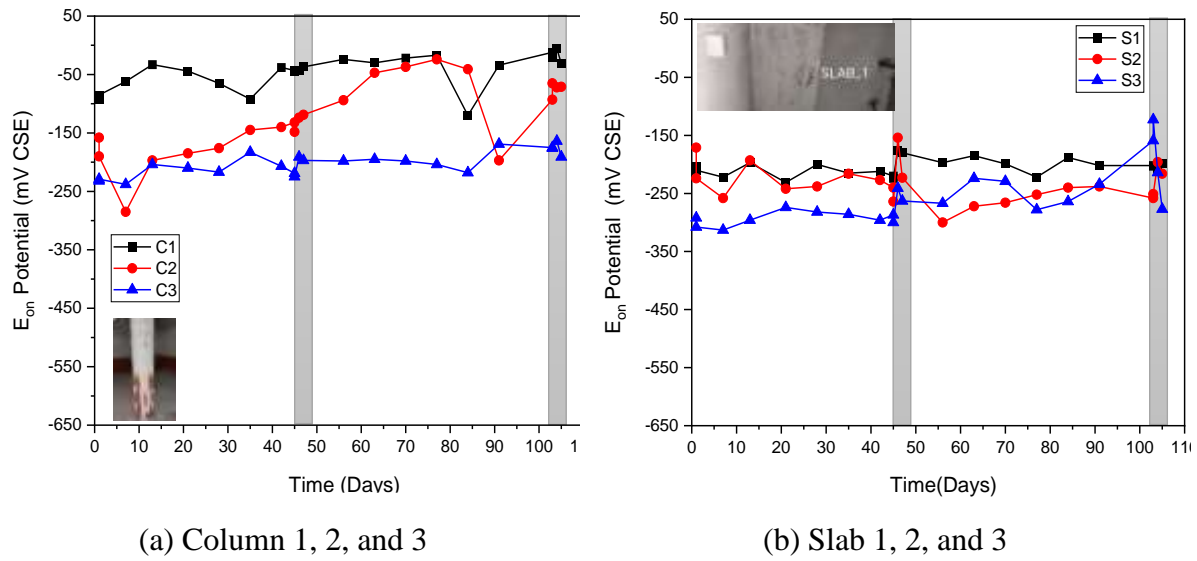
Figure 4.24: E_{on} Potential reading from columns and slabs

(a) Retaining wall 1, 2, and 3

(b) Column 7 and 8
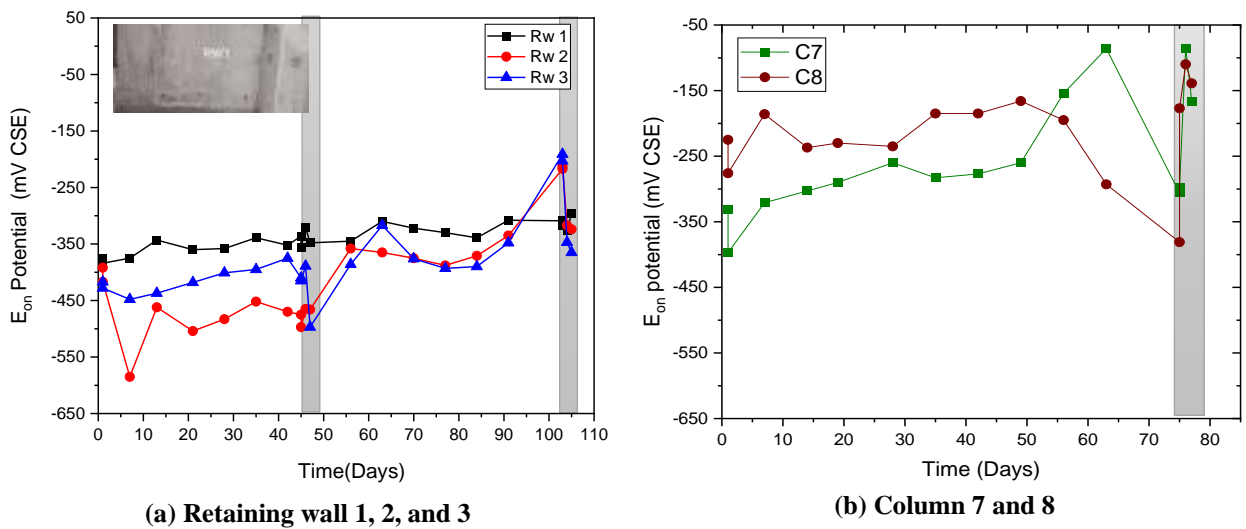
Figure 4.25: E_{on} Potential reading from retaining walls and columns

It can be observed that the E_{on} potential in all the locations is around a –500 mV to –165 mV. For the monitored CP systems in phase-I, depolarisation tests were carried out on the 45th and 103rd days after installation. A depolarisation test was carried out for the CP systems in phase - II at the end of 75 days. The result of the first depolarised test carried out in each

system is shown in Figure 4.26. Interestingly, the observed potential shift in all the locations was less than 100 mV, except for one of the columns (C7). This means that the installed galvanic anodes are not providing adequate protection to the rebars (as per 100 mV criterion in EN ISO 12696).
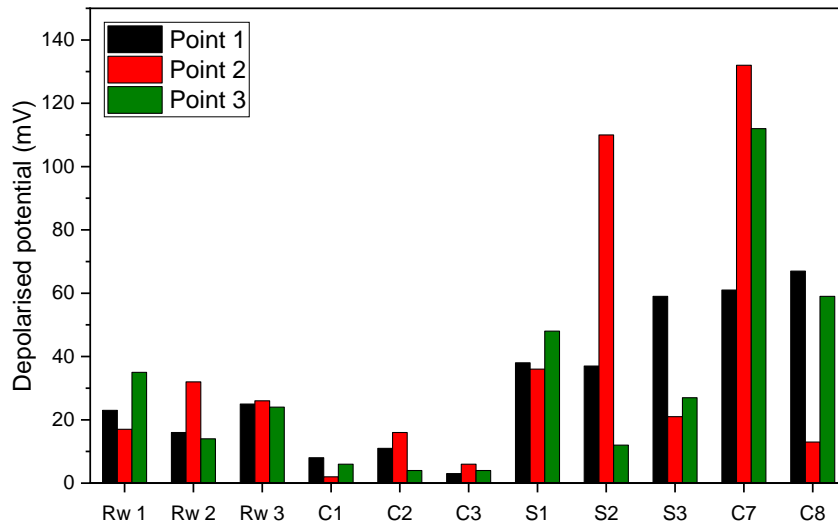
Figure 4.26: Depolarised potential obtained for different CP systems

However, to understand the rate of corrosion of rebars, the Butler-Volmer equation was used to calculate the theoretical corrosion rate. The steel density (ratio of rebar surface area and the concrete surface area) of retaining wall, column, and slabs are taken as 1, 1.1, and 1.28, respectively, to convert the output current to the current density supplied by the anodes. Figure 4.27 shows the output current density supplied by the anodes in various CP systems. In an atmospherically exposed concrete, the steel corrosion rate may be estimated by inserting the applied current density and steel potential shift into the Butler Volmer equation (Eq. (4.3)). Passive steel is indicated by a corrosion rate of less than 2 mA/m² and preferably less than 0.2 mA/m². The steel corrosion rate estimated using the obtained potential shift and the output current density during the depolarisation test is summarised in Table 4.2.

$$i_{corr} = \frac{i_{applied}}{\left\{\exp\left(\frac{2.3\Delta E}{\beta_c}\right) - \exp\left(-\frac{2.3\Delta E}{\beta_a}\right)\right\}} \tag{4.3}$$

where,

i_{corr} = corrosion rate of the rebar

$i_{applied}$ = current density applied to the rebar by the anodes

ΔE = potential shift obtained from the depolarisation test

β_a = anodic Tafel slope (120 mV)

βc = cathodic Tafel slope (120 mV)
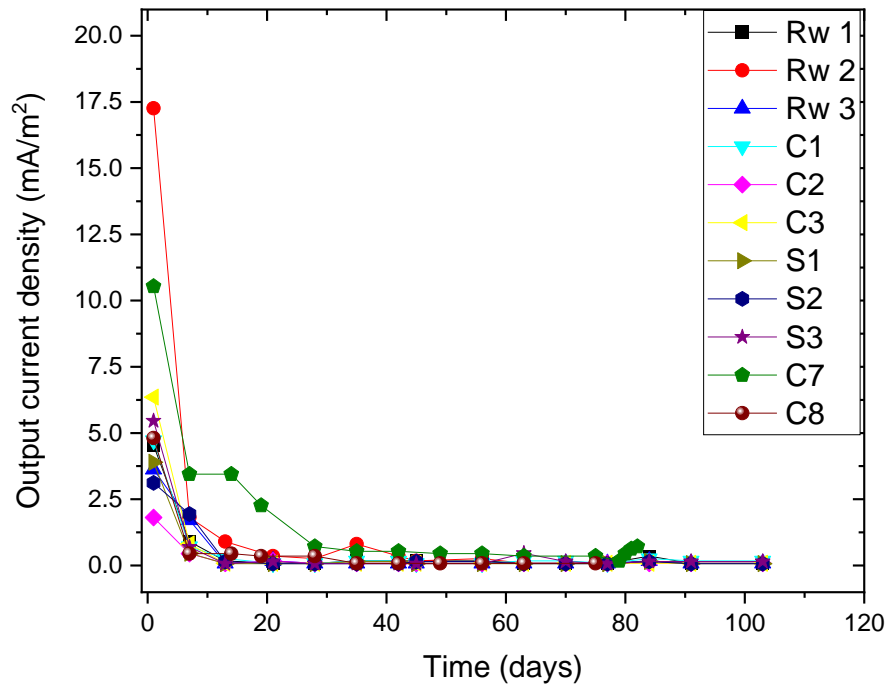
Figure 4.27: Output current density (*i_applied*) from various CP systems

Table 4.2: Estimation of corrosion rate from obtained the potential shift

Time	Member	Steel density (m^2/m^2)	i_{app} by the anodes (mA/m^2)	Potential shift (mV)	i_{corr} of the rebars (mA/m^2)
45th day	Rw 1	1.1	0.2	35	0.126
	Rw 2	1.1	0.2	32	0.139
	Rw 3	1.1	0.1	26	0.088
	C1	1.1	0.1	48	0.043
	C2	1.1	0.1	110	0.011
	C3	1.1	0.1	59	0.033
	S1	1.28	0.1	2	1.019
	S2	1.28	0.2	24	0.164
	S3	1.28	0.1	34	0.056
75th day	C7	1.1	0.4	61	0.125
	C8	1.1	0.1	13	0.181
88th day	C7	1.1	0.6	19	0.733
116th day	RW3	1.1	0.7	12	1.371

The calculated corrosion density of steel at the end of the depolarisation period, in all the locations, is less than 2 mA/m². Also, it is observed that the output current density supplied by the anodes decreased over time with a rising trend of E_{on} potential (towards the more positive side). This indicates that the installed anodes are suppling the current required to regulate the corrosion rate of rebars during the time of testing.

To understand the performance of anodes during high cathodic current density demand, two locations were selected – column 7 and retaining wall 3 for further study. The concrete surface of column 7 and retaining wall 3 was kept moist by alternating wetting and drying for seven days. The continuous wetting of the concrete surface created a low resistance path for the ions to move through the concrete. Therefore, a slight increase in the output current supplied by the anodes in these two test locations (C7 and RW3) was observed during the period of continuous wetting. However, the increase in output current density at these locations

was not very significant. The current density increased from 0.27 to 0.72 mA/m^2 in C7 and 0.18 to 0.90 mA/m^2 in RW3. This can be the reason for the similar values of potential obtained before and after 24 hours of switching Off the system in Column 7 (see Figure 4.20). Also, the calculated corrosion current density in these two locations (C7 and RW3 – on the 88th and 116th day, respectively) is less than 2.0 mA/m^2.

4.4 SUMMARY

This chapter provides the methodology of installing galvanic anodes, its performance assessment based on instantaneous tests, and a review of the present interpretation criteria of the existing test methods for assessing CP systems in reinforced concrete. The efficiency of three types of anodes was assessed in this study. Their short-term instantaneous performance data is monitored. In addition, it was found that a 100 mV potential shift is not always achieved in reinforced concrete structures.

This page is intentionally left blank

5   ELECTROCHEMICAL MODELLING OF

CONCRETE-STEEL-ANODE (C-S-A) SYSTEMS

5.1   INTRODUCTION

This chapter contains the preliminary study conducted towards developing an electrochemical model for a non-destructive test method. The following section describes the need for electrochemical modelling in the concrete-steel-anode (C-S-A) system. Then, the background knowledge to perform modelling using numerical simulation methods is provided. Then, the experimental program conducted to obtain various corrosion kinetic parameters is provided. Finally, the results obtained from the developed electrochemical model is shown.

5.1.1   Electrochemical modelling

Reinforcement steel in concrete undergoes macro and micro level corrosion by segregating its area into cathodic and anodic sites. An electrochemical model for corrosion simulates the various electrical responses associated with corrosion. Figure 5.1 shows the equivalent circuit of corrosion at the steel-concrete interface. The ultimate goal is to estimate the current and potential for a given space and time.

The current density and the corrosion rate of the reinforcing steel at a given point depend upon the electrode potential at that point. Thus, by knowing the potential at the surface of the electrode, the current density can be estimated (Soleimani et al. 2010). Electrochemical modelling of this phenomenon can be used to estimate the current and potential distribution in a reinforced concrete system (Isgor and Razaqpur 2006; Otieno et al. 2011; Ožbolt et al. 2011). This concept of modelling reinforcement corrosion can be adapted to model a galvanic anode cathodic protection system in concrete.

When a more electronegative anodic material is installed in the same system, the incipient anode formation in the rebars is inhibited, and the entire steel rebars act as a cathode. Thus, the current and potential distribution in the concrete (electrolyte) vary depending upon the polarisability of the anode material and the steel rebars. Through electrochemical models, the behaviour of the steel and galvanic anode at any point in the system can be obtained. Such data on the space-time behaviour of steel and anode can be used to obtain the correlation between corrosion potential and corrosion rate of steel rebars in the concrete of various resistivity.
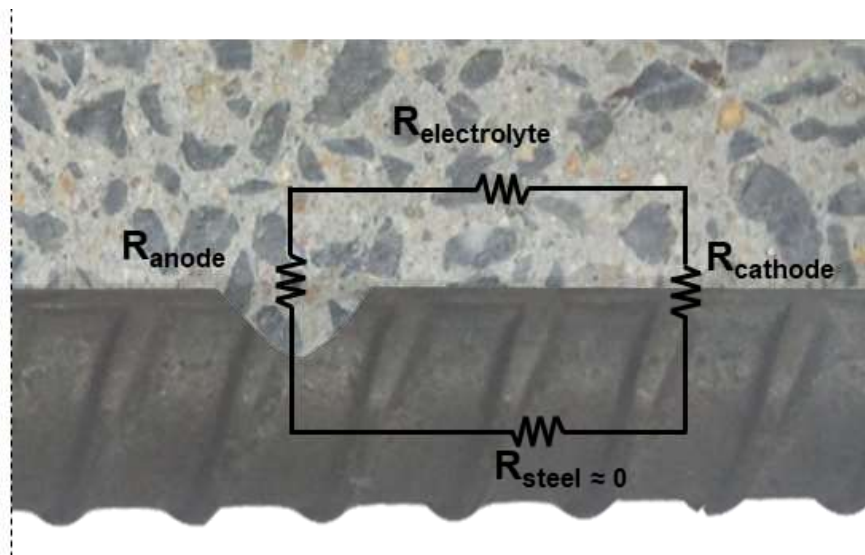
Figure 5.1: Equivalent circuit diagram showing corrosion of reinforcement.

5.1.2   Performance assessment of galvanic anodes in concrete

At present, the test method specified in EN ISO 12696 is used to assess the performance of the CP system in reinforced concrete. This method includes conducting a depolarisation test that uses the half-cell potential (HCP) measurement of rebars before and after connecting them to the anodes. The methodology and testing procedures using this standard are detailed in Section 2.7. However, these HCP measurements depend on the resistivity, temperature,

moisture level, and geometry of the concrete structures and may not always represent the actual condition of the rebar surface. Also, previous research on concrete specimens found that the macrocell activities are significantly suppressed by a relatively lower polarization than 100 mV (see Section 4.2.8 for more details). Therefore, the criteria suggested by EN ISO 12696 (in particular the '100 mV potential shift' criterion) needs to be modified to avoid erroneous estimation of the efficiency of the CP systems in concrete. In addition, the currently adopted practice of installing monitoring boxes at random representative locations in a structure cannot ensure good workmanship and monitor the performance of all the anodes in large concrete structures. Usually, the monitoring boxes malfunction after a few years, and long-term routine and non-destructive performance assessment of concrete-steel-anode (C-S-A) systems become impossible. Figure 5.2 shows some of the photographs from the case studies mentioned in Chapters 3 and 0 showing the damaged monitoring boxes. Hence, many stakeholders are not able to routinely inspect and assess the quality/performance of numerous anodes at random locations inside concrete structures, which are essential to ensure the use of quality CP products and workmanship.

The test methods based on LPR techniques on metal-aqueous systems cannot be used directly in concrete structures because of the difficulty in establishing a confined space for current perturbation. However, there is a lack of sufficient knowledge on the electrical interactions between the steel, concrete, and galvanic anodes, anodes, and the combined system's responses.

Electrochemical models can assess the instantaneous performance of anodes in a concrete structure by collecting and analysing the electrical signals against an external electrical perturbation. This can help develop non-destructive testing equipment that can assess the C-S-A system as and when needed, without multiple monitoring boxes throughout the structure. Such testing techniques can enable routine inspection at random locations on the

structure and assess the quality. Moreover, these correlations can guide Indian entrepreneurs to develop galvanic anodes and condition assessment tools/instruments. However, the scope of this study is limited to developing a numerical model that can predict the current and potential measurement in a concrete system using experimentally obtained polarization data. For this, experiments were conducted on C-S-A systems to determine the extent of polarisability of steel by a cathodic protection system in concrete. The methodology of developing an electrochemical model using the finite element modelling technique and the preliminary results from the model are provided in the subsequent sections.

(a) Monitoring box is missing after 14 years from a Jetty pier (b) Damaged monitoring box in a Jetty pier (c) Damaged electrical connections and conduits in a monitoring box
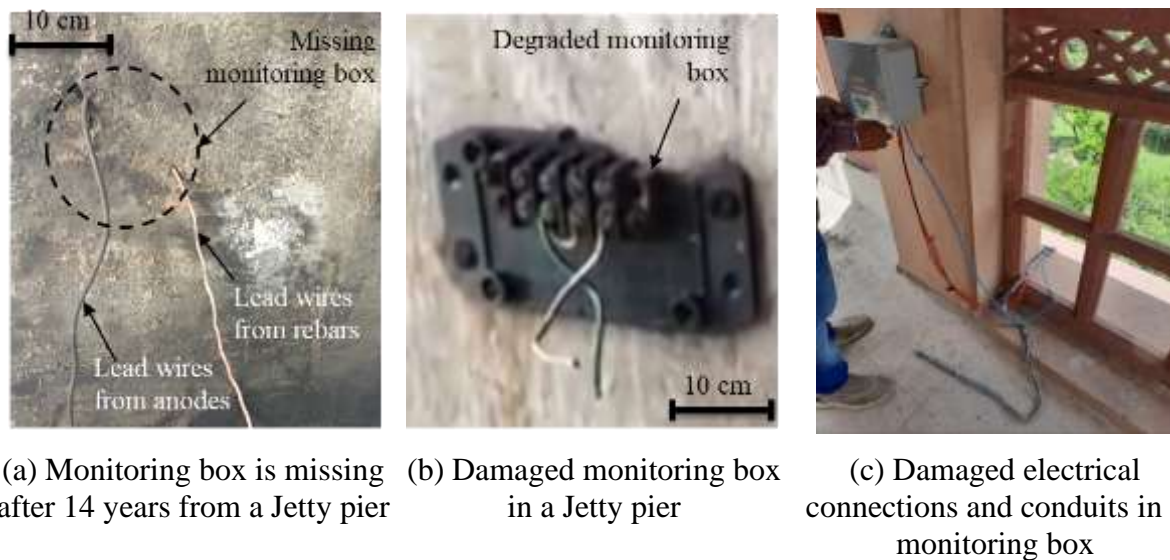
Figure 5.2: Photographs showing damaged monitoring boxes

5.2 NUMERICAL SIMULATIONS USING THE FINITE ELEMENT METHOD

This study uses the finite element method (FEM) to discretize a 3-D geometry of a concrete system containing steel and anode (Bertolini and Redaelli 2009; Bruns and Raupach 2010; Soleimani et al. 2010). An iterative procedure was used to approximate the current and potential distribution. The model starts by using the input kinetic parameters as the initial

values for the boundary conditions. Then, the solutions of the discretized elements are found out. Then the result is compared with the actual value obtained using experimental methods.

In this case, the result of the normal current density is compared with the calculated current density using the experimentally obtained corrosion kinetic parameters. A predefined termination criterion was assumed for refining the solutions of the differential equation. Figure 5.3 shows the schematic of the iteration process used in the EC model. For simplicity in the calculation, the convergence condition is assumed as 0.2% tolerance between the modelled current density and the experimentally obtained current density on the surface of the electrode.
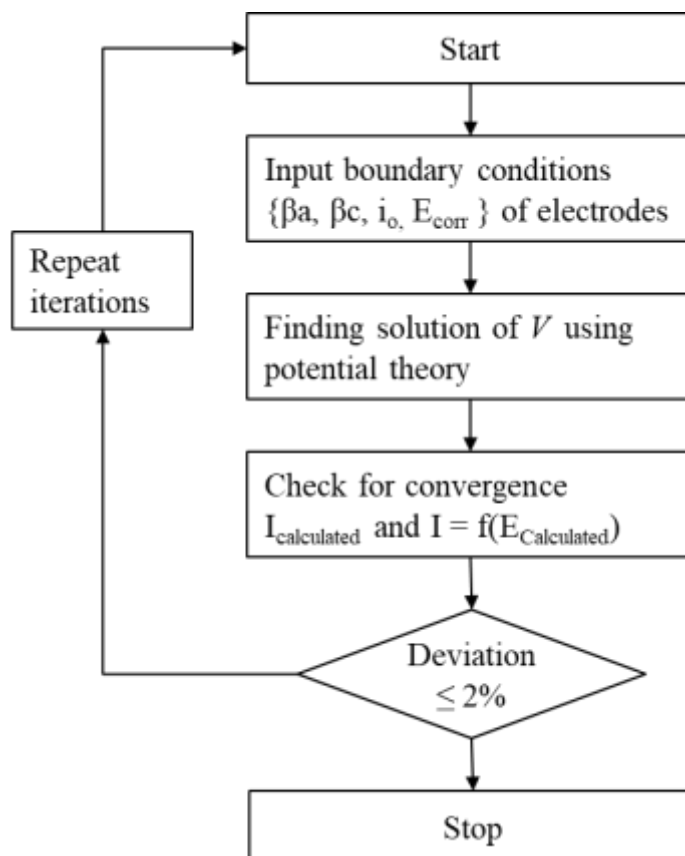
Figure 5.3: Schematic of the iteration process

5.2.1 Assumptions in modelling reinforcement

An ideal model should incorporate all the complex electrochemical processes — such as the secondary effect due to CP in concrete — occurring in concrete due to the inherent corrosion mechanism and the simultaneous application of CP. However, this requires time-dependent information on temperature, moisture, and level of polarisation of the steel to predict the corrosion potential at various locations accurately.

For simplicity and to narrow down the variables, the following assumptions are made:

(i)   The concrete domain is assumed to be homogenous and isotropic. This means that the resistivity of the concrete does not vary locally.

(ii)   All the reinforcement in the system is actively corroding with a lower corrosion potential than the anode metal. The electroneutrality is maintained in the concrete, i.e., the algebraic sum of total cathodic and anodic current is considered 0.

(iii)   Rebars do not intersect among each other but are electrically connected through external connections

5.2.2 Numerical simulation of reinforcement corrosion

Since the electrolyte is assumed to be homogeneous and isotropic, the potential distribution inside the concrete can be obtained by Laplace's equation or the potential theory (Eq. (5.1)),

$$\frac{\partial^2 V}{\partial x^2} + \frac{\partial^2 V}{\partial y^2} + \frac{\partial^2 V}{\partial z^2} = 0 \tag{5.1}$$

where, V [volts] is the potential inside the concrete corresponding to a given x, y, and z Cartesian coordinate. The solution to the above equation gives the potential distribution within

the concrete domain. If the geometry is a three-dimensional object, then the finite formulation, this equation can be written in the integral form of π^h as Eq. (5.2).

$$\pi^h = \frac{1}{2} \iiint_{v1}^{v2} \left[\left(\frac{\partial V}{\partial x}\right)^2 + \left(\frac{\partial V}{\partial x}\right)^2 + \left(\frac{\partial V}{\partial x}\right)^2 \right] dv \tag{5.2}$$

Here, v is the volume of the three-dimensional concrete domain and is expressed in m^3.

Once the potential throughout the concrete domain is known, then the current at that point can be calculated using Ohm's law. Thus, if the potential on the electrode's surface is known, the current passing through that point can be calculated using Eq. (5.3).

$$I_{xj} = -\frac{1}{\rho} \times \frac{\partial V}{\partial x} \tag{5.3}$$

Here, I_{xj}, is the component of the current flowing in xj direction, and ρ is the resistivity of the concrete expressed in kΩ·cm. Therefore, the total current density (I_{total}) at any point in the electrode surfaces can be calculated as Eq. (5.4)

$$I_{total} = \frac{1}{\rho} \times \frac{\partial V}{\partial n} \tag{5.4}$$

where, V is the potential expressed in volts and n is the normal vector from the surface of the electrode.

Now, to help solve the equation Eq. (5.2), necessary boundary conditions must be provided. The current density is a function of the electrode potential, and the same on the surface of each electrode can be obtained out using the known equations Eq. (5.5) and (5.6).

$$i_a = f_a\ (E_a) \tag{5.5}$$

$$i_c = f_c\ (E_c) \tag{5.6}$$

where, i_a and i_c are current densities of anodic and cathodic reactions, respectively, while E_a and E_c are the potentials of anode and cathode. f_a and f_c are functions that relate the current and potentials. Also, the normal current density on all the concrete surfaces ($i_{n, surface}$) can be considered to be zero, i.e., these regions are assumed to be insulated. Therefore, the condition in Eq. (5.7) can be another boundary condition for this model.

$$i_{n, surface} = 0 \tag{5.7}$$

For the present study, a commercial finite element software COMOSL Multiphysics® was used to compute the solutions of the discretised variables. A corrosion module in the COMSOL Multiphysics® software was used to understand the activation polarization and transport modelling of O_2; in particular, a secondary current distribution physics was used. This is because the model has to consider the solution resistance of the concrete, which spatially varies depending upon the composition and the ionic strength, and considers the transport/concentration overpotential at the surface of the electrodes.

5.3   EXPERIMENTAL PROGRAM

5.3.1   Sample preparation and corrosion cell

Experimental programs consist of conducting electrochemical tests on steel and anode samples. Potentiodynamic scan (PDS) tests were conducted in three steel and anode samples to obtain the required corrosion kinetic parameters. These kinetic parameters include Tafel slope constants, exchange current density of the electrodes, and resistivity of the concrete. Since this is a preliminary study, the tests were conducted on steel and anode samples in an alkaline aqueous environment; simulated pore solution was used as the electrolyte for conducting the test. Figure 5.4 shows the test samples used for the study. The steel samples are all 8 mm diameters rebars with a length of 15 cm. A four millimetres hole was drilled on one of the end faces of the rebars to accommodate a stainless-steel rod. This is provided to establish electrical

connections from the rebars. The stainless steel rebars are then covered with a heat shrink tube to insulate them and prevent their influence in the PDS test. In the case of the anodes, the tie wires are insulated using a heat shrink tube of adequate length for the reasons mentioned earlier in this section.

Figure 5.4: Steel and anode samples used for obtaining input parameters
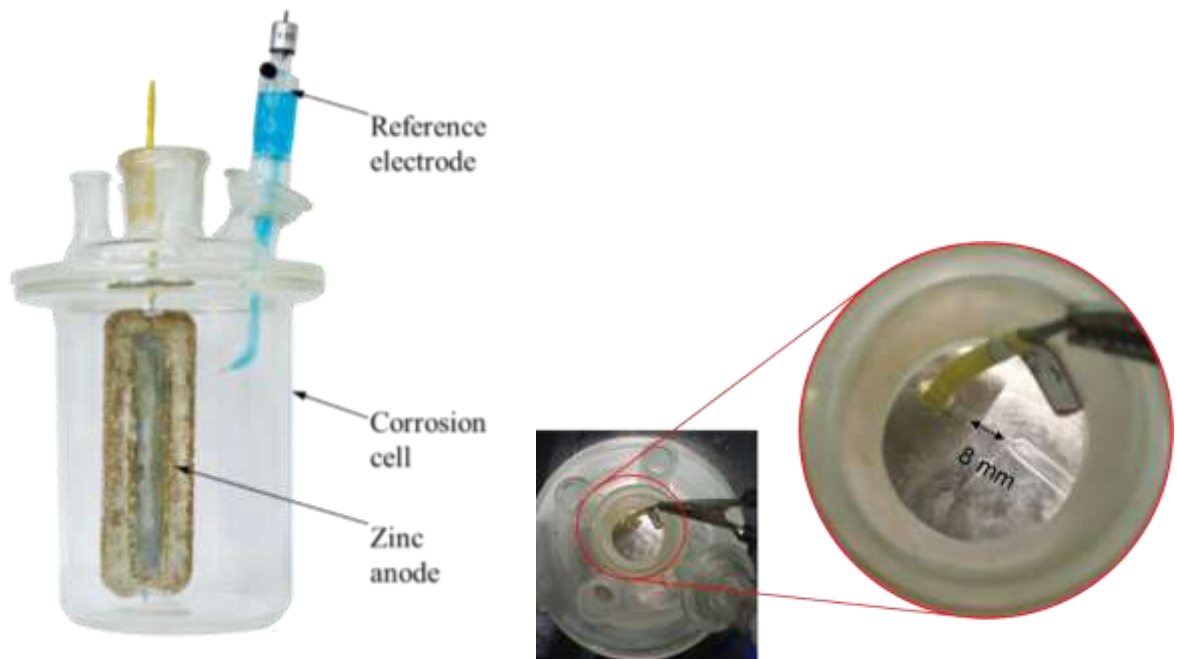
| (a) Photograph of corrosion cell and the arrangement of galvanic anode/steel sample during testing | (a) Photograph showing the clearance (8 mm) maintained between the working electrode and reference electrode during testing |

Figure 5.5: Corrosion cell to accommodate WE, CE, and RE for the PDS study

Figure 5.5 shows the photograph of the corrosion cell and the arrangement of the samples in the corrosion cell for the PDS study. During testing, the distance between the anode and the reference electrode was maintained at 8 mm to prevent the possible shielding effect or short-circuiting. Refer to Rengaraju et al. (2019) for more details on the shielding effect and the position of the reference electrode. All the specimens are placed in the same corrosion cell having a working electrode, counter electrode, and reference electrode embedded in the cementitious mortar. A nichrome wire mesh was used as the counter electrode, and a silver/silver chloride (Ag/AgCl) embedding reference electrode was used as the reference electrode, respectively, for all the test specimens.

5.3.2 Potentiodynamic polarization test

Potentiodynamic polarization technique was used to measure the polarization properties of steel and anode systems separately. Figure 5.6 shows the test setup and the connections to the electrochemical workstations to conduct PDS tests. During a PDS test, the electrode's potential is varied at a selected rate by applying a known current from a potentiostat. In the present study, the potentiodynamic measurements are obtained using a Solartron 1287A. The polarization resistance (Rp) was monitored to calculate the corrosion rate (I_{corr}). The potentiostat uses user inputs such as the electrode's OCP, the amplitude of sweep potential (i.e. the amount of applied overpotential in anodic and cathodic direction), scan rate or the amplitude of potential swept at each step, and finally, the rate at which data is recorded. For the present study, the parameters incorporated are given in Table 5.1.

W_E: Connection to WE
C_E: Connection to CE
R_E: Connection to RE

A: SPS solution
B: Working electrode
    (Rebar/Anode)
C: Embedded reference
    electrode
D: Counter electrode
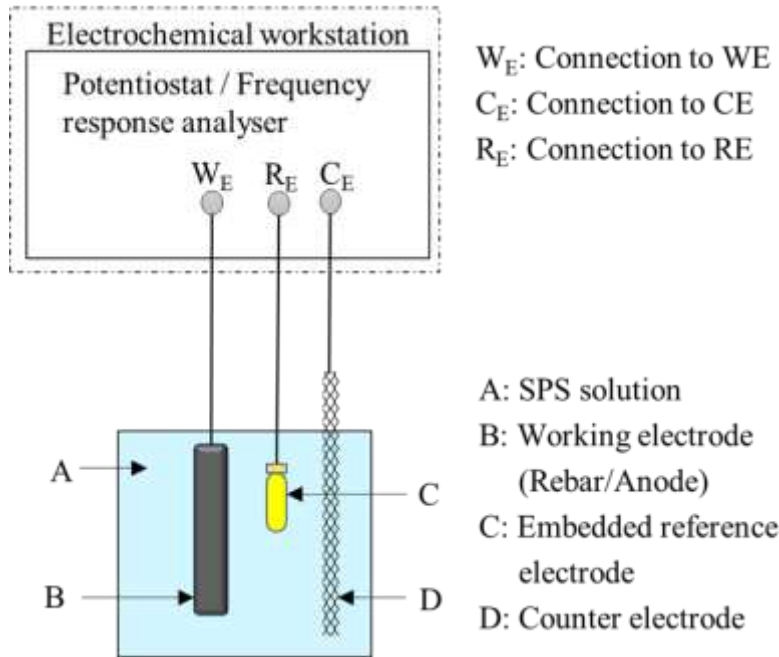
(a) Schematic of test specimens for obtaining potentiodynamic test parameters

(a) Photograph showing the potentiodynamic test setup

Figure 5.6: Experimental setup for conducting the potentiodynamic test

Table 5.1: Adopted test parameters for potentiodynamic measurements

PDS test parameters	Input/Experimentally obtained values
Initial value of overpotential	For steel samples, – 0.80 V For anode samples, – 2.25 V
Final value of overpotential	For steel samples, + 0.80 V For anode samples, + 0.80 V
Scan rate	10 mV per minute
OCP value	Obtained from OCP test of each sample

5.4   RESULTS AND DISCUSSION

5.4.1   EC model development (an attempt)

In this study, a concrete panel geometry of 1000×1000 mm was modelled using the finite element modelling concept.   Figure 5.7 shows the geometry used for the study where cylindrical rods represent rebars and cuboid elements inside the concrete domain represent the anodes; seven rebars and 11 anodes are provided.   All the seven rebars are of 8 mm diameter and are discretely placed with a c/c distance of 150 mm.   As discussed earlier, these rebars are assumed to be electrically connected through external connections.   The total number of anodes are provided based on the concept described in Section 4.2.5 of this thesis.
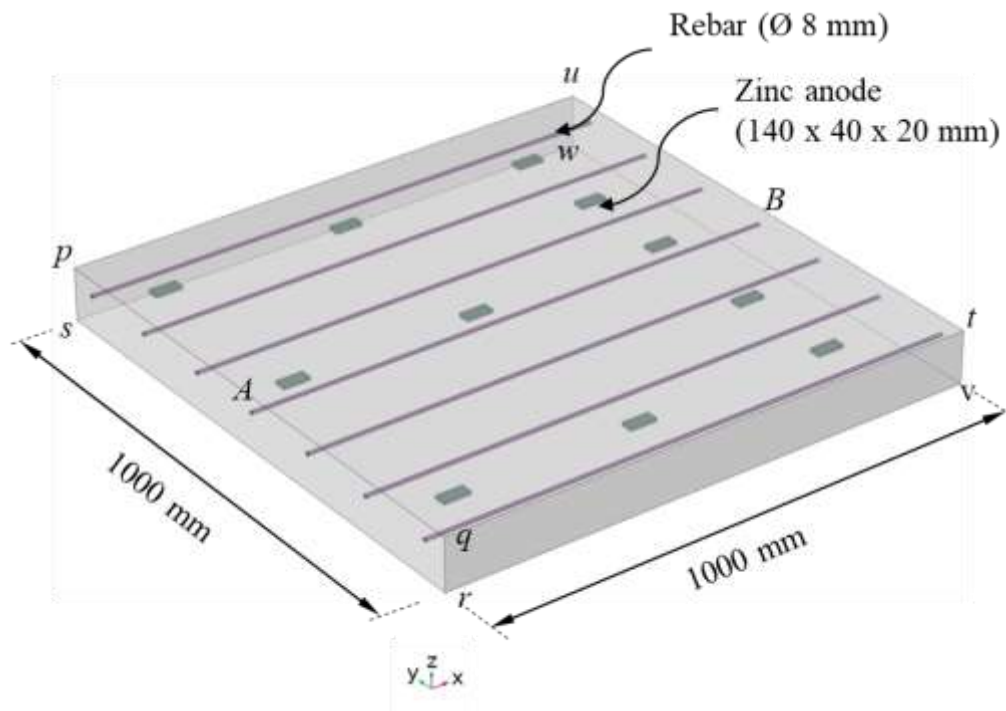
Figure 5.7: Model geometry used for the study

5.4.2 Description of the mesh

This three-dimensional finite element model discretises the rebar and concrete geometry into small tetrahedral and triangular elements. A total of 5,95,369 tetrahedral and 40,352 triangle elements are present in it. To optimise the computational time, discretization of the geometry is less near in the concrete domain without any vertices and edges than locations near a rebar or anode element. The maximum size of the element used is 650.9 µm, and the minimum is 179.8 µm. A detailed representation showing the size of the elements in the mesh is shown in Figure 5.8. To run the model, necessary input parameters characterising the kinetics of the electrode reactions are required. Therefore, the results from the polarisation test measurements are discussed next.
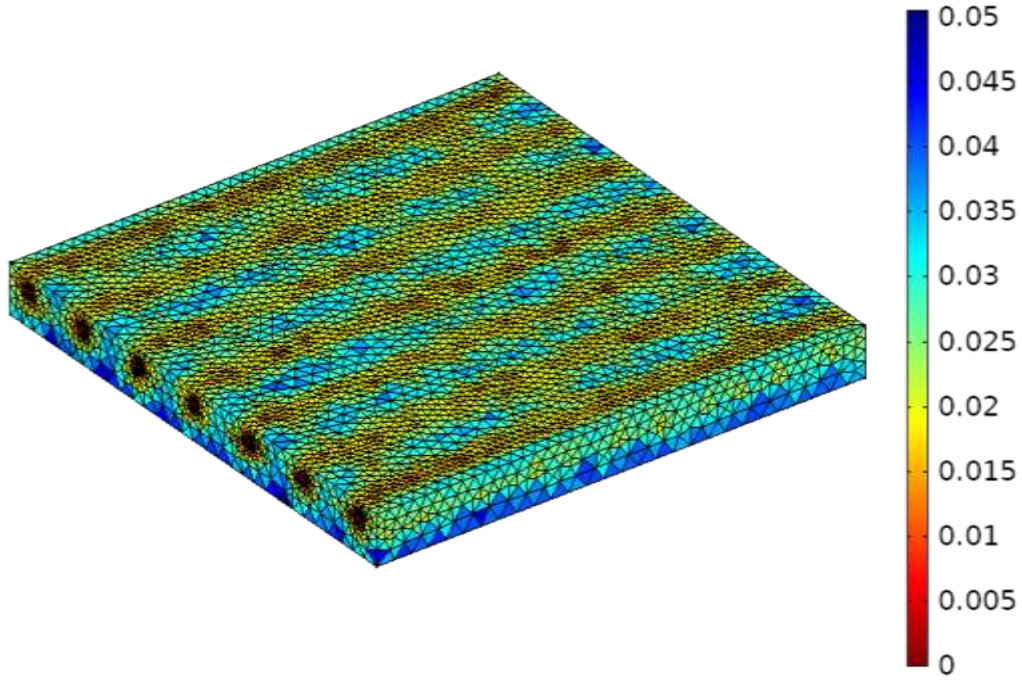
Figure 5.8: Size distribution of each element in the mesh

5.4.3 Results from potentiodynamic scanning

Figure 5.9 (a) and (b) show the PDS tests conducted on steel and anode samples. As all the steel and anode samples are tested under the same temperature with a controlled pH of electrolyte, the obtained PDS curve exhibited an almost similar response. However, one out of the three anode samples showed a drastic variation from the other two during the PDS test. As many factors can cause this deviation, the cause of this variation is not clear and is not investigated in this study. For the sake of calculation, only two samples were considered in this study. The results are then fit appropriately using a linearised Butler-Volmer equation Eq. (5.8), and the obtained kinetic data are presented in Table 5.2.

$$i_{corr} = \frac{i_o}{\left\{exp\left(\frac{2.3\Delta E}{\beta_c}\right) - exp\left(-\frac{2.3\Delta E}{\beta_a}\right)\right\}} \tag{5.8}$$
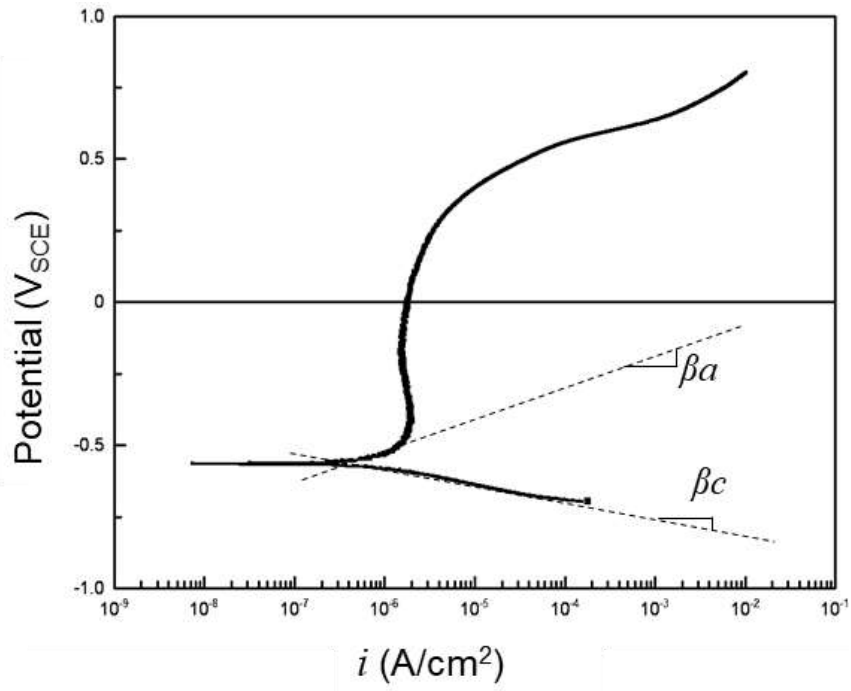
(a) Steel rebar in SPS solution
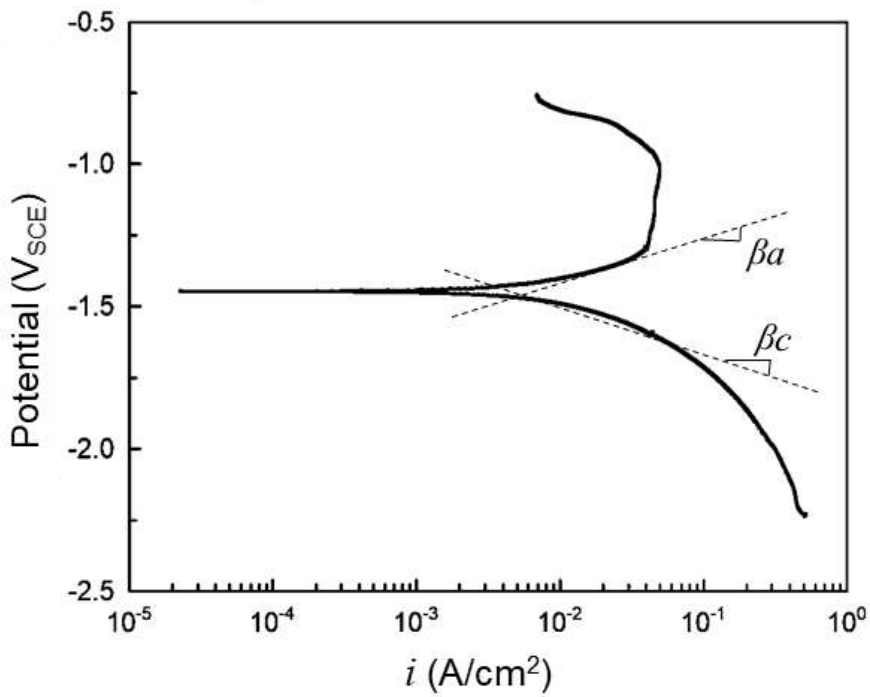
b) Anode (with embedded zinc) in SPS solution

Figure 5.9: Results from PDS test of steel and zinc anode samples in SPS solution

Table 5.2: Corrosion kinetic parameters obtained after fitting PDS curves

Parameter	Anode (with embedded zinc) in SPS solution	Active steel rebar in SPS solution	Unit
i_0	0.01304	0.00678	[A/m²]
E_o	– 1.4	– 0.526	[V vs. SCE]
βa	0.264	0.269	[V/dec]
βc	0.268	0.621	[V/dec]

5.4.4   Results from the parametric study

The COMSOL software aided in estimating the potential of the given geometry of the concrete system of resistivity 10 kΩ·cm, using the methodology mentioned in Section 5.2. Figure 5.10 shows the potential distribution across the steel and the anodes and the current density lines coming from anodes to the rebars. The potential of the rebars is in the range of –700 mV_{SCE} to –550 mV_{SCE} (i.e., with respect to an SCE reference electrode). Note that the reference potential is a saturated calomel electrode because the input values of E_{corr} are in mV_{SCE}. This means that the steel potential can be in the range of –700 to –550 mV_{SCE} by applying the provided number of anodes; essentially, this is the E_{on} potential of the CP system.
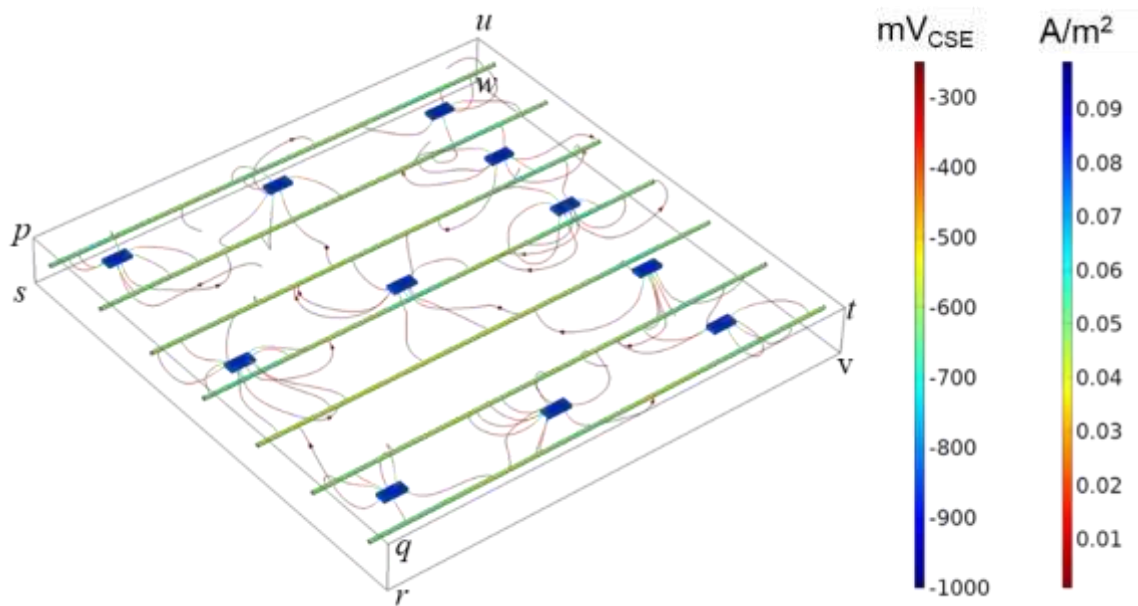
Figure 5.10: Potential and current distribution through concrete with a resistivity of 10 kΩ·cm. Streamlines represent the current output from the anodes.

At the same time, the magnitude of the output current density from the anodes are also estimated. The side view of the model that shows the variation in the magnitude of output current with distance is shown in Figure 5.11. Here, the *pqrs* face of the panel is considered for representation purposes and to better under the variation in the current lines. The zoomed area constitutes two distinctly spaced anodes with two rebars between them. It can be observed that the output current density from these anodes is streamlining towards the rebars. The output current density near the anodes' surface is ≈ 0.09 A/m^2, which decreases to ≈ 0.04 A/m^2 within the first 5 cm. However, the magnitude of the output current density is ≈ 0.01 A/m^2 near the surface of the steel rebars. This means that the current density decreases while travelling through the concrete because of the resistivity of concrete.
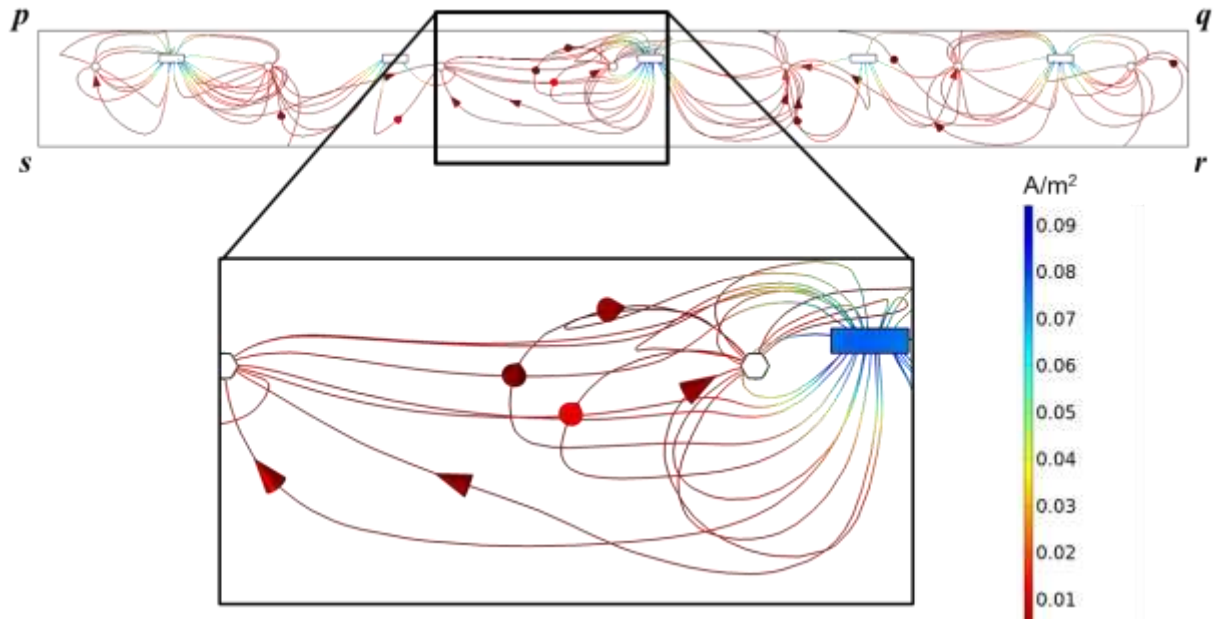
Figure 5.11: Variations in the magnitude of current density as a function of distance.

The green line with the square marker in Figure 5.12 shows the variation of electrolyte current density along the length of the A-B rebar (see Figure 5.7). It can be observed that the magnitude of electrolyte current density fluctuates significantly within a noticeably short length (say 10 cm) of the rebar. Further analysis revealed that this is because of the generation of a capacitive charge at the electrode-electrolyte interface. A double-layer is formed because of the charge separation at the electrode surface and the adjacent electrolyte. This results in generating a capacitive current. This can be conceptualised as a parallel plate capacitor, and the amount of charge separation depends on the charge density on the electrode. Thus, the obtained behaviour comprises the externally applied current from the anodes and the corrosion rate of the steel rebars. As our interest is to understand the output current density from the anodes, the normal current density is plotted against the rebar length and shown as the blue line with the circular marker in Figure 5.12. Hereafter, the current density refers to the normal current density at the surface of the rebar. From Figure 5.12, the current density is increased to the range of ≈ 0.06 A/m^2 wherever there is an influence of an anode. Conversely, the current

density is decreased to ≈ 0.025 A/m^2 when the rebars are far from the anodes – indicating another possible means to identify the influence of galvanic anodes.
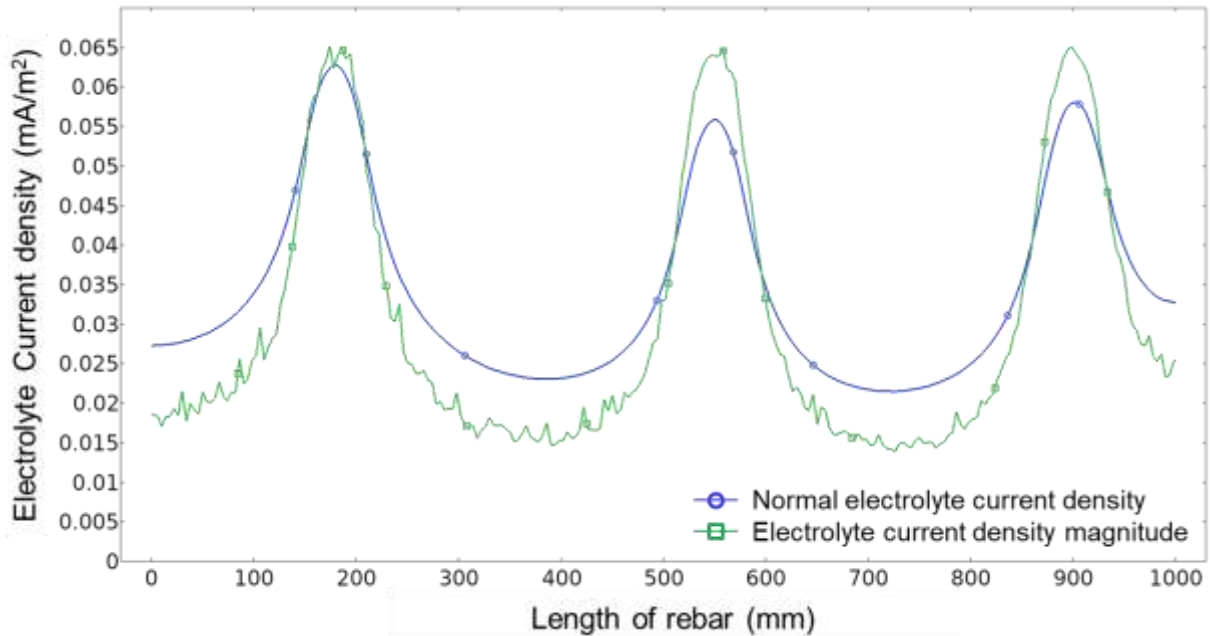
Figure 5.12: Variation of normal current density along with rebar A-B

5.4.5 Parametric study

A parametric study was conducted to understand how the CP system performs in different concrete environments having varying resistivities. The resistivity is varied from 10 kΩ·cm to 150 kΩ·cm by increasing 10 kΩ·cm in each step. Thus, the behaviour of steel and zinc — the resulting E_{on} and current density — are obtained for concrete and is presented in Appendix D.

An important point here is that these results can identify an anode that is not connected to the CP system. For example, s 5.13 (a) and (b) show the Aeon potential variation for the rebar located at 500 mm from the face *puws.* Here, Figure 5.13 (a) shows the variation when all the anodes to the rebars. Assume the corrosion potential of the rebar is known, and the amount of polarisation required for adequate protection is 100 mV. Then the model results

show that the anodes in the concrete of resistivity 10 kΩ·cm are providing adequate protection current. Therefore, the rebars in such a concrete system can be proclaimed protected. Also, all the anodes give a dip in the E_{on} potential curve — indicating all the anodes are working. However, those in the concrete of 100 and 150 kΩ·cm resistivity are not protected at a certain distance between two adjacent anodes.

Now, one of the anodes located at 550 mm from face *puws* and 500 mm from face *pqrs* is disconnected – to simulate the condition of an anode that has stopped functioning. Figure 5.13 (b) shows the variation of E_{on} when an anode is removed from the geometry. Interestingly, in this case, it was observed that the dip in the potential that was observed at 550 mm in Figure 5.13 (a) is absent in all the concrete systems — indicating the evident absence of the removed anodes. In contrast to the previous case, here for the rebar in the concrete system of resistivity 10 kΩ·cm, the region between P1 and P2 is below the required potential value. Thus, it can be inferred that the rebar is not completely protected and thus can be considered partially protected. This can be visually observed in the 2-D surface graph (see Figure 5.14), showing the change in potential in the rebars before and after disconnecting an anode located at the centre of the model geometry. Note the striking difference in the potential of rebars in the two figures, and such results for all the rebar can be obtained using the developed model. This can be a useful tool to develop qualifying/ assessment criteria for a CP system in concrete. Alternatively, the current density at the rebar surface is plotted and shown in Figures (a) and (b). Notably, the current density also shows a similar curve as that of the E_{on} potential response because of the incorporation of Ohm's law in the model. This also paves the way to establishing new assessment criteria based on current density at the rebar surface.
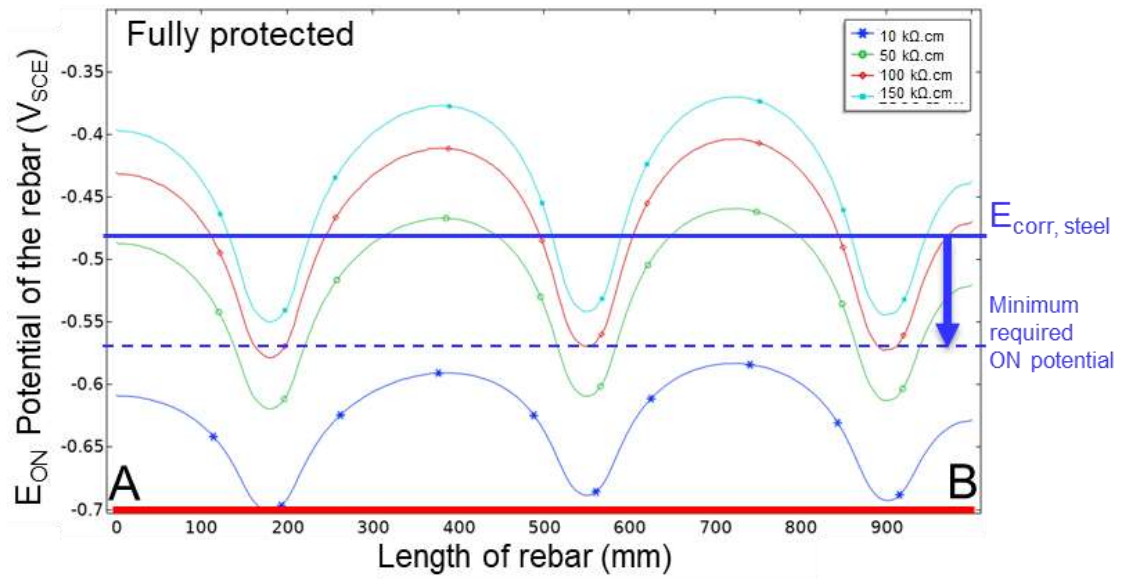
(a) Variation of E_{on} potential when all the anodes are connected. The installed CP system fully protect the rebars in concrete of resistivity 10 kΩ·cm
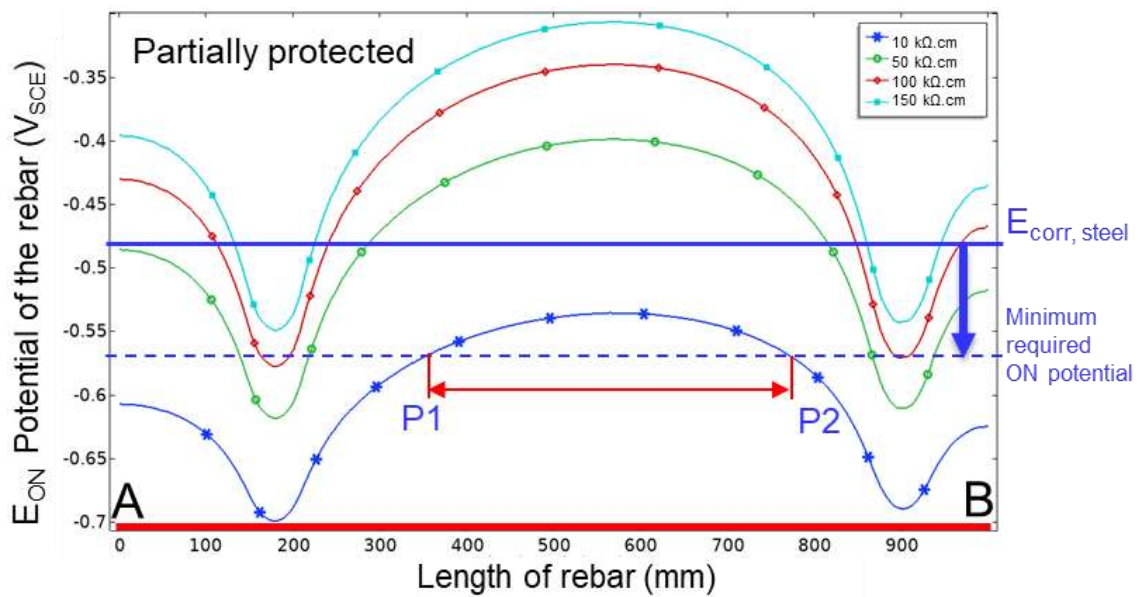
(b) Variation of E_{on} potential when one of the anodes is disconnected. The installed CP system could not protect rebars between 350 and 750 mm in concrete of resistivity 10 kΩ·cm

Figure 5.13: Variation of E_{on} potential along the length of 4th rebar located at a distance of 500 mm from face _puws_
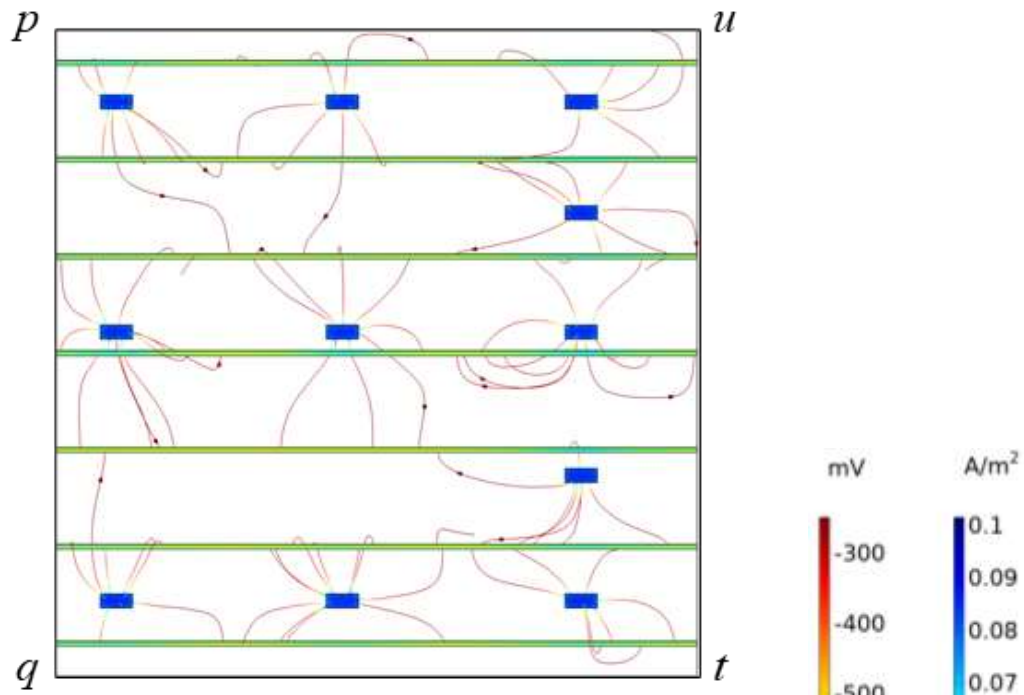
(a) Before disconnecting the anode
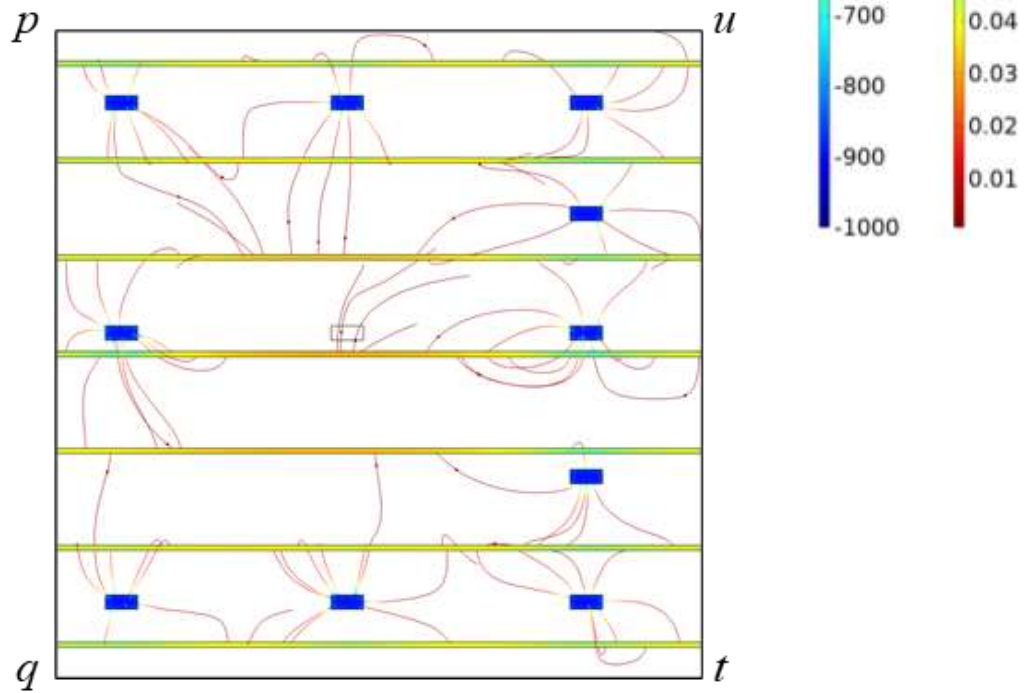
(b) After disconnecting the anode

Figure 5.14: Surface plot showing the effect of removal of one anode in the E$_{on}$
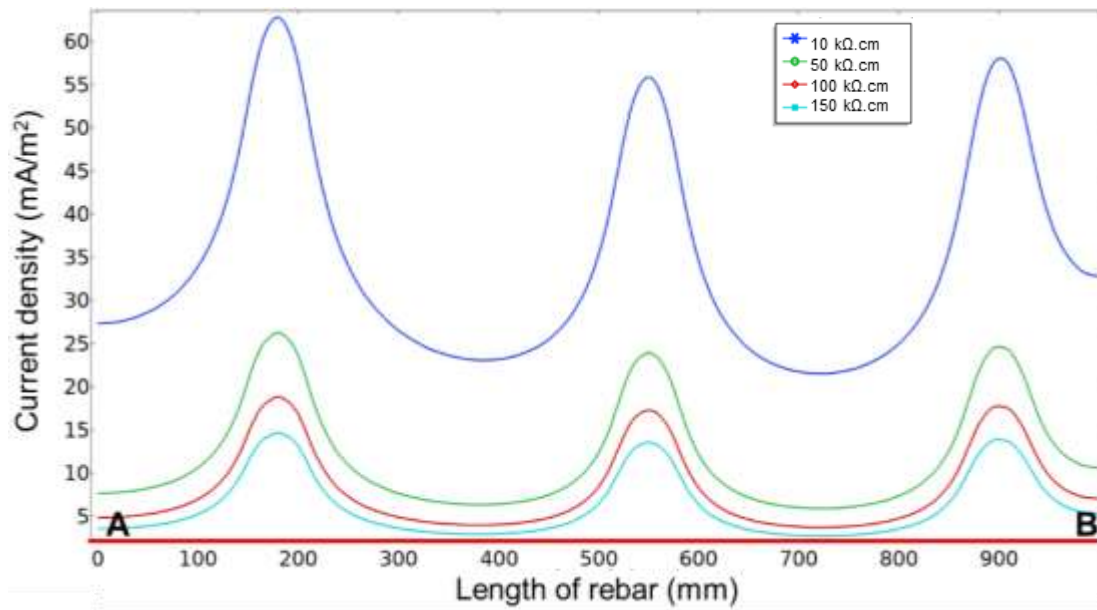
(a) Variation of current density with all anodes in connection
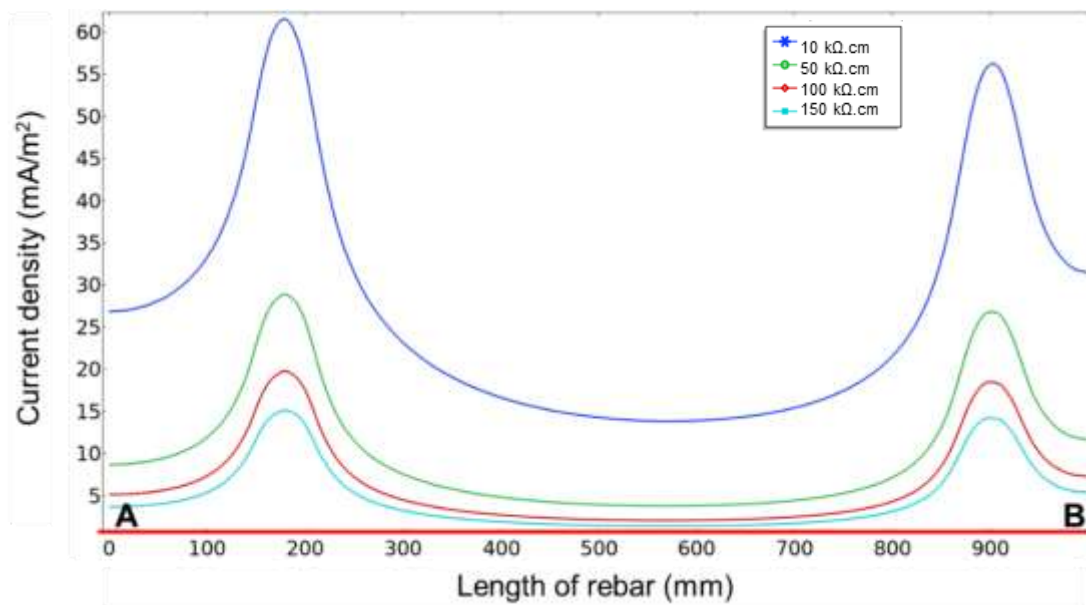
(b) Variation of current density after disconnecting the centre anode

Figure 5.15: Current density at the surface of the rebars in the panel model

5.5 SUMMARY

This chapter discusses the prospects of the electrochemical modelling concept to develop a numerical model that can assess the performance of a CP system non-destructively. An electrochemical model to estimate the potential and current distribution in a concrete-anode-steel system using the polarization properties of the metals is developed. The developed model can be the basis for developing a non-destructive test instrument for assessing the performance of CP systems in reinforced concrete structures.

This page is intentionally left blank

6 SUMMARY, CONCLUSIONS, AND RECOMMENDATIONS

6.1 SUMMARY

This thesis is based on field studies, laboratory results, and electrochemical modelling of cathodic protection (CP) systems in reinforced concrete. First, a survey was conducted among various repair consultants and galvanic anode manufacturers to obtain information on the number of 'repeated' repair projects and galvanic anodes used in various repair projects. Then, CP systems in a 14-year-old jetty structure and a four-year-old salt processing plant were assessed to understand the long-term performance of CP systems. After that, a life cycle cost (LCC) analysis of repairs with and without CP was conducted to understand the long-term cost benefits of CP systems. Then, the instantaneous performance of the CP system from two cases studies was monitored for two years. The reliability of the present criteria to assess the performance of CP systems were studied using this 2-year data. Then, the concept of numerical methods was used and a preliminary electrochemical (EC) model of concrete-steel-anode (C-S-A) systems was developed. For this, experiments on laboratory samples of steel and zinc-based anodes are conducted to obtain the necessary electrochemical parameters. These parameters are then incorporated in the EC model to estimate the potential and current distribution of C-S-A systems. It is anticipated that this thesis work will form the basis for developing a non-destructive test method for a routine inspection of CP systems at random locations in concrete structures.

6.2   CONCLUSIONS

6.2.1   Objective 1: Long-term performance and life cycle cost benefits

➢ The survey conducted among various repair contractors revealed that about 70% of the considered structures that adopted conventional patch repair strategy were re-repaired within about five years after the first repair.

➢ In India, cathodic protection with galvanic anodes is extensively used in coastal structures such as jetties and ports and less used in bridges and highways.

➢ 14-year long-term electrochemical data from the jetty structure shows that galvanic anodes could arrest steel corrosion in a chloride-rich environment for at least 14 years — later age data is yet to be collected.

➢ 30 case studies on repair works showed that employing CP strategy instead of PR strategy would lead to ≈7% more capital cost; however, LCC of the CP strategy can be significantly lower than the PR strategy.

➢ The developed LCC framework shows that, for Jetty structures, the CP strategy can save about 55% and 90% of LCC in 10 and 30 years, respectively, as compared to PR strategy. Moreover, the LCC at 90 years for CP strategy is about half that of the LCC at 45 years for PR strategy.

➢ PR strategy allows continued corrosion (due to halo effect and residual chloride effect) and could not extend service life beyond 30 years after the first repair; whereas, CP and CPrev strategies can enhance the service life to as long as needed by the replacement of anodes at regular intervals (say, when existing anode is consumed) and at a minimal cost of about 5% of the cost of the first repair.

6.2.2 Objective 2: Instantaneous performance of a cathodic protection system

➤ The E_{on} potential of the C-S-A systems with Type I and Type II anodes increased to a more positive potential from installation. However, C-S-A systems with Type II anodes exhibited more negative E_{on} potential than Type I anodes, indicating a higher capability for polarising the Type II anodes.

➤ The output current density from Type I and Type II anodes showed a decreasing trend throughout the test period. This could be due to the passivation of the steel rebars and the subsequent decreased demand for protection current by the steel rebars. Nevertheless, both Type I and Type II anodes provided the minimum protection current, i.e., 2 mA/m^2, throughout the test period.

➤ In Type II anodes, the output current density decreased to a value less than 4 mA/m^2 by about four months from the time of installation — indicating that the shift from Stage 1 (ICCP stage) to Stage 2 (galvanic stage) can happen at about four months.

➤ The depolarised potential at 24 hours (E_{24h}) shifted to a more positive value than -350 mV, indicating that Type II anodes could passivate the steel at about three months. This indicates that the Stage 2 process (i.e., galvanic action from the zinc metal, which started at about four months — as per the previous bullet) in Type II anodes started after the rebars are passivated.

➤ The C-S-A system with about 50 Type I anodes took about 20 more days to passivate the steel than the C-S-A system with about 30 Type II anodes. Type I anode system would need about 50% more anode pieces and about 20 days more than those needed for Type II anodes to passivate steel in concrete.

➢ The C-S-A systems with Type I and Type II anodes can achieve more than 120 mV potential shift at about 700 days after installation – confirming the galvanic action by the installed CP systems and corresponding polarisation/protection of steel.

➢ After 750 days, the Type I anodes showed a potential shift of less than 100 mV. As per EN ISO 12696, this means that the CP system is not working or not protecting the steel. However, it is not distinguishable whether the decrease in potential shift (from 120 to 100 mV) is due to the further passivation of steel rebars, failure of the CP system, climatic variations, or other unnoticed changes in the C-S-A system.

➢ Type III galvanic anodes did not meet the 100 mV potential shift criterion in many cases. However, the calculations indicated negligible corrosion rate (say, ≈ 0.2 mA/m^2) of rebars in concrete, which is a sign of cathodically protected steel. Hence, CP systems must be assessed not only based on the potential shift criterion (as given in EN ISO 12696), but also based on the calculated corrosion rates.

6.2.3 Objective 3: Concept for electrochemical modelling of C-S-A systems

➢ It is possible to model and estimate the distribution of current and potential across the steel surfaces in a C-S-A system using the fundamental electrochemical equations, electrochemical parameters of steel and anode metal (say, zinc) and the electrical resistivity of concrete.

➢ The parametric study showed that the potential and the current distribution in RC systems is dependent on the resistivity of the concrete. Hence, the design of CP systems must consider this factor.

➢ Variation in the E_{on} potential (obtained using the developed EC model) along the length of rebar can be assessed to identify the location of the functioning and malfunctioning galvanic anodes.

Based on the conclusions, the following research questions are answered through this thesis:

- The 14-year performance data from the Jetty structure indicate that galvanic anodes could provide long-term protection and extend the residual service life of the structure for at least 14 years.

- The LCC study found out that employing CP strategy during repair can save about 90% of LCC in 30 years. Therefore, it is worth investing additional cost of galvanic anodes during the implementation of the repair.

- The present interpretation based on 100 mV potential criteria was not always achieved in concrete structures, while the corrosion rate of the steel is negligible. Hence, new interpretation criteria based on the potential shift criterion and calculated corrosion rates need to be developed.

- The results from the numerical study show that the concept of numerical methods can be used to design, optimize, and assess the performance of CP systems in concrete.

6.3   RECOMMENDATIONS FOR FUTURE RESEARCH

➢ This thesis presented the 14-year performance data of CP systems installed in a jetty structure. The monitoring of these CP systems can be continued to understand the probable end of life of the galvanic anodes and the time to replace them. Such long-term results can promote the use of electrochemical treatments during a repair.

➢ This study found that the usage of CP systems in various repair projects of the highway and bridge sector is very less. Therefore, significant efforts are required to promote the use of CP systems in highways, bridges, and buildings for durable and economical repairs.

- The collected data on the repair heads of the jetty structure presented in this study can be used to conduct a life-cycle assessment (LCA) of various repair strategies. LCA helps to understand the environmental impacts of repeated repairs, the production and use of galvanic anodes.

- Since 100 mV potential shift criterion is not always achieved in concrete, it is necessary to establish new interpretation criteria or refine the existing criteria in EN ISO 12696. A deeper understanding of the variation of the iR drop across the cover concrete considering the atmospheric temperature, moisture content of the concrete, and output current density of the anodes is required to qualitatively assess the required amount of polarisation shift for CP systems in concrete.

- The accuracy of the EC model developed in this study depends on the electrochemical input parameters of steel and zinc-based galvanic anodes. More information on the polarization properties of these metals in the concrete system can increase the accuracy of the model.

- Validation of the EC model shall be conducted by casting laboratory panel specimens of the same geometry used in this study and measuring the E_{on} potential from various rebars.

- The EC model can be used to establish correlations between the numerical models and electrical responses from a C-S-A system mimicking various site conditions. This can help develop a non-destructive testing machine for enabling quality assessment of CP systems in concrete structures randomly at any place and time.

- The available database on the time-dependent polarization behaviour of reinforcement steel is limited to assess all long term effects of CP systems. Therefore, time-dependent

polarization studies have to be conducted to understand the change in behaviour of the

metals in the concrete environment to predict the service life of the galvanic anodes.

7   REFERENCES

[1].   Abd El Haleem, S. M., Abd El Aal, E. E., Abd El Wanees, S., and Diab, A. (2010). "Environmental factors affecting the corrosion behaviour of reinforcing steel: I. The early stage of passive film formation in Ca (OH) 2 solutions." *Corrosion Science*, Elsevier, 52(12), 3875–3882.

[2].   Ahmad, S. (2003). "Reinforcement corrosion in concrete structures, its monitoring and service life prediction—a review." *Cement and concrete composites*, Elsevier, 25(4–5), 459–471.

[3].   Andrade, C., and Alonso, C. (2004). "Test methods for on-site corrosion rate measurement of steel reinforcement in concrete by means of the polarization resistance method." *Materials and Structures*, 37(9), 623–643.

[4].   Andrade, C., Rebolledo, N., Bouteiller, V., and Olivier, G. (2007). "Corrosion Characterization of Reinforced Concrete Slabs w ith Different De v ices." (2).

[5].   Angst, U., Elsener, B., Larsen, C. K., and Vennesland, Ø. (2009). "Critical chloride content in reinforced concrete - A review." *Cement and Concrete Research*, Elsevier Ltd, 39(12), 1122–1138.

[6].   Angst, U. M. (2019). "A critical review of the science and engineering of cathodic protection of steel in soil and concrete." *Corrosion*, 75(12), 1420–1433.

[7].   ASTM C876. (2015). "Standard test method for corrosion potentials of uncoated reinforcing steel in concrete." *ASTM International: West Conshohocken, PA, USA*.

[8].   ASTM G100. (2009). "Standard Test Method for Conducting Cyclic Galvanostaircase Polarization."

[9].   ASTM G59. (2014). "ASTM G59 - Standard test method for conducting potentiodynamic polarization resistance measurements." *ASTM Standards*.

[10]. ASTM G96. (2009). "Standard Test Method for Conducting Cyclic Potentiodynamic Polarization Measurements to Determine the Corrosion Susceptibility of Small Implant Devices."

[11]. Barlo, T. J. (2001). "Origin and Validation of the 100 mV Polarization Criterion." *CORROSION 2001*, NACE International.

[12]. Bennett, J. E., and McCord, W. (2006). "Performance of Zinc Anodes used to Extend the Life of Concrete Patch Repair." *CORROSION 2006*, NACE International.

[13]. Bennett, J. E., and Mitchell, T. A. (1990). "Depolarization testing of cathodically protected reinforcing steel in concrete." *MP-Materials performance*, 29(12), 20–25.

[14]. Berkeley, K. G. C., and Pathmanaban, S. (1990). *Cathodic protection of reinforcement steel in concrete*.

[15]. Bertolini, L., Bolzoni, F., Gastaldi, M., Pastore, T., Pedeferri, P., and Redaelli, E. (2009). "Effects of cathodic prevention on the chloride threshold for steel corrosion in concrete." *Electrochimica Acta*, 54(5), 1452–1463.

[16]. Bertolini, L., Bolzoni, F., Pastore, T., and Pedeferri, P. (1996). "Behaviour of stainless steel in simulated concrete pore solution." *British corrosion journal*, Taylor & Francis, 31(3), 218–222.

[17]. Bertolini, L., Carsana, M., and Redaelli, E. (2008). "Conservation of historical reinforced concrete structures damaged by carbonation induced corrosion by means of electrochemical realkalisation." *Journal of Cultural Heritage*, Elsevier, 9(4), 376–385.

[18]. Bertolini, L., Gastaldi, M., Pedeferri, M. P., and Redaelli, E. (2002). "Prevention of steel corrosion in concrete exposed to seawater with submerged sacrificial anodes." *Corrosion Science*, 44(7), 1497–1513.

[19]. Bertolini, L., and Redaelli, E. (2009). "Throwing power of cathodic prevention applied by means of sacrificial anodes to partially submerged marine reinforced concrete piles : Results of numerical simulations." *Corrosion Science*, Elsevier Ltd, 51(9), 2218–2230.

[20]. Böhni, H. (2005). *Corrosion in reinforced concrete structures*. Elsevier.

[21]. Broomfield, J. P., and Tinnea, J. S. (1993). *Cathodic protection of reinforced concrete bridge components*.

[22]. Bruns, M., and Raupach, M. (2010). "Protection of the opposite reinforcement layer of RC-structures by CP - results of numerical simulations." *Materials and Corrosion*, 61(6), 505–511.

[23]. Chess, P. M., and Broomfield, J. P. (2003). *Cathodic protection of steel in concrete*. CRC Press.

[24]. Chess, P. M., and Broomfield, J. P. (2013). *Cathodic Protection of Steel in Concrete and Masonry*. CRC Press.

[25]. Christodoulou, C., Goodier, C., Austin, S., Webb, J., and Glass, G. K. (2013). "Diagnosing the cause of incipient anodes in repaired reinforced concrete structures." *Corrosion Science*, Elsevier, 69, 123–129.

[26]. Christodoulou, C., Goodier, C. I., and Austin, S. A. (2014a). "Site performance of galvanic anodes in concrete repairs." *Concrete Solutions - Proceedings of Concrete Solutions, 5th International Conference on Concrete Repair*, (April 2015), 167–172.

[27]. Christodoulou, C., Sharifi, A., Das, S., and Goodier, C. (2014b). "Cathodic protection on the UK's Midland Links motorway viaducts." *Proceedings of the Institution of Civil Engineers: Bridge Engineering*, 167(1), 43–53.

[28]. Costa, J. (2010). "Corrosion of steel reinforcing in concrete and masonry structures." *Structures Congress 2010*, 2829–2839.

[29].   Dash, D. K. (2017). "23 NH bridges, tunnels over 100 years old." *The Economic Times*.

[30].   Davison, N., Glass, G. K., Roberts, A., and Taylor, J. (2003). "The protective effects of electrochemical treatment in reinforced concrete." *CORROSION 2003*, NACE International.

[31].   Dodds, W., Christodoulou, C., and Goodier, C. (2018a). "Hybrid anode concrete corrosion protection - independent study." *Proceedings of Institution of Civil Engineers: Construction Materials*, 171(4), 149–160.

[32].   Dodds, W., Christodoulou, C., and Goodier, C. I. (2018b). "Long-Term Performance of Hybrid Anodes for Cathodic Protection of Reinforced Concrete." *MATEC Web of Conferences*, 199, 10–13.

[33].   Dugarte, M. J., and Sagüés, A. A. (2009). *Galvanic point anodes for extending the service life of patche areas upon reinforced concrete bridge*. *Department of Civil and Environmental Engineering*.

[34].   Dugarte, M. J., and Sagüés, A. A. (2014). "Sacrificial point anodes for cathodic prevention of reinforcing steel in concrete repairs: Part 1-polarization behavior." *Corrosion*, 70(3), 303–317.

[35].   Elsener, B. (2002). "Macrocell corrosion of steel in concrete–implications for corrosion monitoring." *Cement and concrete composites*, Elsevier, 24(1), 65–72.

[36].   Elsener, B., Andrade, C., Gulikers, J., Polder, R., and Raupach, M. (2003a). "Half-cell potential measurements—Potential mapping on reinforced concrete structures." *Materials and Structures*, Kluwer Academic Publishers-Plenum Publishers, 36(7), 461–471.

[37].   Elsener, B., Andrade, C., Gulikers, J., Polder, R., and Raupach, M. (2003b). "Half-cell potential measurements - Potential mapping on reinforced concrete structures." *Materials and Structures/Materiaux et Constructions*, 36(261), 461–471.

[38].   Ewing, S. P. (1940). *Determination of the Current Required for Cathodic Protection*. American Gas Assoc.

[39].   Feliu, S., Gonzalez, J. A., Feliu, S., and Andrade, M. C. (1990). "Confinement of the electrical signal for in situ measurement of polarization resistance in reinforced concrete." *ACI Materials Journal*, 87(5), 457–460.

[40].   Fontana, M. G. (1987). *Corrosion engineering*. McGraw-Hill series in Meterials Science and Engineering.

[41].   Fontana, M. G., and Greene, N. D. (2018). *Corrosion engineering*. McGraw-hill.

[42].   Ge, J., and Isgor, O. B. (2007). "Effects of Tafel slope, exchange current density and electrode potential on the corrosion of steel in concrete." *Materials and Corrosion*, Wiley Online Library, 58(8), 573–582.

[43].   Genescà Ferrer, J., and Juárez, J. (2000). "Development and testing of galvanic

anodes for cathodic protection." *Contributions to Science*, 1(3), 331–343.

[44]. Glass, G. K., Reddy, B., and Buenfeld, N. R. (2000). "The participation of bound chloride in passive film breakdown on steel in concrete." *Corrosion Science*, Elsevier, 42(11), 2013–2021.

[45]. González, F., Fajardo, G., Arliguie, G., Juárez, C. A., and Escadeillas, G. (2011). "Electrochemical realkalisation of carbonated concrete: An alternative approach to prevention of reinforcing steel corrosion." *International Journal of Electrochemical Science*, 6(12), 6332–6349.

[46]. Gopal, R., and Sangoju, B. (2020). "Carbonation-Induced Corrosion: A Brief Review on Prediction Models." *Journal of The Institution of Engineers (India): Series A*, Springer, 1–11.

[47]. Goyal, A., Pouya, H. S., Ganjian, E., and Claisse, P. (2018). "A review of corrosion and protection of steel in concrete." *Arabian Journal for Science and Engineering*, Springer, 43(10), 5035–5055.

[48]. Goyal, A., Pouya, H. S., Ganjian, E., Olubanwo, A. O., and Khorami, M. (2019). "Predicting the corrosion rate of steel in cathodically protected concrete using potential shift." *Construction and Building Materials*, Elsevier Ltd, 194, 344–349.

[49]. Gummow, R. A., and Eng, P. (2007). "Technical considerations on the use of the 100mV cathodic polarization criterion." *Corrosion 2007*, 1–11.

[50]. Hans Van Den Hondel, A. J., Gulikers, J., Giorgini, R., and Van Den Hondel, A. W. M. (2018). "A 5 year track record on a galvanic CP system applied on a light weight concrete bridge with prestressed steel-Developments in time of the effectiveness as determined by depolarisation values and current densities." *MATEC Web of Conferences*, 199.

[51]. Helm, C., and Raupach, M. (2016). "Development of a numerical simulation model considering the voltage drops within CP anode systems in RC structures." *Materials and Corrosion*, 67(6), 621–630.

[52]. Helm, C., and Raupach, M. (2019). "Numerical study on CP of RC structures regarding the significance of the 100 mV decay criterion considering time dependent processes." *Materials and Corrosion*, 70(4), 642–651.

[53]. Highways Agency. (2002). *Design Manual for Roads and Bridges, Cathodic Protection for Use in Reinforced Concrete Highway Structures. Highway Agency*, London, UK.

[54]. Holland, T. (1998). "Chloride limits in the ACI 318 building code requirements."

[55]. Holmes, S. P., Christodoulou, C., and Glass, G. K. (2013). "Monitoring the passivity of steel subject to galvanic protection." Loughborough University.

[56]. Ihekwaba, N. M., Hope, B. B., and Hansson, C. M. (1996). "Carbonation and electrochemical chloride extraction from concrete." *Cement and concrete Research*, Elsevier, 26(7), 1095–1107.

[57]. International Monetary Fund. (2020). "Interest Rates, Discount Rate for India." *retrived from FRED, Federal Reserve Bank of St. Louis*, <https://fred.stlouisfed.org/series/INTDSRINM193N> (Aug. 15, 2020).

[58]. Isgor, O. B., and Razaqpur, A. G. (2006). "Modelling steel corrosion in concrete structures." *Materials and Structures*, Springer, 39(3), 291–302.

[59]. ISO 12696. (2016). "EN ISO 12696 Standard - Cathodic protection of steel in concrete." 47.

[60]. Joseline, D., Haridasan, H., Rathnarajan, S., Rani, D., Raja, T., Pillai, R. G., Sengupta, A. K., and Menon, A. (2019a). "Restoration of Reinforced Lime Concrete Sunshades of a Century Old Heritage Building in New Delhi, India." *Structural Analysis of Historical Constructions*, Springer, 778–787.

[61]. Joseline, D., Kamde, D. K., Rengaraju, S., and Pillai, R. G. (2019b). "Residual Service Life Estimation and its Importance for Pretensioned Concrete (PTC) Bridges in Coastal Cities."

[62]. Kamde, D. K., and Pillai, R. G. (2020a). "Effect of surface preparation on corrosion of steel rebars coated with cement-polymer-composites (CPC) and embedded in concrete." *Construction and Building Materials*, Elsevier Ltd, 237(117616), 1–11.

[63]. Kamde, D. K., and Pillai, R. G. (2020b). "Effect of Sunlight/Ultraviolet Exposure on the Corrosion of Fusion-Bonded Epoxy (FBE) Coated Steel Rebars in Concrete." *Corrosion*, NACE International, 76(9), 843–860.

[64]. Kean, R. L., and Davies, K. G. (1981). "Cathodic Protection, Guide Prepared British Department Trade and Industry, vol. 2–4." *National Physical Laboratory, Teddington, UK*.

[65]. Krishnan, N., Kamde, D. K., Doosa Veedu, Z., Pillai, R. G., Shah, D., and Velayudham, R. (2021). "Long-term performance and life-cycle-cost benefits of cathodic protection of concrete structures using galvanic anodes." *Journal of Building Engineering*, Elsevier Ltd, 42(February), 102467.

[66]. Krishnan, N., Kamde, D., Pillai, R. G., Sergi, G., Shah, D., and Velayudham, R. (2019). "8-year performance of cathodic protection systems in reinforced concrete slabs and life-cycle cost benefits." *Proceedings of the International Conference on Sustainable Materials, Systems and structures (SMSS)*, RILEM, Rovinj, Croatia, 611–613.

[67]. Lambert, P., and Atkins, C. P. (2005). "Cathodic protection of historic steel framed buildings." *WIT Transactions on the Built Environment*, 83, 491–500.

[68]. Lee, C., and Lee, E.-B. (2017). "Prediction method of real discount rate to improve accuracy of life-cycle cost analysis." *Energy and Buildings*, 135, 225–232.

[69]. Lee, H., Lee, H., Suraneni, P., Asce, A. M., Singh, J. K., and Mandal, S. (2020). "Prediction of Service Life and Evaluation of Probabilistic Life-Cycle Cost for Surface-Repaired Carbonated Concrete." 32(10), 1–9.

[70]. Li, Z., and Madanu, S. (2009). "Highway project level life-cycle benefit/cost analysis under certainty, risk, and uncertainty: Methodology with case study." *Journal of Transportation Engineering*, 135(8), 516–526.

[71]. Martínez, I., and Andrade, C. (2008). "Application of EIS to cathodically protected steel: Tests in sodium chloride solution and in chloride contaminated concrete." *Corrosion Science*, Elsevier Ltd, 50(10), 2948–2958.

[72]. Moreno, M., Morris, W., Alvarez, M. G., and Duffó, G. S. (2004). "Corrosion of reinforcing steel in simulated concrete pore solutions: Effect of carbonation and chloride content." *Corrosion Science*, Elsevier, 46(11), 2681–2699.

[73]. Muehlenkamp, E. B., Koretsky, M. D., and Westall, J. C. (2005). "Effect of Moisture on the Spatial Uniformity of Cathodic Protection of Steel in Reinforced Concrete." 61(6), 519–533.

[74]. Muharemovic, A., Zildzo, H., and Letic, E. (2008). "Modelling of protective potential distribution in a cathodic protection system using a coupled BEM/FEM method." *WIT Transactions on Modelling and Simulation*, WIT Press, 47, 105–113.

[75]. NACE SP0290. (2007). *Impressed Current Cathodic Protection of Reinforcing Steel in Atmospherically Exposed Concrete Structures*.

[76]. NACE SP0408. (2014). *Standard Practice Cathodic Protection of Reinforcing Steel in Buried or Submerged Concrete Structures*.

[77]. Orellan, J. C., Escadeillas, G., and Arliguie, G. (2004). "Electrochemical chloride extraction: efficiency and side effects." *Cement and concrete research*, Elsevier, 34(2), 227–234.

[78]. Ormellese, M., Lazzari, L., Goidanich, S., Fumagalli, G., and Brenna, A. (2009). "A study of organic substances as inhibitors for chloride-induced corrosion in concrete." *Corrosion Science*, Elsevier, 51(12), 2959–2968.

[79]. Otieno, M. B., Beushausen, H. D., and Alexander, M. G. (2011). "Modelling corrosion propagation in reinforced concrete structures–A critical review." *Cement and Concrete composites*, Elsevier, 33(2), 240–245.

[80]. Ožbolt, J., Balabanić, G., and Kušter, M. (2011). "3D Numerical modelling of steel corrosion in concrete structures." *Corrosion science*, Elsevier, 53(12), 4166–4177.

[81]. Pedeferri, P. (1996). "Cathodic protection and cathodic prevention." *Construction and Building Materials*, 10(5 SPEC. ISS.), 391–402.

[82]. Peng, L., and Stewart, M. G. (2016). "Climate change and corrosion damage risks for reinforced concrete infrastructure in China." *Structure and Infrastructure Engineering*, 12(4), 499–516.

[83]. Pistolesi, L., and Zaffaroni, C. (2018). "Corrosion protection of embedded steel bars in concrete." *MATEC Web of Conferences*, 199.

[84].   Polder, R. B., Leegwater, G., Worm, D., and Courage, W. (2013). "Service life and life cycle cost modelling of cathodic protection systems for concrete structures." *Cement and Concrete Composites*, Elsevier Ltd, 47, 69–74.

[85].   Polder, R. B., Peelen, W. H. A., Stoop, B. T. J., and Neeft, E. A. C. (2011). "Early stage beneficial effects of cathodic protection in concrete structures." *Materials and Corrosion*, 62(2), 105–110.

[86].   Polder, R., and Peelen, W. (2018). "Cathodic protection of steel in concrete-experience and overview of 30 years application." *MATEC Web of Conferences*, 199.

[87].   Popov, B. N. (2015). *Corrosion Engineering: Principles and Solved Problems. Corrosion Engineering: Principles and Solved Problems.*

[88].   Pour-Ghaz, M., Isgor, O. B., and Ghods, P. (2009). "The effect of temperature on the corrosion of steel in concrete. Part 1: Simulated polarization resistance tests and model development." *Corrosion Science*, Elsevier, 51(2), 415–425.

[89].   Pourbaix, M. (1974). "Atlas of electrochemical equilibria in aqueous solution." *NACE*, 307.

[90].   Poursaee, A. (2010). "Determining the appropriate scan rate to perform cyclic polarization test on the steel bars in concrete." *Electrochimica acta*, Elsevier, 55(3), 1200–1206.

[91].   Poursaee, A. (2016). "Corrosion of steel in concrete structures." *Corrosion of steel in concrete structures*, Elsevier, 19–33.

[92].   Presuel-Moreno, F. J., Kranc, S. C., and Sagüés, A. A. (2003). "Cathodic prevention distribution in partially submerged reinforced concrete." *Corrosion*, 61(6), 548–558.

[93].   Presuel-Moreno, F. J., Sagues, A. A., and Kranc, S. C. (2005). "Steel activation in concrete following interruption of long-term cathodic polarization." *Corrosion*, 61(5), 428–436.

[94].   Purvis, R. L., Babaei, K., Clear, K. C., and Markow, M. J. (1994). *Life-Cycle Cost Analysis for Protection and Rehabilitation of Concrete Bridges Relative to Reinforcement Corrosion (Report SHRP-S-377). Contract 100.*

[95].   Rathod, N., Sergi, G., Seneviratne, G., and Slater, P. R. (2008). "A suggestion for a two-stage corrosion mitigation system for steel reinforced concrete structures." *EUROCORR 2008*.

[96].   Rathod, N., Sergi, G., Seneviratne, G., and Slater, P. R. (2018). "A suggestion for a two-stage corrosion mitigation system for steel reinforced concrete structures." *EUROCORR 2018*.

[97].   Rathod, N., Slater, P., Sergi, G., Seveviratne, G., and Simpson, D. (2019). "A fresh look at depolarisation criteria for cathodic protection of steel reinforcement in concrete." *MATEC Web of Conferences*, 289, 03011.

146

[98]. Raupach, M. (2006). "Patch repairs on reinforced concrete structures - Model investigations on the required size and practical consequences." *Cement and Concrete Composites*, 28(8), 679–684.

[99]. Rengaraju, S., Neelakantan, L., and Pillai, R. G. (2019). "Investigation on the polarization resistance of steel embedded in highly resistive cementitious systems – An attempt and challenges." *Electrochimica Acta*, 308, 131–141.

[100]. De Rincón, O. T., Torres-Acosta, A., Sagüés, A., and Martinez-Madrid, M. (2018). "Galvanic anodes for reinforced concrete structures: A review." *Corrosion*, 74(6), 715–723.

[101]. Roberge, P. R. (2008). *Corrosion engineering*. McGraw-Hill Education.

[102]. Sandron, F., Whitmore, D. W., and Eng, P. (2005). "Galvanic Protection for Reinforced Concrete Bridge Structures." 1–14.

[103]. Schwarz, W., Bakalli, M., and Donadio, M. (2016). "A novel type of discrete galvanic zinc anodes for the prevention of incipient anodes induced by patch repair." *European Corrosion Congress, EUROCORR 2016*, 3, 2136–2144.

[104]. Sergi. (2011). "Ten-year results of galvanic sacrificial anodes in steel reinforced concrete." *Materials and Corrosion*, 62(2), 98–104.

[105]. Sergi, G., and Page, C. L. (2000). "Sacrificial anodes for cathodic prevention of reinforcing steel around patch repairs applied to chloride-contaminated concrete." *European Federation of Corrosion Publications(UK)*, 31, 93–100.

[106]. Sergi, G., Seneviratne, G., and Simpson, D. (2020). "Monitoring results of galvanic anodes in steel reinforced concrete over 20 years." *Construction and Building Materials*, 269, 121309.

[107]. SHRP-S-330. (1993). "Standard Test Method for Chloride Content in Concrete Using the Specific Ion Probe." Strategic Highway Research Program, National Research Council, Washington, DC.

[108]. Soleimani, S., Ghods, P., Isgor, O. B., and Zhang, J. (2010). "Modeling the kinetics of corrosion in concrete patch repairs and identification of governing parameters." *Cement and Concrete Composites*, Elsevier, 32(5), 360–368.

[109]. Song, H., and Saraswathy, V. (2007). "Corrosion Monitoring of Reinforced Concrete Structures - A Review." 2, 1–28.

[110]. SP0290, N. (2007). "Standard Practice." *ICCP of Reinforcing Steel in Atmospherically Exposed Concrete Structures*.

[111]. Stewart, M. G., and Val, D. V. (2003). "Multiple limit states and expected failure costs for deteriorating reinforced concrete bridges." *Journal of Bridge Engineering*, 8(6), 405–415.

[112]. Stratfull, R. F. (1974). "Experimental cathodic protection of a bridge deck." *Transportation Research Record*, SAGE Publishing, 500, 1–15.

[113]. Tait, W. S. (2018). "Electrochemical corrosion basics." *Handbook of Environmental Degradation of Materials*, Elsevier, 97–115.

[114]. Val, D. V, and Stewart, M. G. (2003). "Life-cycle cost analysis of reinforced concrete structures in marine environments." *Structural safety*, Elsevier, 25(4), 343–362.

[115]. Vukcevic, R. (2010). "Directions for the Future, A Case for a Critical Review of ICCP of Steel in Concrete." *Proc. Corrosion & Prevention*, 14–17.

[116]. Whitmore, D. (2018). "Galvanic cathodic protection of corroded reinforced concrete structures." *MATEC Web of Conferences*, EDP Sciences, 5006.

[117]. Whitmore, D., and Abbott, S. (2003). "Using humectants to enhance the performance of embedded galvanic anodes." *NACE - International Corrosion Conference Series*, 1–9.

[118]. Whitmore, D., Haixue, L., Simpson, D., and Sergi, G. (2019). "Two-Stage, Self-Powered, Corrosion Protection System Extends the Life of Reinforced Concrete Structures." *CORROSION 2019*, NACE International.

[119]. Wilson, K., Jawed, M., and Ngala, V. (2013a). "The selection and use of cathodic protection systems for the repair of reinforced concrete structures." *Construction and Building Materials*, Elsevier Ltd, 39, 19–25.

[120]. Wilson, K., Jawed, M., and Ngala, V. (2013b). "The selection and use of cathodic protection systems for the repair of reinforced concrete structures." *Construction and Building Materials*, Elsevier, 39, 19–25.

[121]. Yehia, S., and Host, J. (2010). "Conductive Concrete for Cathodic Protection of Bridge Decks." *ACI Materials Journal*, 107(6).

[122]. Younis, A., Ebead, U., Suraneni, P., and Nanni, A. (2020). "Cost effectiveness of reinforcement alternatives for a concrete water chlorination tank." *Journal of Building Engineering*, Elsevier Ltd, 27(October 2019), 100992.

[123]. Zaki, A., Chai, H. K., Aggelis, D. G., and Alver, N. (2015). "Non-destructive evaluation for corrosion monitoring in concrete: A review and capability of acoustic emission technique." *Sensors*, Multidisciplinary Digital Publishing Institute, 15(8), 19069–19101.

APPENDIX A

CUMULATIVE FUTURE VALUE OF VARIOUS REPAIR STRATEGIES USED IN THE LCC ANALYSIS

Table 7.1:shows the calculated FV of PR, CP, and CPrev strategy corresponding to various projected ages of the Chennai port structure.

Table 7.1: FV of the PR, CP, and CPrev repair strategy

Year	Cumulative FV of the repair Without CP (INR)	Cumulative FV of the repair With CP (INR)	Cumulative FV of CPrev strategy (INR)
–15*			434,935
–10*			536,605
–5*			679,202
0	24,000,000	25,000,000	879,202
5	57,661,242	25,280,510	1,159,713
10	104,872,874	25,673,941	1,553,143
15	171,089,631	28,984,778	4,863,981
20	263,962,058	29,758,715	5,637,918
25	394,220,442	30,844,202	6,723,404
30	394,220,442	39,978,908	8,245,855
35		42,114,224	10,381,172
40		45,109,116	13,376,063
45		70,312,058	38,579,005
50		76,203,463	44,470,410
55		84,466,463	52,733,410
60		154,002,175	64,322,696
65		170,256,748	80,577,268
70		193,054,626	103,375,147
75		**193,054,626**	103,375,147

*   *Represents the time before the first actual repair of the structure; for instance, –15 means 15 years before the repair, i.e., essentially the time of construction of the structure*

** *Represents the cumulative FV of a repair with CP after 75 years from the time of repair. This value is used to normalise all the costs for representation purposes and is shown in Figure 3.13*

APPENDIX B

METHODOLOGY OF INSTALLATION AND MONITORING OF GALVANIC ANODES

IN REINFORCED SUNSHADE (CASE STUDY I)

a) Checklist to ensure proper installation of galvanic

Date of installation	
Label of the test region	
Length of the concrete segment	
Distance between Row 1 and Row 2 (V1)	
Distance between Row 2 and Row 3 (V2)	
Number of anodes to be provided in Row 1	
Label the anode pockets in row 1 as A1, A2, A3…An	
Spacing of anodes to be provided in Row 1 (S1)	
Number of anodes to be provided in row 2	
Label the anodes pockets in row 1 as B1, B2, B3…Bn	
Spacing of anodes to be provided in Row 2 (S2)	
Number of anodes to be provided in row 3	
Label the anode pockets in row 1 as C1, C2, C3…Cn	
Spacing of anodes to be provided in Row 3 (S3)	

Checklist for installation of galvanic anodes in concrete		
Activity	**Yes/No**	**Details**
Have you located all the top and bottom rebars in the member?		No. of top rebars: No. of bottom rebars:
Have you labelled all top rebars and marked the corresponding position of the rebars on the slab? (eg. T1, T2,……, Tn)		
Have you labelled all bottom rebars and marked the corresponding position of the rebars on the concrete surface? (eg. B1, B2,……, Bn)		
Have you drilled holes of 1 cm diameter on the marked points up to the level of the steel?		
Have you established connections between the steels by inserting the special rebar connectors (with a lead ball plug at the tip of the spring wire) into the holes and striking it using a hammer?		
Have you checked the continuity between each rebar? (Electrical continuity is acceptable if the maximum DC resistance between the two considered locations of the rebar is less than 1 Ω)		

Is the electrical resistance between the first Rebar and the mentioned points is less than 1 ohm?	2 and 1		
	3 and 1		
	4 and 1		
	5 and 1		
	6 and 1		
	7 and 1		
	-		
	-		
	n and 1		
Have you made the anode pockets in the first row?			
Have you ensured that the vertical spacing of anode pockets between the first and second row is V1?			
Have you ensured that the vertical spacing of anode pockets between the second and third row is V2?			
Have you ensured that the spacing of anode pockets in the first row is S1?			
Have you made the anode pockets in the second row?			
Have you ensured that the spacing of anode pockets in the second row is S2?			
Have you made the anode pockets in the third row?			
Have you ensured that the spacing of anode pockets in the third row is S3?			
Have you made grooves along the length of the slab to accommodate wires?			
Have you wet the surface of the pockets with water?			
Have you immersed all the anodes in water for 20 minutes before the installation of anodes?			
Have you checked the continuity between each anode (Electrical continuity is acceptable if the maximum D.C. resistance between the two considered locations of the rebar is less than 1 Ω)			
Is the electrical resistance between the mentioned points is less than 1 ohm?	A1 and A2		
	A1 and A3		
	A1 and A4		
	-		
	A1 and An		
	A1 and B1		
	B1 and B2		
	B1 and B3		
	B1 and B4		
	-		
	B1 and Bn		
	B1 and C1		
	C1 and C2		
	C1 and C3		
	-		

	C1 and Cn		
Have you placed the low resistance mortar in the anode pockets?			
Have you placed the anodes aligned horizontally?			
Have you pressed the anodes into the anode pockets till the anodes get completely covered in the low resistive mortar?			
Have you covered the top surface of the slab with 15 mm thick lime mortar?			
Have you marked ('X' mark) the position of the anodes on the slab before the lime mortar sets?			

b) Step-by-step processes of installation of galvanic anodes

The photographs during the repair of the sunshade of the heritage building are shown in Figure 7.1 of this appendix. The pilot repair work was conducted on a10 m stretches of the sunshade shade. These photographs can reference developing installation guidelines for repair using a galvanic anode cathodic protection system.

(a) The micro-concrete top overlay was removed by chipping by hand

(b) Rebars were located using a rebar locator, and the locations were marked on the sunshade

(c) Several 10 mm Ø holes were drilled to establish an electrical connection with the rebars

(d) Pockets of size 150 x 50 x 15 mm for accommodating anodes

(e) Electrical connectivity was checked using a multimeter

(f) Anodes were pre-wetted to saturate the encasing mortar

(g) Half-cell potential of the anodes was measured using a Cu/CuSO4 reference electrode

(h) Anodes were placed in the low resistive mortar inside the pockets

(i) Weathershade was covered with 20 mm thick waterproofing overlay

Figure 7.1: Photographs showing various steps during the repair of the sunshade

c) Datasheet for accessing the performance of galvanic anodes in concrete

Name of test region				Photograph of test region (Position of the anodes should be marked)
Details of test region				
Dimension of the member				
If rectangular column	Width =	Depth =	Length =	
If circular column	Diameter =	Length =		
If beam	Width =	Depth =	Length =	
If slab/wall	Width =	Thickness =	Length =	
If staircase	Width =	Thickness =	Length =	
Surface area of steel rebars per member (sq. m); including area of stirrup reinforcement				
Steel density (steel area/concrete area				
Number of anodes Installed				
Spacing of anodes (mm)				
Mass of one anode (mg)				
HCP reading before installation (mV)				

Date of testing	Time (days)	E_{ON}	$E_{Instant-Off}$	E_{24}	E_{48}	$E_{Instant-ON}$	Output current (Amp)	Resistivity (kΩ.cm)	Remarks
	1								
	7								
	14								
	21								
	28								
	29								
	30								
	35								
	42								
	49								
	56								
	57								
	58								
	63								
	70								
	77								
	84								
	85								
	86								
	91								
	98								
	105								
	112								
	113								
	114								
	119								
	126								
	133								
	140								
	141								
	142								

Measurements from embedded reference electrode

**Figure 7.2: Screenshot of the datasheet for monitoring galvanic anodes**

APPENDIX C

PILOT PROJECT CONDUCTED ON THE APARTMENT COMPLEX IN KOLKATA (CASE STUDY II))

Three types of anodes were used in the structure: Type I, Type II, and Type II. The study determined the type of anode and checked whether the spacing provided is adequate to prevent further corrosion of the rebars. Four locations in four different towers (Tower 2, 4, 8, and 9) of the residential building mentioned as Case study II in Chapter 4 were selected for pilot studies. The selected locations and the position of the anodes are given in Figure 7.4, Figure 7.3, and Table 7.2.

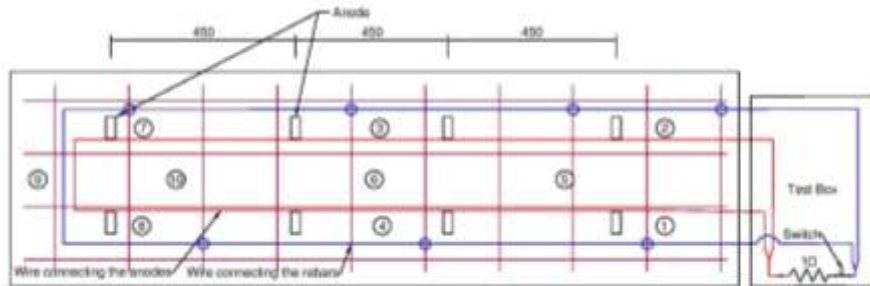**(a) Location 1**
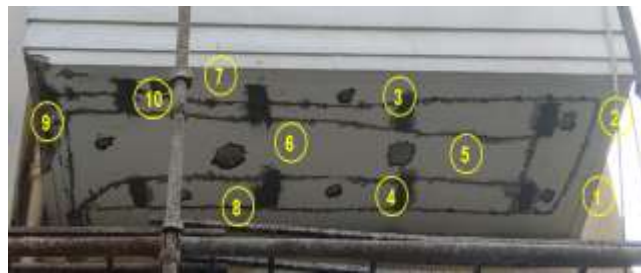
(b) Location 2
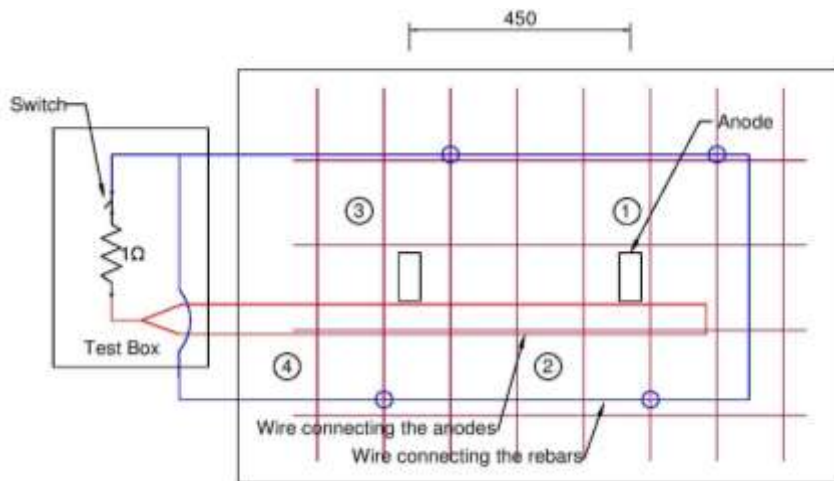

(c) Location 3

Figure 7.3: Selected locations for the installation of anodes
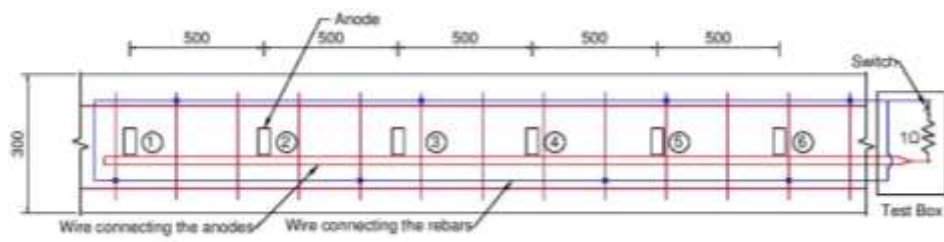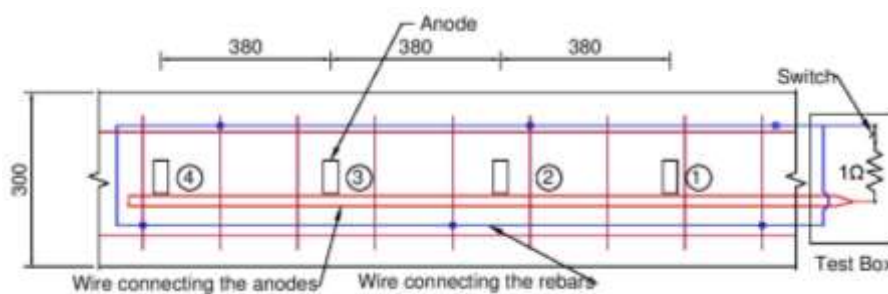
(a) Layout of the anodes in location 1 (tower 9)

(b) Layout of the anodes in location 2 (tower 2)

(c) Layout of the anodes in location 3 (tower 4)

(d) Layout of the anodes in location 4 (tower 8)

Figure 7.4: Layout of installed anodes at various locations

Table 7.2: Location and type of anodes used

Location	Member	Type of Anode	Number of Anodes	Spacing of Anodes (mm)
1	Staircase beam in tower 9	Hybrid fusion anode	6	500
2	Balcony slab in tower 2	Hybrid fusion anode	8	500
3	Sunk slab in tower 4	Flat anode	2	450
4	Staircase beam in tower 8	Hybrid fusion anode	4	380

d) Results

Figure 7.5, Figure 7.6, and Figure 7.7 show the results obtained from various test locations (L1, L2, L3, and L4). It is observed that there is a less negative potential at L2 and L6 of location 1 (see Figure 7.5 (a)). The use of a bonding agent (between the substrate concrete and the repair mortar) while installing the anode could be a reason for the observed lower potential at L6 (the bonding agent might act as a barrier for the ionic conduction from the anode). A reduction is observed in the output current from the anode (see Figure 7.7) at the locations where the hybrid fusion anodes are installed (L1), indicating the steel's repassivation. The current output from L2 is zero throughout these days, indicating a breakage in the system's connection.
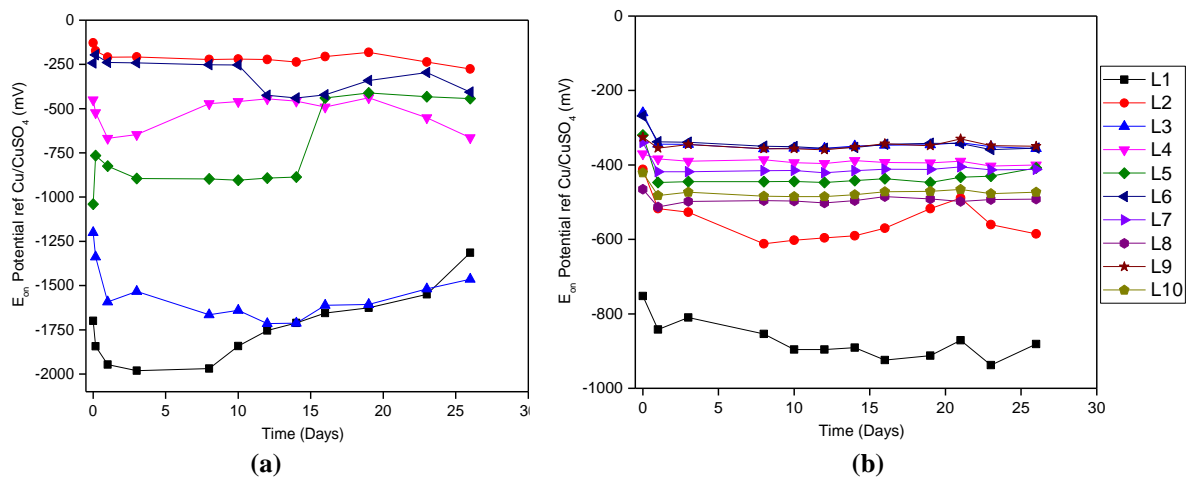

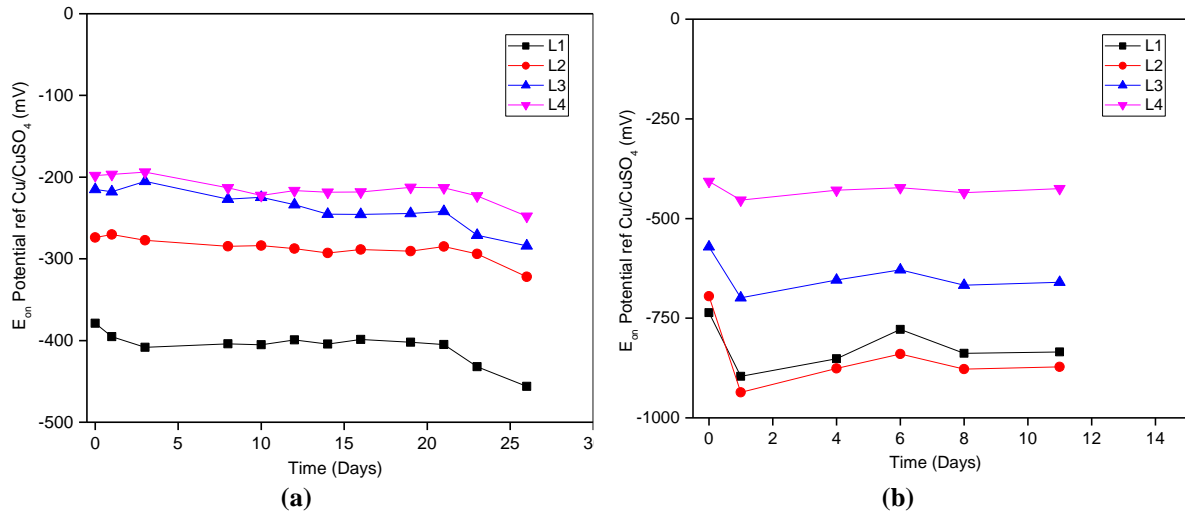**Figure 7.5: Variation of E_{on} potential with time at (a) Location 1 and (b) Location 2**

Figure 7.6: Variation of E$_{on}$ potential with time at (a) Location 3 and (b) Location 4
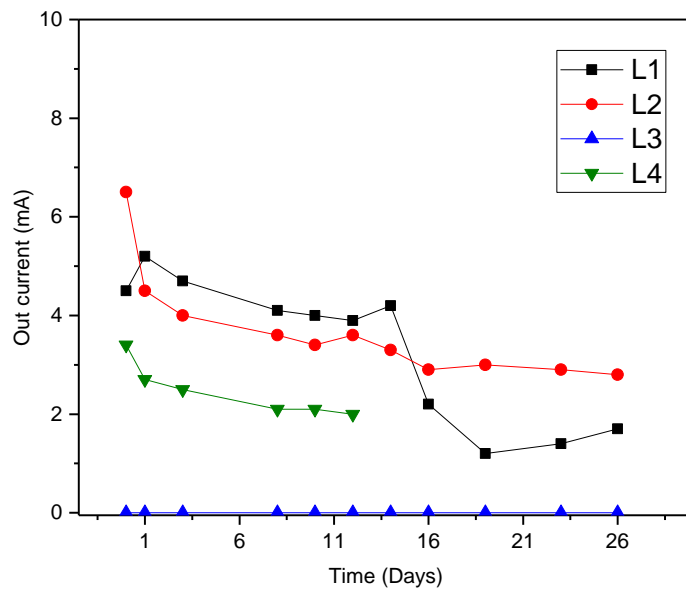

Figure 7.7: Variation of output current from anodes in various locations with time

e) Evaluation of passivity verification technique (PVT)

The efficiency check of cathodic protection without switching off the current is made through the Passivity verification technique (PVT). Gecor8 gives corrosion potential, corrosion rate and an indication of the efficiency of the CP (as well protected, protected or non-protected). For analyzing the efficiency of the PVT technique, a location that showed more positive depolarized potential was selected. Figure 7.8 shows the photograph of the location where

anodes were installed. The red line in the diagram shows how the anodes are connected through external connections. Figure 7.9 shows the contour of the 24 hours depolarized potential. The potential before the installation of anodes at this location was already shown in Figure 4.20. Figure 7.10 shows the results from the passivity verification test.
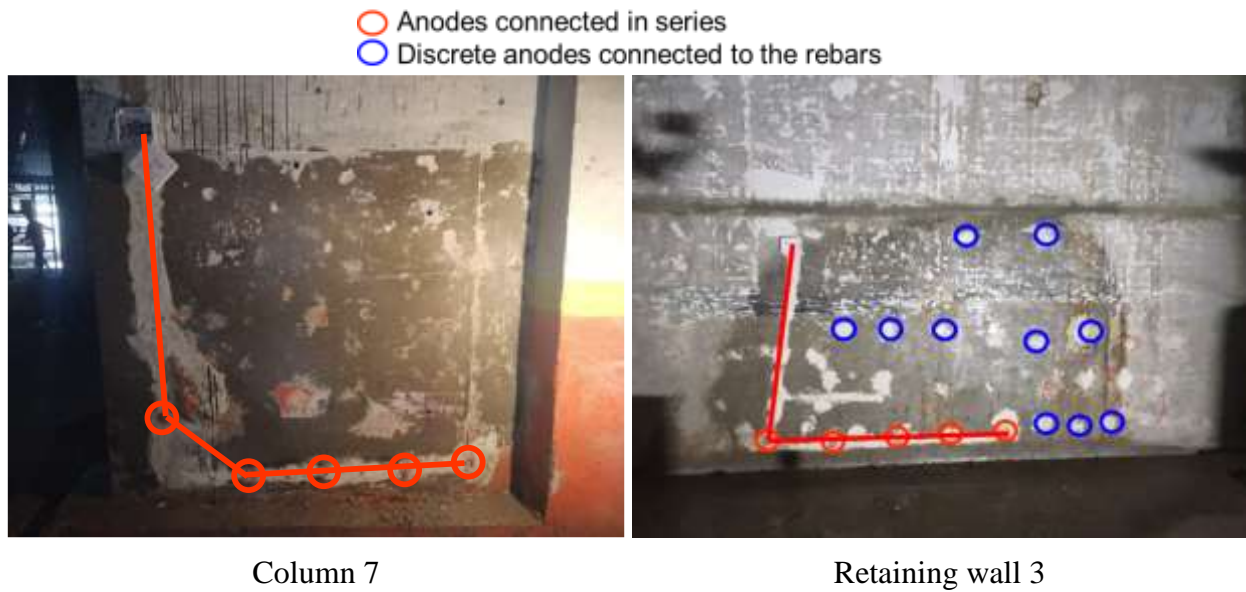

Column 7   Retaining wall 3

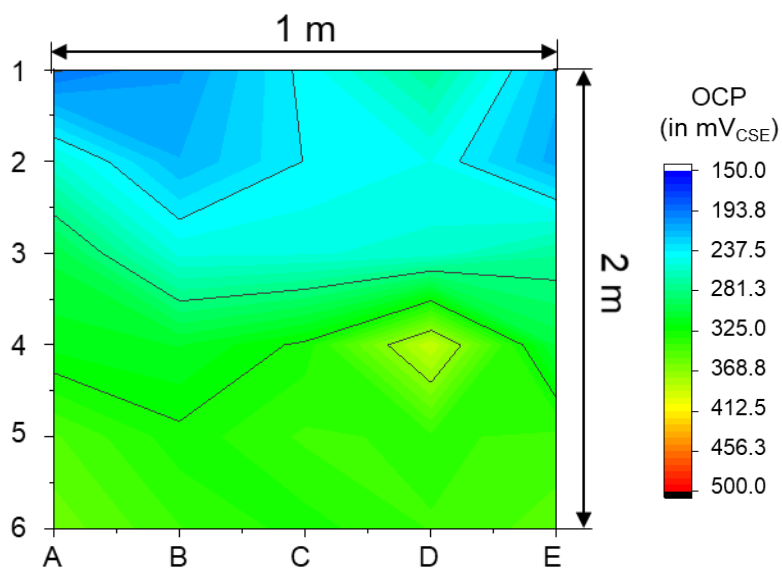**Figure 7.8: Locations considered for obtaining measurements during the site visit**

Figure 7.9: Contour plot of E$_{24}$ potential of a column in Tower D

| Column 7 – result displayed 'Protected' | Retaining wall 3 – result displayed 'Well protected' |

Figure 7.10: Result of passivation verification test obtained using GECOR instrument

f) Examples showing improper implementation of galvanic anodes

Improper embedment of galvanic anodes: Photographs taken from Case Study II
Carrying out a full-scale inspection (walk-through) on all the installed anodes and checking for the proper embedment of anodes post-installation is a must to avoid such poor practices.

APPENDIX D

RESULTS FROM PARAMETRIC STUDY CONDUCTED USING

THE ELECTROCHEMICAL MODEL

This section contains the results obtained from the parametric studies conducted on the concrete geometry by varying the resistivity. Figure 7.11 and Figure 7.12 shows the variation in E_{on} potential of the 3rd and 4th rebar in the model, respectively, along its length. It can be observed that the 3rd rebar at 200 mm from the face *utvw* is influenced by two anodes, whereas the 4th rebar at the same distance is influenced only by only one anode.
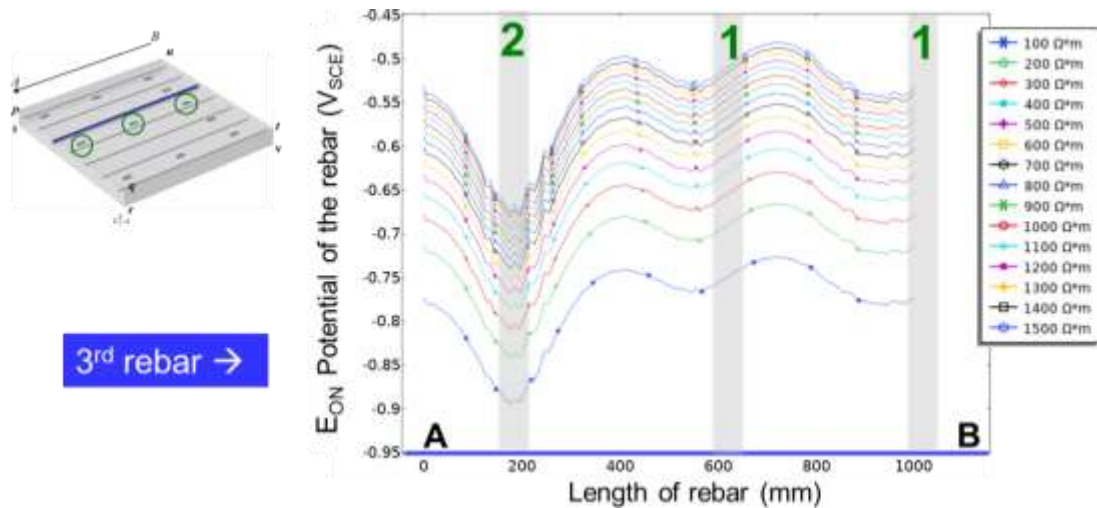

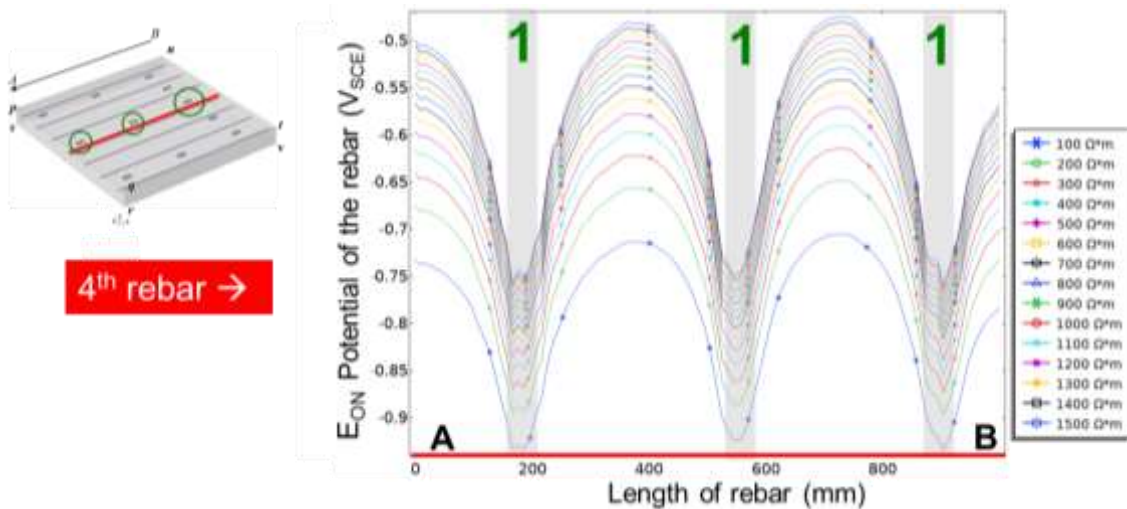
Figure 7.11: Influence of the anodes on protecting 3rd rebar

Figure 7.12: Influence of the anodes on protecting 4th rebar

161

This page is intentionally left blank

MOST IMPORTANT CONTRIBUTION

The following are the major contributions from this research:

a) Long-term field data showing the performance of the galvanic anode cathodic protection system is presented. A framework to estimate the future cost of various repair strategies is developed. This will help practicing engineers compare the LCC of various possible repair strategies during the decision-making stages.

b) Instantaneous performance results of the new two-stage hybrid galvanic anodes are presented. This data can promote the two-stage hybrid anodes in the concrete repair industry to achieve fast passivation of the steel rebar.

c) An electrochemical model to estimate the potential and current distribution in a concrete-anode-steel system using the polarization properties of the metals is developed. The developed EC model can aid in instrumenting a non-destructive test for assessing the performance of the CP system in concrete.

This page is intentionally left blank

CURRICULUM VITA

Naveen Krishnan was born in Kollam, Kerala, India and was brought up in Alappuzha, Kerala. In June 2017, he earned Bachelor of Technology degree in Civil Engineering from Government Engineering College Kottayam (Rajiv Gandhi Institute of Technology), Kerala. Then, he worked as a Project Associate at the Building Technology and Construction Management (BTCM) division of the Department of Civil Engineering, Indian Institute of Technology (IIT) Madras, Chennai. Later, he started master of science studies in Civil Engineering (specialising in construction materials performance) in the Department of Civil Engineering, Indian Institute of Technology Madras, Chennai, Tamil Nadu. During the post-graduate studies, he worked as a half-time research/teaching assistant in the Department of Civil Engineering, IIT Madras.

Naveen Krishnan can be contacted at

c/o Mr K. C. Krishnakumar
Kannampallil house, Palace Ward,
Krishnapuram P.O., 690533
Kayamkulam, Alappuzha District,
Kerala, India
Ph. +91 79078 31149
Email: naveenkrishnankc@gmail.com

This page is intentionally left blank

GENERAL TEST COMMITTEE (GTC) MEMBERS

CHAIRPERSON   Dr Manu Santhanam
                         Professor and Head
                         Department of Civil Engineering

GUIDE   Dr Radhakrishna G. Pillai
                         Associate Professor
                         Department of Civil Engineering

MEMBERS   Dr Sankaran Aniruddhan
                         Associate Professor
                         Department of Electrical Engineering

                         Dr Piyush Chaunsali
                         Assistant Professor
                         Department of Civil Engineering

This page is intentionally left blank